THE TIDAL MOTIONS OF A ROTATING , ELLIPTICAL, ELASTIC AND OCEANLESS EARTH

John Matthew Wahr

THE TIDAL MOTIONS OF A ROTATING, ELLIPTICAL, ELASTIC AND OCEANLESS EARTH

by

John Matthew Wahr

B.A., University of Michigan, 1973

M.A., University of Colorado, 1975

A thesis submitted to the Faculty of the Graduate School of the University of Colorado in partial fulfillment of the requirements for the degree of

Doctor of Philosophy

Department of Physics

1979

This Thesis for the Doctor of Philosophy Degree by

John Matthew Wahr

has been approved for the

Department of

Physics

by

Martin L. Smith

Peter L. Bender

Date 4-16-79

Wahr, John Matthew (Ph.D., Geophysics)

The Tidal Motions of a Rotating, Elliptical, Elastic and Oceanless Earth

Thesis directed by Assistant Professor Martin L. Smith

A theoretical study is presented of the response of a rotating, elliptical and elastic Earth to the combined gravitational attraction of the Sun and Moon. Five of the most heavily constrained contemporary models of the Earth's material structure are considered (all have a fluid outer core and a solid inner core). The non-orbital part of the response is separated into the body tide (the Earth's deformation), the precession and nutation of the Earth, and changes in the Earth's rotation rate. In particular, the nutations are shown to be the best represented by motion of the 'Tisserand mean figure axis of the surface', which also is essentially a mean mantle fixed axis.

An eigenfunction expansion technique is developed and used to compute the total induced displacement. The computed results at the surface are shown to be accurate to at least 1 part in 300. Observational effects of the displacements are examined, with all rotational, elliptical and inertial effects included. The results show slight ($\lesssim$ 1%) latitude dependence in the Love numbers and in the gravimetric and diminishing factors. A 10% reduction in amplitude of the tidally induced changes in the Earth's rotation

rate is found and is due to the fluid core. Only small numerical differences are observed between results for the different structural models, suggesting that observations will probably not impose additional constraints on these models within the near future.

This abstract is approved as to form and content. I recommend its publication.

Signed _____
Faculty member in charge of thesis

ACKNOWLEDGEMENT

I would like to gratefully acknowledge the help and guidance of a number of people who contributed to this work. First and foremost is Martin L. Smith whose advice and intellectual support throughout really made this thesis possible. I have greatly profited from our association.

I thank P. L. Bender, J. C. Harrison and T. Sasao for many long, invaluable discussions which helped to significantly improve the content and orientation of much of this work. Their help and encouragement has left me greatly in their debt. Mrs. B. Sloan did an excellent job of typing the manuscript. The National Aeronautics and Space Administration provided financial support under grant NSG 7319. The Cooperative Institute for Research in Environmental Sciences at Boulder, Colorado provided office space and clerical assistance.

Finally, I thank my wife, Ann Brady Wahr. Her unflagging patience and support during these long years has helped me more than she can know.

TABLE OF CONTENTS

LIST OF TABLES

LIST OF FIGURES

CHAPTER I

INTRODUCTION

Ground based geodetic and astrometric observations have long contributed to our understanding of the structure and dynamical behavior of the Earth. The newly developed precision space techniques of VLBI (Counselman, 1976; Robertson, et al., 1978) and lunar and satellite ranging (Williams, 1977; Silverberg, 1978; Smith, 1978) should offer even better opportunities for constraining terrestrial models in the future. One particular consequence should be improved observation of the Earth's response to the combined gravitational attractions of the Sun and Moon. This response is conveniently referred to as the Earth's tidal motion and is important both as a useful geophysical signal and as a source of noise for other phenomena.

It is usual to separate the tidal motion into three conceptually disjoint effects: body tides, tidally induced changes in the Earth's rotation rate, and the forced precession and nutation of the Earth. The body tide (or Earth tide) is defined as the lunisolar induced deformation of the Earth. Most of the important response occurs at (approximately) semi-diurnal, diurnal and zero frequencies. For a spherical Earth, a description of this deformation at the outer surface usually employs a convenient set of dimensionless parameters, the Love numbers. As will be shown, both rotation and ellipticity modify this simple representation.

The long period tidal deformation perturbs the Earth's principal moment of inertia. To conserve angular momentum the Earth must correspondingly alter its rotation rate. These long period (from $\sim$ 10 days to 18.6 years) rotational perturbations affect the instantaneous angular position of the Earth and are observed in precision time measurements of stellar transits.

The precession and nutation of the Earth is the result of the Earth's rotation and accompanying ellipticity of figure and has important astrometric consequences. Because of the ellipticity the luni-solar tidal force exerts a torque on the Earth about an equatorial axis. Since the Earth is rotating it responds gyroscopically: its figure axis precesses about the normal to the ecliptic plane. The angle of inclination is 23.5° and the precessional period is about 26,000 years. To further complicate matters the Sun and Moon are both moving relative to the Earth's center of mass. Consequently, the Earth's instantaneous axis of precession is actually moving through inertial space. This may be accommodated conceptually by superimposing a set of higher frequency wiggles or 'nutations' onto the ecliptic precession. These nutations occur at periods of from $\sim$ 10 days to 18.6 years in inertial space but are observed at any sidereally rotating Earth fixed observatory as approximately diurnal phenomena.

The success of modelling these different aspects of tidal motion depends on assumptions about the Earth's dynamical behavior. Nutations have been shown to be reasonably well represented by the tidal response of a rotating, elliptical but rigid Earth (Woolard, 1953; Kinoshita, 1977). Conversely, the body tide is traditionally computed for an Earth which is elastic, but non-rotating and spherically symmetric (see e.g. Longman, 1962, 1963; Farrell, 1972). Tidal changes in the Earth's rotation rate are usually computed directly from the long period body tide results by assuming a completely solid Earth (see Munk and McDonald, 1960).

The two most important omissions in these models are probably the effects of oceans (see e.g. Farrell, 1972; Beaumont and Lambert, 1972; Warburton et al., 1975; Beaumont and Berger, 1975; Zschau, 1976) and local, near-surface inhomogeneities in geology and topography (see e.g. Beaumont and Berger, 1974; Harrison, 1976; Berger and Beaumont, 1976). Identification of these contributions offers a means of improving our understanding of both the dynamics of the oceans and local geological structure (see Baker, 1979, for a general review).

As observations improve, more complete dynamical models of the Earth's interior become necessary. Of particular importance are the effects of non-rigidity on the nutations and of rotation

and ellipticity on the body tides. These considerations may be combined into a more general problem: computation of the complete tidal motion on a rotating, elliptical, elastic Earth. This problem is made increasingly important by the presence of the fluid core and its treatment has a long history. Hough (1895) and Poincare (1910) demonstrated the presence of a free nutational mode for a fluid ellipsoid contained in an invariably rotating rigid cavity. Jeffreys (1948, 1949, 1950) considered the geophysical consequences of this mode for both the free and forced nutational motions of the Earth.

Jeffreys and Vicente (1957a, 1957b) and Molodensky (1961) greatly extended these results by including more realistic, elastic stratification throughout the Earth. In both cases mantle deformation is computed for a spherical non-rotating shell and only particularly simple core structures are considered. Furthermore, both theories rely almost totally on analytical techniques which demand varying degrees of approximation, of often obscure significance.

Shen and Mansinha (1976) and Sasao et al. (1979) extended these theories of the free nutational and diurnal tidal motions to include more complete dynamical and structural models of the fluid core. Sasao et al. (1979) use a predominantly analytical approach

conceptually similar, in many respects, to that of Molodensky (1961). Shen and Mansinha (1976), relying more heavily on numerical techniques, are able to include even more general representations of the flow in the fluid core. In both cases mantle deformation is computed for a spherically stratified, non-rotating solid shell.

Smith (1976, 1977) used a more complete description of the infinitesimal motion of a rotating, slightly elliptical, elastic Earth (see Smith, 1974) to numerically investigate portions of the Earth's low frequency normal mode spectrum. He relies principally on a truncated representation of the response throughout the Earth which is similar to that used by Shen and Mansinha (1976) in the fluid core.

We use, here, the linearized equations of Smith (1974) to examine the complete tidal motion on a rotating, slightly elliptical, linearly elastic, self-gravitating, hydrostatically pre-stressed Earth. Unlike earlier theories, elliptical and rotational effects are considered throughout the Earth. Calculations have been performed for five of the most heavily constrained elastic Earth models currently available, all of which have a fluid outer core and a solid inner core. Although the dynamical equations must necessarily be truncated, the approximation used has an apparently minimal affect. In particular, numerical investigations suggest our results are probably accurate to better than one percent.

The dynamical problem is formulated in Chapter II. Vector and scalar equations are developed and the tidal potential is defined. A unique approach to the tidal problem, developed in Chapter IV, is an expansion of the tidal motion as a sum of normal modes of the Earth. As a preliminary, the normal modes of a rotating, slightly elliptical, elastic Earth are described in Chapter III.

The complete computational procedure used to solve the dynamical equations is presented in Chapter V. The truncation process is described and its numerical consequences discussed.

Chapters VI, VII and VIII separate and identify the body tide, nutations and changes in rotation rate, respectively. Observational effects of each phenomenon are discussed with all rotational, elliptical and inertial modifications included. The nutations are shown to be described by the inertial space motion of a well defined, observationally meaningful axis, B, the Tisserand mean figure axis of the surface. Finally, numerical results are presented in Chapter IX and a brief summary offered in Chapter X.

Other dynamical processes in the Earth's interior may yet prove important. Zschau (1978) demonstrated the importance of mantle anelasticity on the ocean loading tide. In addition,

independent sources of core mantle coupling (e.g. core viscosity, electromagnetic effects) are useful in damping the predicted core resonance (see, e.g. Toomre, 1974; Rochester, 1976; McClure, 1976; Sasao et al., 1977). Non-inertial core-mantle coupling could also be important in modelling the tidal angular position changes since it would damp the angular rotation between core and mantle (see Section 9.4 below).

CHAPTER II

FORMULATION OF THE TIDAL PROBLEM

The combined gravitational fields of the Sun and Moon cause acceleration of the Earth's center of mass as well as displacements relative to the center of mass. The relative displacements are referred to as the Earth's 'tidal motion' and are the subject of this study. To compute them we work in a reference frame which follows the Earth's center of mass through space. The applied gravitational force is seen in this frame as the negative gradient of an appropriately defined function: the luni-solar tidal potential. Section 2.1 describes the dynamical model assumed here for the Earth and develops the invariant equations of motion. These are expanded in Section 2.3 into scalar equations over radius. The tidal potential is developed in Section 2.2.

2.1 Equations of Motion

The Earth's tidal response is computed here as the first order infinitesimal deviation from equilibrium induced by the luni-solar tidal force. It consists of perturbations in the particle displacement vector, the gravitational potential and the stress tensor.

At equilibrium the Earth is assumed uniformly rotating about the $\hat{\underset{\sim}{z}}$ axis with angular velocity $\underset{\sim}{\Omega}$. It is assumed hydrostatically

prestressed and is consequently an axisymmetric ellipsoid of revolution. The (small) ellipticity of constant density surfaces is found from the equilibrium density distribution, ρ, and angular velocity $\underset{\sim}{\Omega}$ using Clairaut's equation (Jeffreys, 1970). The Earth is self-gravitating and has a constitutive relation assumed as linear, elastic and isotropic with equilibrium Lame parameters, λ and μ, constant over any constant density (elliptical) surface.

Define the equilibrium coordinate system, $\mathcal{R}$, with origin at the Earth's instantaneous center of mass and uniformly rotating with constant angular velocity $\underset{\sim}{\Omega} = \Omega\hat{\underset{\sim}{z}}$. (The center of mass is in a non-infinitesimal orbit around the Sun and Moon. We choose $\mathcal{R}$ to follow its motion through inertial space and will adjust the luni-solar gravitational potential accordingly, in Section 2.2). We conform to tradition by orienting the $\hat{\underset{\sim}{x}}$ axis along the equilibrium Greenwich meridian.

To represent deviations from equilibrium in $\mathcal{R}$, we must adopt some method of labelling the material within the Earth. We choose here the Lagrangian formulation where every material point is represented by its equilibrium position vector. The Eulerian position, $\underset{\sim}{r}$, in $\mathcal{R}$ of any infinitesimally displaced Lagrangian material point, $\underset{\sim}{x}$, at time t is

$$\underset{\sim}{r}(\underset{\sim}{x},t) = \underset{\sim}{x} + \underset{\sim}{s}(\underset{\sim}{x},t) \tag{2.1}$$

where $\underset{\sim}{s}(\underset{\sim}{x},t)$ is the infinitesimal Lagrangian displacement of $\underset{\sim}{x}$.

The linearized infinitesimal Lagrangian equations of motion of the Earth are written in R as (see e.g. Dahlen, 1972).

$$+\rho\partial_t^2 \underset{\sim}{s} + 2\partial_t \rho\underset{\sim}{\Omega} \times \underset{\sim}{s} = \rho\nabla\phi_1^E - \rho\underset{\sim}{s}\cdot\nabla[\nabla(\phi + \psi)] + \nabla\cdot\underset{\sim}{T} + \rho\underset{\sim}{f}$$

$$\nabla^2\phi_1^E = -4\pi G\nabla\cdot(\rho\underset{\sim}{s}) \tag{2.2}$$

$$\underset{\sim}{T} = \lambda(\nabla\cdot\underset{\sim}{s})\,\hat{\underset{\sim}{1}} + \mu[\nabla\underset{\sim}{s} + (\nabla\underset{\sim}{s})^T]$$

with boundary conditions

$$\begin{aligned}
&\underset{\sim}{s}\cdot\hat{\underset{\sim}{n}} && \text{continuous across any boundary}\\
&\underset{\sim}{s} && \text{continuous across any welded boundary}\\
&\hat{\underset{\sim}{n}}\cdot\underset{\sim}{T} && \text{continuous across any boundary}\\
&\phi_1^E && \text{continuous across any boundary}\\
&\hat{\underset{\sim}{n}}\cdot(\nabla\phi_1^E + 4\pi G\rho\underset{\sim}{s}) && \text{continuous across any boundary}
\end{aligned} \tag{2.3}$$

Here, ϕ_1^E, $\underset{\sim}{T}$ and $\underset{\sim}{f}$ are the incremental Eulerian gravitational potential, infinitesimal Cauchy elastic stress tensor and applied body force, respectively; G is the gravitational constant; $\hat{\underset{\sim}{1}}$ the second rank identity tensor, ϕ and ψ the equilibrium gravitational and centripetal potentials, and $\hat{\underset{\sim}{n}}$ the local (outward) normal at the boundary.

Elliptical modifications to the equilibrium material parameters are given to first order as (see Dahlen, 1972)

$$\rho(r,\theta,\phi) = \rho_o(r) + \frac{2}{3} r\varepsilon(r)\, \partial_r \rho_o P_2(\cos\theta)$$

$$\lambda(r,\theta,\phi) = \lambda_o(r) + \frac{2}{3} r\varepsilon(r)\, \partial_r \lambda_o P_2(\cos\theta)$$

$$\mu(r,\theta,\phi) = \mu_o(r) + \frac{2}{3} r\varepsilon(r)\, \partial_r \mu_o P_2(\cos\theta) \qquad (2.4)$$

$$\phi(r,\theta,\phi) + \psi(r,\theta,\phi) = \phi_o(r) + \frac{2}{3} r\varepsilon(r)\, \partial_r \phi_o P_2(\cos\theta)$$

$$\psi(r,\theta,\phi) = -\frac{1}{3}\Omega^2 r^2 P_2(\cos\theta)$$

where $\varepsilon(r)$ is the ellipticity. The normal to any constant density surface is

$$\hat{\underset{\sim}{n}} = \hat{\underset{\sim}{r}} - \frac{2}{3} r\varepsilon(r) \underset{\sim}{\nabla} P_2(\cos\theta) \qquad (2.5)$$

(Smith, 1974).

The radially dependent ϕ_o, ρ_o, λ_o and μ_o define an Earth model and are determined from free oscillation and body wave data. In particular, every model considered here has a solid inner core, a fluid outer core and a solid mantle capped by a thin continental crust.

2.2 Tidal Potential

We wish to solve (2.2) and (2.3) for

$$\underset{\sim}{f} = \rho \underset{\sim}{F}_T \tag{2.6}$$

where $\underset{\sim}{F}_T$ is the luni-solar tidal acceleration. Although $\underset{\sim}{F}_T$ has been studied extensively (see, e.g. Bartels, 1957; Melchior, 1966) a brief, independent description is offered here.

The total external gravitational acceleration of the Moon (or Sun) may be written as the negative gradient of a scalar function

$$\underset{\sim}{F} = - \underset{\sim}{\nabla} V \tag{2.7}$$

where V is interpreted as the gravitational potential energy per unit mass. Let $\underset{\sim}{x}$ be any fixed Lagrangian point within the Earth and $\underset{\sim}{R}$ the vector between the centers of mass of the Earth and Moon (see Figure 1). Assuming $|\underset{\sim}{R}|$ is much larger than the Moon's diameter we may approximate

$$V = \frac{GM_m}{|\underset{\sim}{x}-\underset{\sim}{R}|} \tag{2.8}$$

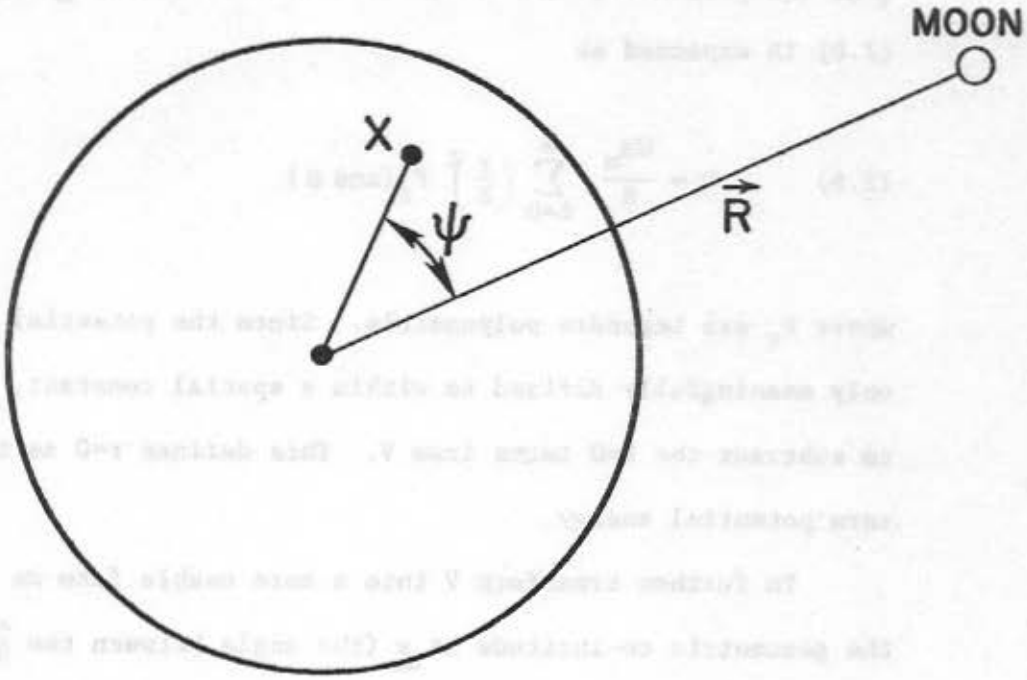

Figure 1. ψ is the geocentric zenith distance of the Moon at the point $\underset{\sim}{x}$.

where M_m is the Moon's mass. By defining $r = |\underset{\sim}{x}|$, $R = |\underset{\sim}{R}|$ and ψ as the geocentric zenith distance of the Moon at $\underset{\sim}{x}$ (see figure 1), (2.8) is expanded as

$$(2.9) \qquad V = \frac{GM_m}{R} \sum_{\ell=0}^{\infty} \left(\frac{r}{R}\right)^{\ell} P_{\ell}(\cos\psi)$$

where P_{ℓ} are Legendre polynomials. Since the potential energy is only meaningfully defined to within a spatial constant, we choose to subtract the $\ell=0$ terms from V. This defines r=0 as the point of zero potential energy.

To further transform V into a more usable form we define θ as the geocentric co-latitude at $\underset{\sim}{x}$ (the angle between the $\hat{\underset{\sim}{z}}$ axis and $\underset{\sim}{x}$) and δ and h_M as the declination (the angle between the equator and $\underset{\sim}{R}$) and hour angle (between the equatorial projections of $\underset{\sim}{x}$ and $\underset{\sim}{R}$) of the Moon (see figures 2a and 2b). The addition theorem for spherical harmonics gives

$$(2.10) \qquad P_{\ell}(\cos\psi) = \mathrm{Re} \sum_{m=-\ell}^{\ell} \frac{(\ell-m)!}{(\ell+m)!} P_{\ell}^{m}(\cos\theta)\, P_{\ell}^{m}\left(\cos\left(\frac{\pi}{2} - \delta\right)\right) e^{imh_M}$$

where the P_{ℓ}^{m} are associated Legendre polynomials and Re denotes the real part.

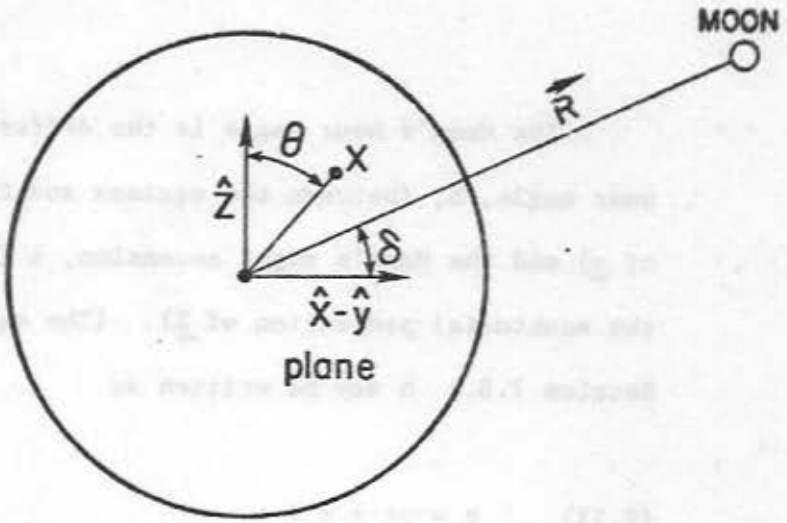

FIGURE 2a

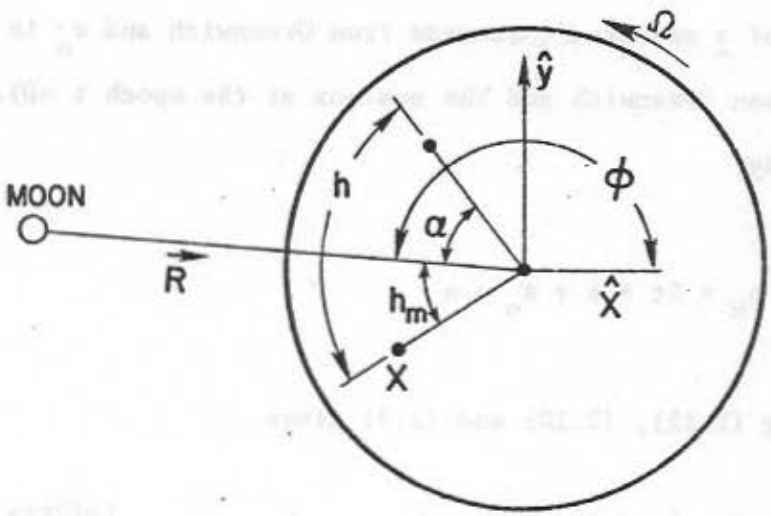

FIGURE 2b

Figure 2. A number of angles are shown which relate the Earth-Moon vector, $\underset{\sim}{R}$, and the material point, $\underset{\sim}{x}$, to the $\hat{\underset{\sim}{x}}$, $\hat{\underset{\sim}{y}}$, $\hat{\underset{\sim}{z}}$ equatorial coordinate system. Figures 2a and 2b are, respectively, perpendicular to and concident with the Earth's equator.

The Moon's hour angle is the difference between the sidereal hour angle, h, (between the equinox and the equatorial projection of $\underset{\sim}{x}$) and the Moon's right ascension, α (between the equinox and the equatorial projection of $\underset{\sim}{R}$). (The equinox is defined in Section 7.8.) h may be written as

$$h = \Omega t + \phi + \phi_o \tag{2.11}$$

where Ω is the sidereal angular velocity of rotation, ϕ is the longitude of $\underset{\sim}{x}$ measured eastwards from Greenwich and ϕ_o is the angle between Greenwich and the equinox at the epoch t =0). Consequently,

$$h_M = \Omega t + \phi + \phi_o - \alpha \tag{2.12}$$

Using (2.12), (2.10) and (2.9) gives

$$V = \mathrm{Re}\ \frac{GM_m}{R} \sum_{\ell=1}^{\infty} \sum_{m=-\ell}^{\ell} \left(\frac{r}{R}\right)^{\ell} \frac{4\pi}{2\ell+1}\, Y_\ell^{m*}\left(\frac{\pi}{2} - \delta, \alpha\right)\, Y_\ell^m(\theta,\phi)\ e^{im(\Omega t+\phi_o)} \tag{2.13}$$

where the Y_ℓ^m are surface spherical harmonics with normalization described in Appendix A, and * denotes complex conjugation. A similar expression describes V for the Sun.

The Earth moon distance, R, and angles α and δ are time dependent. Writing R_E as the equatorial radius of the Earth (the equator is chosen to coincide with the development of Cartwright and Tayler, 1971) and noting

$$Y_\ell^{-m} = (-1)^m Y_\ell^{m*}$$

(2.14)

$$\mathrm{Re}Y_\ell^m = \mathrm{Re}Y_\ell^{m*}$$

gives

$$V = - \mathrm{Re} \sum_{\ell=1}^{\infty} \sum_{m=0}^{\ell} \left(\frac{r}{R_E}\right)^\ell C_\ell^m(t)\, Y_\ell^m(\theta,\phi) \tag{2.15}$$

where the time dependence is confined to

(2.16)

$$C_\ell^m(t) = - 2 \frac{GM_m}{R(t)} \left(\frac{R_E}{R(t)}\right)^\ell \frac{4\pi}{2\ell+1} Y_\ell^{m*}\left(\frac{\pi}{2} - \delta(t),\, \alpha(t)\right) e^{im(\Omega t + \phi_o)}$$

for $m \neq 0$ and

$$C_\ell^o(t) = - \frac{GM_m}{R(t)} \left(\frac{R_E}{R(t)}\right)^\ell \frac{4\pi}{2\ell+1} Y_\ell^{o*}\left(\frac{\pi}{2} - \delta(t),\, \alpha(t)\right) \tag{2.17}$$

Equation (2.15) represents the total gravitational potential of the moon (or sun), including that part responsible for the Earth's orbital motion. The tidal response at any point is defined as the displacement relative to the Earth's instantaneous center of mass. Consequently, the tidal acceleration, denoted by $\underset{\sim}{F}_T$, is the total gravitational acceleration minus the acceleration of the center of mass:

$$\underset{\sim}{F}_T(x) = \underset{\sim}{F}(x) - \underset{\sim}{F}_{CM} \tag{2.18}$$

where

$$\underset{\sim}{F}_{CM} = \frac{1}{M} \int_{V_E} \rho \underset{\sim}{F} \tag{2.19}$$

with ρ, M and V_E the density, total mass and volume of the Earth and $\underset{\sim}{F}$ the total luni-solar tidal acceleration.

The spatially constant vector, $\underset{\sim}{F}_{CM}$, can be written

$$\underset{\sim}{F}_{CM} = - \underset{\sim}{\nabla} V_{CM}(\underset{\sim}{x}) \tag{2.20}$$

Using (2.15) and (2.7) and some laborious algebra gives

$$V_{CM}(\underset{\sim}{x}) = - \mathrm{Re}\left[\sum_{m=0}^{1} \frac{r}{R_E} C_1^m(t)\, Y_1^m(\theta,\phi) - \right.$$

$$\left. \frac{C-A}{MR_E^2} \frac{r}{R_E} \left[\sqrt{21}\ C_3^o(t)\, Y_1^0(\theta,\phi) + \sqrt{\frac{7}{2}}\, C_3^1(t)\, Y_1^1(\theta,\phi) \right] \right] \tag{2.21}$$

where C and A are the Earth's greatest and least moments of inertia. Equation (2.21) is accurate to first order in the dynamical ellipticity, $\frac{C-A}{A}$.

Finally, the tidal potential is defined as

$$V_T(\underset{\sim}{x}) = V(\underset{\sim}{x}) - V_{CM}(\underset{\sim}{x}) \tag{2.22}$$

From (2.21) and (2.15):

$$V_T(t) = - \mathrm{Re}\left[\frac{C-A}{MR_E^2} \frac{r}{R_E} \sqrt{7} \left[\sqrt{3}\, C_3^0(t)\, Y_1^0(\theta,\phi) + \right.\right.$$

$$\left. \frac{1}{\sqrt{2}}\, C_3^1(t)\, Y_1^1(\theta,\phi) \right] \tag{2.23}$$

$$\left. + \sum_{\ell=2}^{\infty} \sum_{m=-0}^{\ell} \left(\frac{r}{R_E} \right)^{\ell} C_\ell^m(t)\, Y_\ell^m(\theta,\phi) \right]$$

with the C_ℓ^m given by (2.16) and (2.17) and

$$F_T(\underset{\sim}{x}) = -\underset{\sim}{\nabla} V_T(\underset{\sim}{x}) \tag{2.24}$$

Equations (2.16) and (2.17) show the C_ℓ^m to decrease with ℓ as $\left(\frac{R_E}{R(t)}\right)^\ell$. Since for the moon $\frac{R_E}{R(t)} \approx \frac{1}{60}$ (and is much smaller for the sum), it is sufficient for our purposes to keep only $\ell \leq 3$ terms in (2.23).

The $\ell=1$ terms in V_T are not found in the usual spherical developments of the tidal potential. They are needed for an elliptical Earth to keep the coordinate system centered at the center of mass: they negate the orbital motion induced by the $\ell=3$ terms in V_T. (Contemporary models of the Earth's ephemeris take the non-sphericity into account.) These terms do not cause any deformation within the Earth.

The $C_\ell^m(t)$ are usually Fourier transformed into the frequency domain as

$$C_\ell^m(t) = \sum_\omega H_s(\omega)\, e^{i\omega t} \tag{2.25}$$

Historical treatments (see, e.g. Darwin, 1883; Doodson, 1922) express $\delta(t)$, $\alpha(t)$ and $R(t)$ as truncated, finite harmonic expansions in t. Algebraically combining terms results in a finite expansion of the form (2.25). Cartwright and Tayler (1971), in a recent study, generate a time series for each $C_\ell^m(t)$ from corresponding series for δ, α and R and they then use filtering techniques to reduce $C_\ell^m(t)$ to the form (2.25). Only those terms which exceed a specified amplitude are kept.

Since the important variations in δ, α and R have periods of a month or longer, the $C_\ell^m(t)$ time dependence exhibited in (2.16) and (2.17) consists of frequencies closely grouped around $m\Omega$. Consequently, m=0,1,2 and 3 terms in V_T are referred to as long period, diurnal, semi-diurnal and ter-diurnal, respectively.

The Fourier expansion (2.25), of $C_\ell^m(t)$ is particularly convenient for tidal calculations. The dynamical equations, (2.2), are transformed to the frequency domain (by replacing ∂_t with $i\omega$) and solved for

$$\underset{\sim}{f} = -\rho\nabla\left[\left(\frac{r}{R_E}\right)^\ell Y_\ell^m(\theta,\phi)\right] \tag{2.26}$$

Once computations have been completed for a representative set of frequencies, results may be convolved with the $H_s(\omega)$ to obtain a time series solution.

2.3 Scalar Equations

The Lagrangian equations of motion (2.2) and (2.3), are defined over the elliptically symmetric equilibrium Earth. To minimize computational difficulties we transform this domain into an equivalent spherical domain (the ESD). The ESD is pointwise identical to the equilibrium Earth except near boundaries, where each elliptical surface is smoothly mapped onto a spherical surface in the ESD. The boundary conditions are altered appropriately. (For a more complete discussion of the ESD, see Smith, 1974.)

The invariant vector equations (2.2) and (2.3) are conveniently transferred to scalar equations over radius in the ESD by using the generalized spherical harmonics, $D^{\ell}_{m\alpha}(\theta,\phi)$, described in Appendix A. In particular, the completeness of the $D^{\ell}_{m\alpha}$ allows us to expand the Fourier transformed gravitational potential, displacement, stress and luni-solar tidal force as:

$$\phi_1^E(r,\theta,\phi,\omega) = \sum_{\ell,m} (\phi_1^E)^m_\ell(r,\omega)\ D^{\ell}_{mo}(\theta,\phi)$$

$$\underset{\sim}{s}(r,\theta,\phi,\omega) = \sum_{\ell,m,\alpha} \hat{\underset{\sim}{e}}_\alpha\ s^{m\alpha}_\ell(r,\omega)\ D^{\ell}_{m\alpha}(\theta,\phi)$$

(2.27)

$$\underset{\sim}{T}(r,\theta,\phi,\omega) = \sum_{\substack{\ell,m \\ \alpha,\beta}} \hat{\underset{\sim}{e}}_\alpha \hat{\underset{\sim}{e}}_\beta\ T^{m\alpha\beta}_\ell\ (r,\omega)\ D^{\ell}_{m(\alpha+\beta)}(\theta,\phi)$$

$$\underset{\sim}{f}(r,\theta,\phi,\omega) = -\rho \underset{\sim}{\nabla} \sum_{\ell,m} \left(\frac{r}{R_E}\right)^{\ell} D^{\ell}_{mo}(\theta,\phi)$$

Here, the $\hat{\underset{\sim}{e}}_{\ell i}$ are complex unit vectors described in Appendix A. Substituion of (2.27) into (2.2) and (2.3) transforms the dynamical vector equationsinto a formidable, infinite system of ordinary differential equations over radius. The mechanics of this process, together with the resulting scalar equations for $\underset{\sim}{f} = 0$, can be found in Smith (1974).

We have followed Smith (1974) (see also Phinney and Burridge, 1973) in choosing as our complete independent set of unknown scalar functions:

$$U_\ell^m(r,\omega),\ V_\ell^m(r,\omega),\ W_\ell^m(r,\omega),\ P_\ell^m(r,\omega),\ Q_\ell^m(r,\omega),$$

$$R_\ell^m(r,\omega),\ (\phi_1^E)_\ell^m(r,\omega),\ (g_1^E)_\ell^m(r,\omega) \tag{2.28}$$

where

$$U_\ell^m = S_\ell^{mo} \quad ; \quad V_\ell^m = S_\ell^{m+} + S_\ell^{m-} \quad ; \quad W_\ell^m = S_\ell^{m+} - S_\ell^{m-}$$

$$P_\ell^m = T_\ell^{moo} \quad ; \quad Q_\ell^m = T_\ell^{mo+} + T_\ell^{mo-} \quad ; \quad R_\ell^m = T_\ell^{mo+} - T_\ell^{mo-} \tag{2.29}$$

$$g_{1\ell}^m = \partial_r \phi_{1\ell}^m + 4\pi G \rho_o(r)\ U_\ell^m$$

and $\rho_o(r)$ is the spherical part of the equilibrium density distribution.

For each ℓ and m the set of 8 scalars, (2.28), can be conveniently separated into two groups:

1) a spheroidal set, σ_ℓ^m, containing U_ℓ^m, V_ℓ^m, P_ℓ^m, Q_ℓ^m, $(\phi_1^E)_\ell^m$, $(g_1^E)_\ell^m$

2) a toroidal set, τ_ℓ^m, containing W_ℓ^m, R_ℓ^m

(The σ_ℓ^m and τ_ℓ^m may alternatively refer to just the relevant displacement components, in which case they are represented in the text as vectors.)

This division is useful for the following reasons:

a) no σ_ℓ^m is dynamically coupled to any other $\sigma_{\ell'}^m$, unless $\ell-\ell'$ is even

b) no τ_ℓ^m is coupled to any other $\tau_{\ell'}^m$, unless $\ell-\ell'$ is even.

c) no τ_ℓ^m is coupled to any $\sigma_{\ell'}^m$, unless $\ell-\ell'$ is odd

These properties come directly from the invariance of (2.2) and (2.3) under spatial inversion through the center of mass. In addition, the assumed rotational invariance demands that no σ_ℓ^m or τ_ℓ^m may be coupled to any other $\sigma_\ell^{m'}$ or $\tau_\ell^{m'}$ unless $m = m'$.

The coupling rules prove valuable for calculations of both tides and normal modes. In either case the exact solution to (2.2) and (2.3) has the form

$$u = \sigma_m^m + \tau_{m+1}^m + \ldots\ldots + \tau_{\ell-1}^m + \sigma_\ell^m + \tau_{\ell+1}^m + \ldots\ldots$$

(2.30)

$$u = \tau_m^m + \sigma_{m+1}^m + \ldots\ldots + \tau_{\ell-1}^m + \sigma_\ell^m + \tau_{\ell+1}^m + \ldots\ldots$$

As a comparison, the corresponding solutions for a spherically symmetric, non-rotating Earth are

$$u = \sigma_\ell^m \quad \text{for an } \ell,m \text{ tide, and either} \tag{2.31}$$

$$u = \sigma_\ell^m \quad \text{or} \quad u = \tau_\ell^m \text{ for a normal mode.}$$

CHAPTER III

NORMAL MODE CATALOG

In Chapter IV the forced solution to (2.2) and (2.3) will be written as a sum of normal modes of the rotating, elliptical Earth (the case $\underset{\sim}{f}=0$ in (2.2)). We anticipate this by examining the Earth's normal mode spectrum.

The best known normal modes are the seismic free oscillations, a denumerably infinite set of modes, all with period less than one hour. The dynamical behavior of these modes is determined by elastic restoring forces. They are the only modes with non-zero eigenfrequency for a non-rotating, everywhere solid Earth and are altered only slightly by rotation and ellipticity (Dahlen, 1968, 1969).

An important class of modes for an Earth with a stably stratified fluid core is the set of internal gravity waves, an infinite family of normal modes with motion confined predominantly to the core. Although these modes can be correctly computed for a non-rotating Earth (see, e.g. Pekeris and Accad, 1972) the effects of rotation should be large and are presently unknown. The results of Kudlick (1966) (see also Greenspan, 1968) for a confined homogeneous, incompressible rotating fluid suggest characteristic eigenfrequencies of less than two cycles per day with an accumulation point at infinite period.

A third group of eigenfunctions which are of prime importance to this study, are a set of three free nutations. These are:

1) The Eulerian free nutation of the mantle, commonly called the Chandler Wobble (CW), with period of about 14 months. The CW is predominantly a slow wobble of the mantle figure axis about the mantle rotation axis. The Earth's non-rigidity has an important effect on the CW eigenfrequency and there is some accompanying deformation (see, e.g. Hough, 1895; Love, 1909; Larmor, 1909; Jeffreys and Vicente, 1957a, 1957b; Molodensky, 1961; Smith, 1977).
2) The Nearly Diurnal Free Wobble (NDFW), predominantly a relative incremental rotation between the fluid core and the solid mantle with period slightly less than one day. This relative rotation is maintained through inertial pressure coupling across the elliptical core-mantle boundary. There is some elastic deformation associated with the NDFW (see, e.g. Hough, 1895; Jeffreys and Vicente, 1957a, 1957b; Molodensky, 1961; Smith, 1977).
3) The tilt-over-mode (TOM), a mode with exactly diurnal frequency, representing a rotation around an axis slightly different than $\underset{\sim}{\Omega}$. The TOM does not depend in any way on the constitution of the Earth and has no accompanying deformation. Yet, despite its simplicity, it is a very

important eigenfunction representing free periodic motion relative to the invariably rotating reference frame, R, and must be included in our normal mode catalog. (See, e.g. Hough, 1895; Dahlen and Smith, 1975; Smith, 1977.) In particular, the TOM will be seen to be strongly excited by the $\ell=2$ diurnal tides.

All three of these nutational modes are characterized by a large, nearly linear (in r) $\underset{\sim}{\tau}^{m=1}_{\ell=1}$ displacement component in the mantle. (In rectangular coordinates a linear $\underset{\sim}{\tau}^{1}_{1}$ term represents $(\hat{\underset{\sim}{x}} + i\hat{\underset{\sim}{y}}) \times \underset{\sim}{r}$ motion, where $\hat{\underset{\sim}{x}}$ and $\hat{\underset{\sim}{y}}$ are unit vectors.) The CW and NDFW have, in addition, fairly sizable $\underset{\sim}{\sigma}^{m=1}_{\ell=2}$ elastic components.

There are two other sets of modes of some importance to this study, all of which are associated with particular zero-frequency normal modes of a non-rotating Earth. These are 1) the axial spin modes of the inner core, fluid core and mantle, representing rotations about the $\hat{\underset{\sim}{z}}$-axis, and 2) the set of 3 uniform translations - one for each spatial dimension. These modes are all complicated by the fact that they contain both constant and secular (linear in time) parts (see Dahlen and Smith, 1975).

The translational displacements may be written as $\underset{\sim}{s}^{T}_{Z}$, a translation in the $\hat{\underset{\sim}{z}}$ direction, and $\underset{\sim}{s}^{T}_{x+iy} = \underset{\sim}{s}^{T}_{x} + i\underset{\sim}{s}^{T}_{y}$, $\underset{\sim}{s}^{T}_{x-iy} = \underset{\sim}{s}^{T}_{x} - i\underset{\sim}{s}^{T}_{y}$, where $\underset{\sim}{s}^{T}_{x}$ and $\underset{\sim}{s}^{T}_{y}$ represent translations in the $\hat{\underset{\sim}{x}}$ and $\hat{\underset{\sim}{y}}$ directions, respectively. $\underset{\sim}{s}^{T}_{Z}$ has zero eigenfrequency and the functional form

$$(3.1) \qquad \underset{\sim}{s}^{T}_{Z} = \hat{\underset{\sim}{z}}(\alpha + \beta t)$$

where α and β are constants. Equation (3.1) is a special form of a $\underset{\sim}{\sigma}^{m=0}_{\ell=1}$ spheroidal displacement. The two modes $\underset{\sim}{s}^{T}_{x+iy}$ and $\underset{\sim}{s}^{T}_{x-iy}$ have eigenfrequencies $+\Omega$ and $-\Omega$, respectively (corresponding to zero frequency in non-rotating inertial space) and the functional form:

$$(3.2) \qquad \underset{\sim}{s}^{T}_{x\pm iy} = [\hat{\underset{\sim}{x}} \pm i\hat{\underset{\sim}{y}}]\ (\alpha+\beta t)\ e^{\pm i\Omega t}$$

representing a $\underset{\sim}{\sigma}^{m=\pm 1}_{\ell=1}$ displacement.

The constant, α, terms in both (3.1) and (3.2) represent an Earth which is not centered on the origin of the reference system. The secular, β, terms describe uniform motion at a constant velocity away from the origin.

The zero-frequency axial spin mode (ASM) for a given region is more complex. Its time independent component has a displacement

$$(3.3) \qquad \alpha\hat{\underset{\sim}{z}} \times \underset{\sim}{r}$$

representing an Earth which has been rotated slightly about the $\hat{\underset{\sim}{z}}$-axis relative to the reference frame. Equation (3.3) is equivalent to a linear $\underset{\sim}{\tau}^{m=0}_{\ell=1}$ displacement. The ASM also has a secular part which describes an Earth which is rotating at a

faster rate than the reference frame. The principal displacement of this latter mode is $\beta t \hat{\underset{\sim}{z}} \times \underset{\sim}{r}$. However, the increased centrifugal forces connected with such motion must also deform the Earth slightly. The accompanying deformation will be constant in time (not secular) and must be found from the equations of motion, (2.2) and (2.3).

Other well-known modes of the Earth include inner core translations (the Slicher modes) (see, e.g. Slichter, 1961; Alsop, 1963; Busse, 1974; Smith, 1976) and nutations (see, e.g. Busse, 1970). These will be of decreased importance importance here, since they describe motion confined mainly to the deep interior.

CHAPTER IV

EIGENFUNCTION EXPANSION

An analytical technique often applied to forced physical systems is to represent the motion as a linear combination of the normal modes of the system. This method is used in geophysics, for example, to compute synthetic seismograms from a given seismic source and a sufficiently dense suite of spherical Earth free oscillations. We describe, here, a similar technique in which the tidal response is represented as a sum of rotating, elliptical normal modes. The process is considerably complicated by non-sphericity. Both ellipticity and rotation affect the Earth's normal modes (see Chapter III) making computation difficult and expensive. The Coriolis force (represented by $\underset{\sim}{\Omega} \times \partial_t \underset{\sim}{s}$ in (2.2)) has the additional effect of seriously degrading the usual method of expansion: it couples normal modes together into an infinite algebraic system (see Dahlen and Smith, 1975). A modified formulation must be used and is developed, below.

4.1 Transformation to a Six Dimensional Solution Space

Taking the Fourier transform (in the time variable) of (2.2) gives

$$(4.1) \qquad -\omega^2 \rho \underset{\sim}{s} + \rho i\omega N s + K \underset{\sim}{s} = \underset{\sim}{f}\,\delta$$

where ω is the perturbing frequency and the operators K and N are defined as

$$(4.2) \qquad K\,\underset{\sim}{s} = \rho\nabla\phi_1^E + \rho\underset{\sim}{s}\cdot\nabla\,[\nabla(\phi+\psi)] - \nabla\cdot\underset{\sim}{T}$$

$$(4.3) \qquad N\,\underset{\sim}{s} = 2\underset{\sim}{\Omega} \times \underset{\sim}{s}$$

(ϕ_1^E and $\underset{\sim}{T}$ are determined from $\underset{\sim}{s}$ using the second and third of (2.2)).

Let L^2 be the set of all square integrable, vector valued, complex functions defined over the equilibrium volume of the Earth. Define X as the (dense) subspace of L^2 containing all sufficiently differentiable functions (i.e. functions in the domain of K) which satisfy the boundary conditions (2.3). Given the applied force, $\underset{\sim}{f}$, we must find $\underset{\sim}{s} \in X$ which solves (4.1).

It is convenient to reformulate (4.1) so that only first derivatives in time are present. Define the function space, H, as the cartesian product

$$(4.4) \qquad H = L^2 \times L^2$$

Any element, $\underset{\sim}{z}$, in H is a six-dimensional vector field of the form

$$(4.5) \qquad \underset{\sim}{z} = \begin{pmatrix} \underset{\sim}{s}_1 \\ \underset{\sim}{s}_2 \end{pmatrix}$$

where $\underset{\sim}{s}_1$ and $\underset{\sim}{s}_2$ are both in L^2. We further define the dense subspace, $\mathcal{D} \subset H$ as

$$\mathcal{D} = X \times X \tag{4.6}$$

Suppose $\underset{\sim}{s}_o \in X$ solves (4.1). Then the six-dimensional vector $\underset{\sim}{z}_o \in \mathcal{D}$:

$$\underset{\sim}{z}_o = \begin{pmatrix} \underset{\sim}{s}_o \\ i\omega \underset{\sim}{s}_o \end{pmatrix} \tag{4.7}$$

solves

$$\rho i\omega \underset{\sim}{z}_o = \begin{pmatrix} 0 & \rho \\ -K & -\rho N \end{pmatrix} \underset{\sim}{z}_o + \begin{pmatrix} 0 \\ \underset{\sim}{f} \end{pmatrix} \delta \tag{4.8}$$

Conversely, if $\underset{\sim}{z}_o = \begin{pmatrix} \underset{\sim}{s}_o \\ \underset{\sim}{s}_1 \end{pmatrix}$ solves (4.8) and $\underset{\sim}{z}_o \in \mathcal{D}$, it is easy to see that $\underset{\sim}{s}_o \in X$ and $\underset{\sim}{s}_o$ solves (4.1). Consequently, the two formulations, (4.1) and (4.8), are equivalent.

Define the six-dimensional differential operator

$$A = i \begin{pmatrix} o & -1 \\ K/\rho & N \end{pmatrix} \tag{4.9}$$

and the vector

$$\underset{\sim}{F} = \begin{pmatrix} 0 \\ f\underset{\sim}{k}\Phi \end{pmatrix} \tag{4.10}$$

Then (4.8) is

$$i\omega \underset{\sim}{z}_o = iA\underset{\sim}{z}_o + \underset{\sim}{F} \tag{4.11}$$

The solutions to (2.2) and (2.3) are exactly represented by those $\underset{\sim}{z}_o \in \mathcal{D}$ which satisfy (4.11). This equivalence extends to the special case $f=0$, where the solutions, $\underset{\sim}{z}_i$, are the normal modes of the Earth and solve

$$\omega_i \underset{\sim}{z}_i = A\underset{\sim}{z}_i \tag{4.12}$$

with ω_i the eigenvalue associated with $\underset{\sim}{z}_i$. Equation (4.12) represents the non-secular normal modes on a rotating Earth as solutions to a linear eigenvalue problem. Such a linear description is not available using the original formulation, (2.2), because of the Coriolis term, $\underset{\sim}{\Omega} \times \partial_t \underset{\sim}{s}$.

4.2 Inner Product of H

It is reasonable to expect that the forced Fourier transformed solution to (4.11), $\underset{\sim}{z}_o \in \mathcal{D}$, can be expanded in terms of the eigenfunctions, $\underset{\sim}{z}_i$, as

$$\underset{\sim}{z}_o = \sum_i a_i \underset{\sim}{z}_i \tag{4.13}$$

To develop (4.13) effectively it is useful to first find an inner product on H which orthogonalizes the $\underset{\sim}{z}_i$.

Let $\underset{\sim}{y} = \begin{pmatrix} \underset{\sim}{s}_1 \\ \underset{\sim}{s}_2 \end{pmatrix}$ and $\underset{\sim}{z} = \begin{pmatrix} \underset{\sim}{t}_1 \\ \underset{\sim}{t}_2 \end{pmatrix}$ be any two elements in $\mathcal{D}$. We define a bilinear form $((\ , \ ))$ on $\mathcal{D}$ according to

$$((\underset{\sim}{y},\underset{\sim}{z})) = \left(\underset{\sim}{s}_1, \frac{K}{\rho} \underset{\sim}{t}_1 \right) + (\underset{\sim}{s}_2, \underset{\sim}{t}_2) \tag{4.14}$$

where $(\underset{\sim}{s},\underset{\sim}{t})$ denotes the usual three-dimensional inner product

$$(\underset{\sim}{s},\underset{\sim}{t}) = \int_{V_E} \rho \underset{\sim}{s} \cdot \underset{\sim}{t}^* \tag{4.15}$$

with * denoting complex conjugation, ρ the density and V_E the volume of the Earth. We continuously extend (4.14) to all of H.

It proves necessary to modify H to make $((\ ,\ ))$ an inner product. Let C be the set of all elements in H where

$$(4.16) \qquad \underset{\sim}{z}_C \in C \Rightarrow ((\underset{\sim}{z}_C, \underset{\sim}{z}_C)) \leq 0$$

Define an equivalence relation, '$\equiv$' on H as

$$(4.17) \qquad \underset{\sim}{y} \equiv \underset{\sim}{z} \quad \text{iff} \quad \underset{\sim}{y}-\underset{\sim}{z} \in C$$

Any $\underset{\sim}{c} \in C$ is consequently equivalent to $\underset{\sim}{0}$. The vector space, H, together with the equivalence relation, (4.17), is conventionally written as H/C, the 'quotient space of H modulo C' (quotient spaces are rigorously defined by e.g. Rudin, 1973).

The equivalence relation, (4.17), is introduced so that $((\underset{\sim}{z},\underset{\sim}{z}))$ is positive definite on $H/C - \{\underset{\sim}{0}\}$. ($((\underset{\sim}{z},\underset{\sim}{z}))$ will be defined as 0 for $\underset{\sim}{z} \equiv \underset{\sim}{0}$). It can then be verified that (4.14) is an inner product. Completing H/C under the norm

$$(4.18) \qquad |\underset{\sim}{z}| = ((\underset{\sim}{z},\underset{\sim}{z}))^{1/2}$$

defines a Hilbert space which we continue to denote as H/C.

4.3 Eigenfunction Expansion on H/C

Consider the operator A (4.9) with domain restricted to $\mathcal{D}/C \subset H/C$. It is not difficult to show that for any $\underset{\sim}{y},\underset{\sim}{z} \in \mathcal{D}/C$:

$$(4.19) \qquad ((\underset{\sim}{y},A\underset{\sim}{z})) = ((A\underset{\sim}{y},\underset{\sim}{z}))$$

Consequently, A is symmetric. It is beyond the scope of this work to rigorously decide if A has a self-adjoint extension on H/C. We assume this to be the case and denote the extension also by A. We also assume the spectrum of A to be discrete (it must be real since A is assumed self-adjoint).

From the spectral theorem (see, e.g. Rudin, 1973) we can then expand any $\underset{\sim}{z}_o \in H/C$ as

$$(4.20) \qquad \underset{\sim}{z}_o \equiv \sum_n a_n \underset{\sim}{z}_n$$

where the $\underset{\sim}{z}_n$ are eigenvectors of A in H/C and the a_n are scalar coefficients. (Note the equivalence relation, $\equiv$, in (4.20).) The $\underset{\sim}{z}_n$ are orthogonal under the inner product, (4.41). (They are eigenvectors of a self-adjoint operator.) Letting $\underset{\sim}{z}_o$ in (4.20) be the forced solution to (4.11) and taking the inner product of (4.11) with $\underset{\sim}{z}_n$, we can solve for the coefficients, a_n

$$a_n = \frac{i((F, z_n))}{(\omega_n - \omega)((z_n, z_n))} \tag{4.21}$$

where ω_n is the eigenvalue associated with z_n.

4.4 Composition of C

Let

$$z_c = \begin{pmatrix} s_c \\ i\omega_c s_c \end{pmatrix} \tag{4.22}$$

be any eigenvector of A in C. Then

$$((z_c, z_c)) = \left(s_c, \frac{K}{\rho} s_c \right) + \omega_c^2 (s_c, s_c) \leq 0 \tag{4.23}$$

It is possible to show that

$$\left(s_c, \frac{K}{\rho} s_c \right) = E(s_c, s_c) + G(s_c, s_c) + \Phi(s_c, s_c) \tag{4.24}$$

where $E(s_c, s_c)$, $G(s_c, s_c)$ $\Phi(s_c, s_c)$ and (s_c, s_c) are, respectively, the elastic, gravitational, centripetal potential and relative kinetic energy bilinear forms (see Dahlen, 1972, and Dahlen and Smith, 1975).

As a result,

$$(4.25) \qquad ((\underset{\sim}{z}_c, \underset{\sim}{z}_c)) = 2[\overline{T} + \overline{V}] \leq 0$$

where $\overline{V}$ and $\overline{T}$ represent the time averages over one harmonic cycle of the potential and relative kinetic energies, respectively ($\overline{T}$ is not the total kinetic energy on a rotating Earth).

The dissipationless momentum equation (2.2) for $\underset{\sim}{s}_c$ can be used to independently derive the conservation of energy (Dahlen and Smith, 1975)

$$(4.26) \qquad \frac{d}{dt}(T + V) = 0$$

where V and T are the instantaneous potential and relative kinetic energies of the deformation. For a dissipative system (4.26) is replaced by

$$(4.27) \qquad \frac{d}{dt}(T + V) < 0$$

Consequently, in the presence of dissipation, T + V (and thus $\overline{T} + \overline{V}$) is continuously decreasing. In this case, any $\underset{\sim}{z}_c$ with $((\underset{\sim}{z}_c, \underset{\sim}{z}_c)) < 0$ which is initially excited will continue to grow: i.e., $\underset{\sim}{z}_c$ is secularly unstable. For an Earth with 'realistic' material

properties in the mantle and inner core and with a stable fluid core, no secularly unstable modes are expected to exist.

There is, however, a set of modes in C satisfying $((\underset{\sim}{z}_C, \underset{\sim}{z}_C)) = 0$ which can never have accompanying dissipation: the static axial spin modes and center of mass translations. These modes are all associated with simple conservation properties of the Earth (as will be seen), and their union is assumed to span the set, C.

4.5 New Modes in H/C

The eigenfunctions of A form a mathematically complete set only in H/C - not in H. This is reflected by the equivalence relation, '$\equiv$', in (4.21). It introduces two distinct complications: First, the forced solution, $\underset{\sim}{z}_o$, is determined by (4.21) only to within an arbitrary member of C. This undetermined component (the 'projection' of $\underset{\sim}{z}_o$ onto C) must be found independently. This is done in Section 4.6.

Second, and discussed here, the eigenfunctions of A in H/C are not quite the same as those in H. More precisely, the linear eigenvalue equation (4.12) is modified on H/C by replacing '=' with '$\equiv$':

$$A\underset{\sim}{z}_i \equiv \omega_i \underset{\sim}{z}_i \tag{4.28}$$

The solutions to (4.28) which are not equivalent to zero, include all those normal modes in H (i.e., those satisfying (4.12)) which are not in C.

In addition, since any $\underset{\sim}{z}_c \in C$ is equivalent to $\underset{\sim}{0}$ in H/C, there will be solutions, $\bar{\underset{\sim}{z}}$, to (4.28) which satisfy

$$A\bar{\underset{\sim}{z}}_i = \omega_i \bar{\underset{\sim}{z}}_i + \underset{\sim}{z}_c \tag{4.29}$$

in H, where $\bar{\omega}_i$ is the eigenvalue associated with $\bar{\underset{\sim}{z}}_i$. Consequently A has an additional set of normal modes $\bar{\underset{\sim}{z}}_i$, in $\mathcal{D}/C$, each of which may be identified with one of the normal modes in C (the ASM's and translations). To find these new modes in H/C for a given normal mode $\underset{\sim}{z}_c \in C$, we write

$$\bar{\underset{\sim}{z}}_i = \begin{pmatrix} \bar{\underset{\sim}{s}}_i \\ \bar{\underset{\sim}{v}}_i \end{pmatrix} \tag{4.30}$$

Using (4.22) for $\underset{\sim}{z}_c \in C$, and solving (4.29) for $\bar{\underset{\sim}{s}}_i$ and $\bar{\underset{\sim}{v}}_i$ gives

$$\bar{\underset{\sim}{v}}_i = i\bar{\omega}_i \bar{\underset{\sim}{s}}_i + i\underset{\sim}{s}_c \tag{4.31}$$

and

$$\left[\frac{K}{\rho} + i\,N\bar{\omega}_i - \bar{\omega}_i^2\right]\bar{\underset{\sim}{s}}_i = \left[\bar{\omega}_c + \bar{\omega}_i - iN\right]\underset{\sim}{s}_c \tag{4.32}$$

where ω_c is the eigenvalue of A in H, associated with $\underset{\sim}{z}_c$.

Using the appropriate expressions for each $\underset{\sim}{s}_c$ as given in Chapter III we solve (4.31) and (4.32) to find

1) $\hat{z}$-translations ($\underset{\sim}{s}_c = \hat{z}$, $\omega_c = 0$)

$$(4.33) \qquad \bar{\underset{\sim}{s}} = 0 \quad , \quad \bar{\underset{\sim}{v}} = i\hat{z}, \quad \bar{\omega} = 0$$

2) $\hat{x}\pm i\hat{y}$ translations ($\underset{\sim}{s}_c = \hat{x}\pm i\hat{y}$, $\omega_c = \pm\Omega$)

$$(4.34) \qquad \bar{\underset{\sim}{s}}_{\pm} = 0, \quad \bar{\underset{\sim}{v}}_{\pm} = i(\hat{x}\pm i\hat{y}) \quad , \quad \bar{\omega}_{\pm} = \pm\Omega$$

3) axial spin modes ($\underset{\sim}{s}_c = \hat{z} \times \underset{\sim}{r}$, $\omega_c = 0$)

$$(4.35) \qquad \frac{K}{\rho}\bar{\underset{\sim}{s}} = -\, iN\,(\hat{z} \times \underset{\sim}{r}) \quad , \quad \bar{\underset{\sim}{v}} = i\hat{z} \times \underset{\sim}{r} \quad , \quad \bar{\omega} = 0$$

Equations (4.33), (4.34) and (4.35) describe new modes in H/C which must be included in the expansion (4.20). For the translations, (4.33) and (4.34), the displacement component, $\bar{\underset{\sim}{s}}$, vanishes. Consequently, excitation of (4.33) and (4.34) will not contribute to any forced displacement. On the other hand, the associated ASM displacement solution, $\bar{\underset{\sim}{s}}$, in

(4.36) is non-zero; it actually represents the elastic deformation in the secular ASM (see Chapter III). Since every $\underset{\sim}{s}_c \in C$ safisfies

$$(4.36) \qquad \frac{K}{\rho}\,\underset{\sim}{s}_c = 0$$

$\bar{\underset{\sim}{s}}$ is only determined by (4.35) to within an element of C. We choose to define $\bar{\underset{\sim}{s}}$ for the ASM so that

$$(4.37) \qquad (\bar{\underset{\sim}{s}}, \underset{\sim}{s}_c) = 0$$

for all $\underset{\sim}{s}_c \in C$.

Consideration of (4.33)-(4.35) and (4.37) then shows that each $\underset{\sim}{z}_{c_i} \in C$ can be identified with a new normal mode, $\bar{\underset{\sim}{z}}_i \in H/C$ according to

$$(4.38) \qquad \bar{\underset{\sim}{z}}_i = \begin{pmatrix} \bar{\underset{\sim}{s}}_i \\ i\underset{\sim}{s}_{c_i} \end{pmatrix}$$

where $(\bar{\underset{\sim}{s}}_i, \underset{\sim}{s}_{c_j}) = 0$ for all $\underset{\sim}{s}_{c_j} \in C$.

4.6 Expansion of the displacement in H

The eigenfunctions of A in H/C thus consists of the non-translational and non-ASM normal modes in H, with the form

$$\underset{\sim}{z}_n = \begin{pmatrix} \underset{\sim}{s}_n \\ i\omega_n \underset{\sim}{s}_n \end{pmatrix} \tag{4.39}$$

as well as a set of new modes, $\underset{\sim}{\bar{z}}_l$, each associated with an element of C and with the form, (4.38). By summing (4.20) over all these modes and using (4.14) for ((,)) and (4.21) for a_n, we find the forced solution $\underset{\sim}{z}_o$, in H/C as

$$\underset{\sim}{z}_o = \sum_n a_n \underset{\sim}{z}_n + \sum_m \bar{a}_m \underset{\sim}{\bar{z}}_m \tag{4.40}$$

where

$$a_n = \frac{1}{2} \frac{(\underset{\sim}{f}, \underset{\sim}{s}_n)}{(\omega_n - \omega)\ [\omega_n (\underset{\sim}{s}_n, \underset{\sim}{s}_n) - (\underset{\sim}{s}_n, i\Omega \underset{\sim}{x} \underset{\sim}{s}_n)]} \tag{4.41}$$

$$\bar{a}_m = \frac{(\underset{\sim}{f}, \underset{\sim}{s}^m_c)}{(\bar{\omega}_m - \omega)\ [(\underset{\sim}{s}^m_c, \underset{\sim}{s}^m_c) - (\underset{\sim}{\bar{s}}_m, \frac{K}{\rho} \underset{\sim}{\bar{s}}_m)]} \tag{4.42}$$

Since $\underset{\sim}{z}_o$ as given by (4.40) is only determined in H to within an element of C, we must further find the projection of $\underset{\sim}{z}_o$ onto C and add it to (4.40). Write

$$\underset{\sim}{z}_o = \sum_n a_n \underset{\sim}{z}_n + \sum_m a_m \underset{\sim}{z}_m + \sum_m b_m \underset{\sim}{z}_{c_m} \tag{4.43}$$

in H. The b_m represent excitation coefficients of normal modes in C (i.e. the translations and $A3M^{S}$) and must now be found. Using (4.43) in (4.11) and noting that

$$A\bar{\underset{\sim}{z}}_m = \underset{\sim}{z}_{c_m} + \bar{\omega}_m \bar{\underset{\sim}{z}}_m \tag{4.44}$$

we find

$$\sum_n i(\omega-\omega_n)\, a_n \underset{\sim}{z}_n + \sum_m i(\omega-\omega_{c_m})\, b_m \underset{\sim}{z}_{c_m} \tag{4.45}$$

$$+ \sum_m \bar{a}_m \left[i(\omega-\bar{\omega}_m)\, \bar{\underset{\sim}{z}}_m + \underset{\sim}{z}_{c_m} \right] = \underset{\sim}{F}$$

where ω_{c_m} is the eigenvalue of $\underset{\sim}{z}_{c_m}$ ($\omega_{c_m} = \bar{\omega}_m$ for every m). Taking the upper (displacement) component of (4.45) and then the conventional three-dimensional inner product with $\underset{\sim}{s}_{c_k}$ gives

$$(4.46)\qquad \sum_n i(\omega-\omega_n)\, a_n(\underset{\sim}{s}_{c_k}, \underset{\sim}{s}_n) + \sum_m i(\omega-\omega_{c_m})\, b_m(\underset{\sim}{s}_{c_k}, \underset{\sim}{s}_{c_m})$$

$$+ \sum_m \bar{a}_m(\underset{\sim}{s}_{c_k}, \underset{\sim}{s}_{c_m}) = 0$$

Since the $\underset{\sim}{\text{ASM}}^{S}$ and translational modes satisfy

$$(4.47)\qquad (\underset{\sim}{s}_{c_k}, \underset{\sim}{s}_{c_m}) = 0$$

unless k=m, we get

$$(4.48)\qquad b_k = \frac{1}{2}\left[\frac{1}{\omega-\omega_{c_k}}\right]^2 \left[\frac{(\underset{\sim}{f}, \underset{\sim}{s}_{c_k})}{(\underset{\sim}{\bar{s}}_k, \underset{\sim}{\frac{K}{\rho}}\underset{\sim}{\bar{s}}_k) - (\underset{\sim}{s}_{c_k}, \underset{\sim}{s}_{c_k})}\right] +$$

$$\frac{1}{2}\,\frac{1}{(\underset{\sim}{s}_{c_k}, \underset{\sim}{s}_{c_k})(\omega-\omega_{c_k})} \sum_n \frac{(f, \underset{\sim}{s}_n)\,(\underset{\sim}{s}_{c_k}, \underset{\sim}{s}_n)}{\omega_n(\underset{\sim}{s}_n, \underset{\sim}{s}_n) - (\underset{\sim}{s}_n, i\underset{\sim}{\Omega} \times \underset{\sim}{s}_n)}$$

So, all together

$$\underset{\sim}{s} = \sum_n a_n \underset{\sim}{s}_n + \sum_{\text{ASM}^{\underline{s}}} \left[\bar{a}_{\text{ASM}} \left(\underset{\sim}{\bar{s}}_{\text{ASM}} + \hat{\underset{\sim}{z}} \times \underset{\sim}{r} \right) + b_{\text{ASM}} \hat{\underset{\sim}{z}} \times \underset{\sim}{r} \right] +$$

(4.49)

$$b_z \hat{\underset{\sim}{z}} + b_{x+iy} (\hat{\underset{\sim}{x}} + i\hat{\underset{\sim}{y}}) + b_{x-iy} (\hat{\underset{\sim}{x}} - i\hat{\underset{\sim}{y}})$$

where the sum over n includes all normal modes except for the $\text{ASM}^{\underline{s}}$ and translations, a_n is given by (4.41), $\underset{\sim}{\bar{s}}_{\text{ASM}}$ represents the elastic deformation associated with the secular part of the ASM, and

$$\bar{a}_{\text{ASM}} = \frac{-(\underset{\sim}{f}, \hat{\underset{\sim}{z}} \times \underset{\sim}{r})}{\omega^2 \left[(\underset{\sim}{\bar{s}}_{\text{ASM}}, i\underset{\sim}{\Omega} \times (\hat{\underset{\sim}{z}} \times \underset{\sim}{r})) + (\hat{\underset{\sim}{z}} \times \underset{\sim}{r}, \hat{\underset{\sim}{z}} \times \underset{\sim}{r}) \right]} \tag{4.50}$$

$$b_{\text{ASM}} = \frac{1}{2} \frac{1}{\omega} \frac{1}{(\hat{\underset{\sim}{z}} \times \underset{\sim}{r}, \hat{\underset{\sim}{z}} \times \underset{\sim}{r})} \sum_n \frac{(\underset{\sim}{f}, \underset{\sim}{s}_n) (\hat{\underset{\sim}{z}} \times \underset{\sim}{r}, \underset{\sim}{s}_n)}{\omega_n (\underset{\sim}{s}_n, \underset{\sim}{s}_n) - (\underset{\sim}{s}_n, i\underset{\sim}{\Omega} \times \underset{\sim}{s}_n)} \tag{4.51}$$

$$b_z = \frac{-(\underset{\sim}{f}, \hat{\underset{\sim}{z}})}{\omega^2 M} \tag{4.52}$$

$$b_{x \pm iy} = \frac{-(\underset{\sim}{f}, \hat{\underset{\sim}{x}} \pm i\hat{\underset{\sim}{y}})}{(\omega \mp \Omega)^2 \, 2M} \tag{4.53}$$

where M is the mass of the Earth

$$M = \int_{V_E} \rho \tag{4.54}$$

and the sum in (4.51) is over all normal modes except the ASM^s and translations. (To find b_z and $b_{x\pm iy}$ we have used $(\hat{z}, \underset{\sim}{s}_n) = (\hat{x}\pm i\hat{y}, \underset{\sim}{s}_n) = 0$ for any $\underset{\sim}{s}_n$ not in C.)

Equations (4.49)-(4.53) represent the complete forced displacement of the Earth for any $\underset{\sim}{f}$. The contributions from the translational modes merely reflect Newton's second law ($\underset{\sim}{F} = m\underset{\sim}{a}$) for motion of the Earth's center of mass.

In particular,

$$b_z = \frac{-F^z_{CM}}{\omega^2 M}$$

$$b_{z\pm iy} = \frac{-F^x_{CM} \mp i\, F^y_{CM}}{(\omega\mp\Omega)^2\, 2M} \tag{4.55}$$

where $\underset{\sim}{F}_{CM}$ is the total force on the Earth. Since the tidal force is defined so that $\underset{\sim}{F}_{CM} = 0$ (see Section 2.2) the translational contributions to (4.49) will not appear in the tidal solution.

The ASM contributions are associated with Euler's equation for the $\hat{z}$-component of the Earth's angular momentum

$$\frac{d}{dt} H_z = N_z \tag{4.56}$$

where $\underset{\sim}{N}$ and $\underset{\sim}{H}$ are the torque and angular momentum. A non-zero N_z (proportional to $(\underset{\sim}{f}, \hat{z} \times \underset{\sim}{r})$) will cause the Earth to spin more rapidly about the $\hat{z}$ axis, an incremental displacement proportional to $\hat{z} \times \underset{\sim}{r}$. The resulting increase in centripetal force which results produces an elastic-gravitational deformation, $\underset{\sim}{\bar{s}}_{ASM}$. For the tides on an axisymmetric Earth, $N_z = 0$ and $\bar{a}_{ASM}$ will vanish.

The other ASM contribution, represented by b_{ASM}, describes the increased spin needed to offset inertia tensor perturbations: angular momentum must be conserved. This term is not dependent on the applied torque and must be included in the tidal solution. (It will be shown to describe changes in the Earth's rotation rate.)

For the luni-solar force, then, the complete solution is

$$\underset{\sim}{s} = \sum_n a_n \underset{\sim}{s}_n + \sum_{ASM} b_{ASM} \hat{z} \times \underset{\sim}{r} \tag{4.57}$$

with a_n and b_{ASM} given by (4.41) and (4.51).

4.7 Significance of the Expansion

The resonance factor, $\frac{1}{\omega_m - \omega}$, in (4.41) implies that if the Earth is forced at a frequency near a particular normal mode eigenfrequency, that mode may be highly excited. This phenomenon will be shown responsible for perturbations both in the Love numbers near ψ_1 and in the annual and semi-annual nutations (both due to excitation of the NDFW) as well as for the observed nutational resonance at exactly one retrograde sidereal day (caused by excitation of the TOM). (Note: a retrograde diurnal frequency in our invariably rotating frame is equivalent to zero frequency in inertial space.)

Conversely, for any narrow band of perturbing frequencies far removed from theset of excited normal modes, the response is smooth. This can be used to reduce the number of calculations needed for many of the tidal groups.

However useful (4.57) is as a conceptual tool, its computational utility is often limited. Successful application of (4.57) is only possible once a sufficient number of rotating, elliptical normal modes have been computed. Since such normal mode calculations are not trivial, it is often easier to integrate the forced equations (2.2) and (2.3) directly.

The one tidal exception is the set of computations for the $\ell=2$, $m=1$ (diurnal) tides. Both the NDFW and TOM eigenfrequencies

lie within the diurnal band, and their eigenfunctions are highly excited. To recover the considerable frequency dependent structure, results must be found at many perturbing frequencies. In this case, (4.57) permits a very efficient means of computation. The efficiency is, in fact, increased by first directly integrating (2.2) and (2.3) for the response $\underset{\sim}{s}_o$ at some diurnal frequency, ω_o away from any resonance. The response, $\underset{\sim}{s}$, at any other frequency ω, is then

$$\underset{\sim}{s} = \underset{\sim}{s}_o + \frac{1}{2} \sum_n \left[\frac{(\underset{\sim}{f},\underset{\sim}{s}_n)}{\omega_n(\underset{\sim}{s}_n,\underset{\sim}{s}_n) - (\underset{\sim}{s}_n, i\underset{\approx}{\Omega}\underset{\sim}{s}_n)} \frac{\omega - \omega_o}{(\omega_n - \omega)(\omega_n - \omega_o)} \right] \underset{\sim}{s}_n \tag{4.58}$$

(The ASM is not excited by the diurnal tides on an axisymmetric Earth.) Since the free oscillation contribution to $\underset{\sim}{s}$ is nearly the same as to $\underset{\sim}{s}_o$ (a fact reflected by the correspondingly small factor $(\omega_o - \omega)/(\omega_m - \omega)$ in (4.58)) fewer modes are needed in (4.58) than in (4.57). In fact, by comparing results computed from (4.58) with directly integrated solutions, it is found that nine normal modes (six free oscillations and the three mantle nutations) are sufficient to guarantee accuracy well above one part in 300.

CHAPTER V

COMPUTATIONAL PROCEDURE

The infinitely coupled system of equations developed in Section 2.3 is truncated, here, in 5.1 and solved numerically in 5.2. Errors introduced by the truncation are investigated in 5.3 and an attempt is made to correct for them. Section 5.4 summarizes the computational procedure used for each tidal group.

5.1 Truncation

The Earth's tidal response is found either by computing normal modes and using (4.57) or (4.58) or by integrating the forced equations, (2.2)-(2.3), directly. The exact, coupled infinite set of scalar equations over radius for both cases are described in Section 2.3 and have solutions of the form (2.30). Since it is not feasible to solve infinite systems, some form of truncation is needed. In particular, (2.30) is arbitrarily restricted to a finite number of σ_{ℓ}^{s} and τ_{ℓ}^{s},

$$U = \begin{matrix}\sigma_{\ell-i} \\ \text{or} \\ \tau_{\ell-i}\end{matrix} + \ldots + \tau_{\ell-1} + \sigma_{\ell} + \tau_{\ell+1} + \ldots + \begin{matrix}\sigma_{\ell+j} \\ \text{or} \\ \tau_{\ell+j}\end{matrix} \tag{5.1}$$

This procedure results in a finite system of equations and unknowns and can be handled, at least in principle, with existing numerical techniques. Remeber that the truncated equations

represent only an approximation to the dynamical behavior of the Earth. It is not safe to accept the results of such a calculation if they cannot be substantiated by independent means.

Consider, as the important example here, the tidal case. It will be shown in Section 5.3, below, that the tidal solution in the upper mantle for an ℓ,m potential term can be expressed accurately to at least one part in 300 as

$$u = \sigma^m_{\ell-2} + \tau^m_{\ell-1} + \sigma^m_{\ell} + \tau^m_{\ell+1} + \sigma^m_{\ell+2} \tag{5.2}$$

To understand the significance of this series of spheroidal and toroidal components, consider the familiar spherical, non-rotating case. There, the tidal response simplifies to

$$u = \sigma^m_{\ell} \tag{5.3}$$

The set of displacement and gravitational potential scalars represented by (5.3) is simply:

$$U^m_{\ell}(r,\omega),\ V^m_{\ell}(r,\omega),\ (\phi^E_1)^m_{\ell}(r,\omega) \tag{5.4}$$

(see section 2.3).

The surface values of these three scalar functions are proportional to the Love numbers, h_ℓ, ℓ_ℓ and k_ℓ, respectively, and, in fact, are independent of m.

For an elliptical rotating Earth the set of pertinent scalars represented by the approximate solution (5.2), is expanded to:

$$(5.5) \qquad U^m_{\ell-2},\ V^m_{\ell-2},\ (\phi^E_1)^m_{\ell-2},\ W^m_{\ell-1},\ U^m_\ell,\ V^m_\ell,\ (\phi^E_1)^m_\ell,$$

$$W^m_{\ell+1},\ U^m_{\ell+2},\ V^m_{\ell+2},\ (\phi^E_1)^m_{\ell+2}$$

To describe this enlarged scalar set using Love number terminology, it is necessary to introduce a new group of Love numbers, each proportional to the surface value of a particular member of (5.5). Another approach is described in Chapter VI, where the physically observable quantities are related directly to the scalars in (5.5).

5.2 Solving a Truncated Problem

The approximation (5.2) represents, in general, 22 scalar unknowns with an equal number of scalar differential equations. Although a system this size is in principle directly solvable, the effort needed is extreme.

Instead, a more indirect technique has been employed which takes, as its starting point, an algorithm developed by Smith (1974, 1976, 1977). Smith was interested in the normal modes of a rotating, elastic, slightly elliptical Earth, the problem corresponding to $\underset{\sim}{f} = 0$ in equation (2.2) above. To solve the resulting infinite set of scalar equations, he took as a truncated form for his solution

$$u = \tau^m_{\ell-1} + \sigma^m_\ell + \tau^m_{\ell+1} \tag{5.6}$$

(Equation (5.6) is the same approximation used by Crossley (1975) and Shen and Mansinha (1976) to describe motion in the fluid outer core.) The resulting system is tenth order, and its numerical solution is straightforward.

Smith's normal mode algorithm need be modified only slightly to find the approximate tidal solution to (2.2) and (2.3) with the truncated form (5.6). First, $\phi_{Tot} = V_T + \phi^E_1$ is defined as the sum of the tidal and induced potentials. Since $\nabla^2 V_T = 0$, it is straightforward to show that the set of equations (2.2) and (2.3) with $\underset{\sim}{f} = -\underset{\sim}{\nabla} V_T$, is equivalent to (2.2) and (2.3) with $\underset{\sim}{f} = 0$ and ϕ^E_1 replaced by ϕ_{Tot}. The only exception is at the outer surface, where ϕ_{Tot} must satisfy different boundary conditions than ϕ^E_1. (This is a standard technique in tidal calculations.)

5.3 Truncation Errors

Use of the truncated series (5.6) naturally results in discrepancies between the computed and exact solutions. As shown below, the errors could conceivably be large in the core. However, in the mantle the relative error should be the order of the ellipticity, and a correction is computed as a first order perturbation.

Internal Waves in the Fluid Core

Smith (1977) has found serious discrepancies between his calculations of internal gravity-inertial waves in the core for simple Earth models and known analytical results. He attributes the differences to the truncation scheme used, (5.6).

A corresponding problem can be anticipated in the tidal solution. Consider the forced response, $\underset{\sim}{s}$, as a sum of excited normal modes, as in (4.57). Errors in $\underset{\sim}{s}$ due to truncation can then be related directly to corresponding errors in the normal mode results. Since the internal gravity waves cannot, at this writing, be adequately computed, their contribution to the sum in (4.57) is unknown; the solution in the core must always be assumed suspect. However, these modes probably represent motion confined almost entirely to the fluid core, and, as such, appreciably affect the mantle tidal response only when the perturbing frequency lies very close to a gravity wave eigenfrequency. Although such a coincidence

is certainly conceivable, we are obliged to omit these modes when using the eigenfunction expansion (4.57), and to look carefully for any evident excitation when integrating the equations directly. Naturally, should these core waves ever be accurately computed, they can be incorporated into the solution at a later date by including appropriate terms in (4.57).

Size of the Error in the Mantle

The tidal solution for a spherical, non-rotating Earth is exactly $u = \sigma_\ell^m$. The combined effects of ellipticity and the rotationally induced Coriolis and centripetal forces serve to couple spheroidal and toroidal components together yielding a solution of the form (2.30). Using a truncated solution form, such as (5.6), is exactly equivalent to ignoring certain coupling terms in the dynamical equations. To see this, consider first a spherical Earth with a Coriolis force. The Coriolis force couples σ_ℓ terms to $\tau_{\ell\pm1}$ terms. The order ℓ body tide for such an Earth is a solution to an equation of the form

$$\begin{bmatrix} & & \vdots & & & \vdots & \\ \cdots\ B_{\ell+2} & C_{\ell+2} & D_{\ell+2} & 0 & 0 & 0 & 0\cdots \\ 0 & B_{\ell+1} & C_{\ell+1} & D_{\ell+1} & 0 & 0 & 0 \\ 0 & 0 & B_{\ell} & C_{\ell} & D_{\ell} & 0 & 0 \\ \cdots\ 0 & 0 & 0 & B_{\ell-1} & C_{\ell-1} & D_{\ell-1} & 0\cdots \\ 0 & 0 & 0 & 0 & B_{\ell-2} & C_{\ell-2} & D_{\ell-2} \\ & & \vdots & & & \vdots & \end{bmatrix} \begin{bmatrix} \vdots \\ \sigma_{\ell+2} \\ \tau_{\ell+1} \\ \sigma_{\ell} \\ \tau_{\ell-1} \\ \sigma_{\ell-2} \\ \vdots \end{bmatrix} = \begin{bmatrix} \vdots \\ 0 \\ 0 \\ f_{\ell} \\ 0 \\ 0 \\ \vdots \end{bmatrix}$$

(5.7)

where f_{ℓ} is a term in the luni-solar tidal force with angular order ℓ, and each B_{ℓ}, C_{ℓ} and D_{ℓ} is a vector valued operator. (The $\{C_{\ell}\}$ lie on the diagonal.) The $\{B_{\ell}\}$ and $\{D_{\ell}\}$ represent coupling between spheroidal and toroidal components and are due totally to Coriolis effects.

Equation (5.7) has the form

$$M \cdot z = f \tag{5.8}$$

where z is the exact tidal solution. When we truncate the solution to (5.6) and solve (2.2) and (2.3) we are, in reality, solving

$$M' \cdot u = f \tag{5.9}$$

for the truncated solution, u, where M' is a matrix identical to M except with the coupling terms $D_{\ell+2}$ and $B_{\ell-2}$ set arbitrarily to zero.

We may always write the exact solution, z, as the sum of the truncated solution, u, plus a correction, Δu:

$$z = u + \Delta u \tag{5.10}$$

Then, Δu satisfies

$$M \cdot \Delta u = [M' - M] \cdot u \equiv F \tag{5.11}$$

where

$$F = - \begin{bmatrix} \vdots \\ 0 \\ D_{\ell+2}\ \tau_{\ell+1} \\ 0 \\ 0 \\ 0 \\ B_{\ell-2}\ \tau_{\ell-1} \\ 0 \\ \vdots \end{bmatrix} = \begin{bmatrix} \vdots \\ 0 \\ F_{\ell+2} \\ 0 \\ 0 \\ 0 \\ F_{\ell-2} \\ 0 \\ \vdots \end{bmatrix} \tag{5.12}$$

with $\tau_{\ell\pm1}$ the tidal components of u.

This process may be extended to include the corrections due to both the centripetal force and ellipticity. The latter poses some added difficulties since it couples together components through the boundary conditions, as well. However, it is always possible to transform a homogeneous volume equation with non-homogeneous

boundary conditions to a non-homogeneous volume equation with homogeneous boundary conditions. This is done by adding or subtracting to the solution any well-behaved function which satisfies the boundary conditions, athough not necessarily the volume equations. Suffice it to say that when appropriate modifications are effected, we write the total truncation correction, Δu, for elliptical, rotating Earth as the solution to (5.11) where, for the general case, F has the form:

$$F = [M' - M]u = \begin{bmatrix} \vdots \\ F_{\ell+3} \\ F_{\ell+2} \\ 0 \\ 0 \\ 0 \\ F_{\ell-2} \\ F_{\ell-3} \\ 0 \\ \vdots \end{bmatrix} \tag{5.13}$$

Here, M is the exact dynamical operator for an elliptical, rotating Earth and M' is the approximate operator used to find the truncated solution, u.

Consequently, the truncation correction, Δu, is represented as the response of the rotating elliptical Earth to a fictitious

force, F. As such, it may be expanded as a sum of eigenfunctions according to (4.57), with $f_\ell = F_c$ in (4.41).

Since (M'-M) is a known operator and u is calculable (it is the solution to the truncated problem) it is always possible to find F. In fact, for each tidal computation the components of F are observed to be everywhere smaller than the tidal forces, f_ℓ, by a factor of at least 200.

As a result, it is tempting to conclude that Δu should be smaller than the complete solution, z, by about the same factor. This assertion must be regarded carefully.

The equivalent force, F, though pointwise much smaller than f_ℓ, is also of markedly different character. In particular, F would appear to excite normal modes with large $\sigma_{\ell\pm2}$ or $\tau_{\ell\pm2}$ components, while f_ℓ mainly excites those with large σ_ℓ terms. The consequences of this observation for Δu are mixed. The seismic mode contribution to Δu poses little problem. All such modes have periods of less than one hour, far removed from any pertinent tidal band. This eliminates the possibility of resonance excitation of these modes by F. As a result, it is safe to conclude that although F may excite different seismic modes than does f_ℓ, the total contribution of these modes to Δu should still be smaller than the seismic mode contribution to z by about 1/200, the ratio of F to f_ℓ.

Other modes are more of a problem. As expected, little can be said about the internal gravity wave contribution to Δu. Suppose, for example, there was a gravity wave with eigenfrequency near the tidal frequency, and which happened to 'look' significantly more like F than like f_ℓ. Such a circumstance could conceivably overcome the small F to f_ℓ ratio, so that the gravity wave contributions to Δu might be as large or even larger than their corresponding contributions to z. However, we must again seek solace in the fact that these modes probably consist almost entirely of core motion. As a result, their contribution to Δu in the upper mantle should, in any case, be much smaller than the seismic mode contribution to z.

There are three tidal cases where F excites other modes. For the $\ell=2$ $m=0$ (long period) tides, the $F_{\ell-2(=0)}$ component of F excites the zero frequency axial spin modes. However, as will be discussed below, each ASM is excited approximately 300 times as much by the corresponding tidal force, f_ℓ, itself. So again, the ASM contribution to Δu will be much smaller than its contribution to the complete solution, z.

The $\ell=3$ $m=1$ and $\ell=3$ $m=0$ tides are slightly more of a problem. The $F_{\ell-2(=1)}$ components for these tides excite both the Slichter modes and the center of mass translations, none of which are present in the truncated solution, u. Little can be said about the Slichter mode excitation coefficients. However, neither of the

two tidal groups has a representative period near those of the Slichter modes (4-5 hours, see Smith, 1975) implying no evident resonant responses. Furthermore, these modes exhibit very little mantle motion, suggesting that their contribution to the tidal surface motion should be small indeed.

In contrast, the translations are highly excited by $F_{\ell-2}$ for these tides. The discussion of Section 2.2 shows that the $\ell=3$ $m=1$ and $\ell=3$ $m=0$ components of f_ℓ impart a net linear momentum to an elliptical Earth. Due to the restrictive truncation, (5.6), for u, the resulting large translational motion is absorbed entirely by Δu. However, as shown in 2.2, this net center of mass motion should be exactly balanced by the Earth's response to additional $\ell=1$ terms in the tidal potential, (2.23). Computationally, these extra terms may be added directly to F when solving for Δu. The result is that almost all of the translational motion disappears from Δu. The small amount remaining comes simply from the fact that the truncated solution, u, does not quite conserve momentum. Consequently, a weakly excited translational mode must be present in Δu to preserve a stationary center of mass. The net contribution from this mode to Δu will be, however, about 300 times smaller than the seismic mode contribution to z.

Method of Computing Δu

Let z be the complete tidal solution, u the truncated solution, and $\Delta u = z-u$ the correction to u. It was shown above that the magnitude of u should be about 200 times smaller than that of z throughout the upper mantle. This suggests the following first order method of finding Δu.

Consider equation (5.11) for the truncation correction Δu. This equation represents the response of a rotating, elliptical Earth to the fictitious force, F. Like the original tidal problem, (5.11) is not solvable exactly. As before, a trunction scheme is needed. Since Δu is so small we do not require great relative accuracy in its determination. In fact, the scheme we adopt is to approximate u as the response of a non-rotating, spherical Earth to the force, F. Write the total dynamical operator of (5.11) as:

$$M = M_o + \delta M \tag{5.14}$$

where M_o is the operator for a non-rotating, spherical Earth, and δM represents the corrections due to rotation and ellipticity. We then solve for an approximation to Δu from

$$M_o \overline{\Delta u} = F \tag{5.15}$$

The solution, $\overline{\Delta u}$, should adequately represent Δu with the following two exceptions:

1) Since rotation is vitally important to the core response and is not included in M_o, $\overline{\Delta u}$ will undoubtedly suffer in the core. This problem is presumably of little importance for the upper mantle response, as discussed above.

2) The axial spin mode is excited by $F_{\ell-2}$ for the $\ell=2$ $m=0$ tides and so must be present in Δu. However, its contribution will not show up on $\overline{\Delta u}$ due to the absence of rotational terms in M_o. This mode must be put into $\overline{\Delta u}$ separately, as discussed in Section 5.4

One other condition is imposed on $\overline{\Delta u}$: only the spheroidal terms are included. This is equivalent to ignoring $F_{\ell\pm3}$ in (5.13). These components are the result of elliptical terms in M-M' acting on the $\tau_{\ell\pm1}$ parts of u. They are significant only in the core (they are observed to be $\sim 1 \times 10^6$ times smaller than the corresponding f_ℓ terms in the mantle). As a result, one would expect minimal accompanying excitation of seismic or other mantle modes. In any case, the strong dependent of $F_{\ell\pm3}$ on the poorly computed internal gravity wave contribution to u, would make inclusion of $F_{\ell\pm3}$ of questionable value.

The numerical technique used in solving (5.15) is not much different from the standard free oscillation technique described in Section 5.2. The first step is to compute a particular solution, satisfying all non-homogeneous volume and internal boundary equations. This solution will not, in general, satisfy the free surface boundary conditions. Next, a complete set of regular, independent homogeneous solutions are found. These are added to the particular solution in such a way that the free surface conditions are satisfied.

5.4 Computations for Each Tidal Group

This section offers a brief description of the calculation process for each tidal group. Throughout, z will represent the exact tidal solution, u the truncated solution with the form (5.6), $\Delta u = z - u$ the truncation correction to u, and $\overline{\Delta u}$ the approximation to Δu found from (5.15). The final adopted approximation to the tidal response will then be $u + \overline{\Delta u}$. From the discussion above, we may conclude that the upper mantle values of $u + \overline{\Delta u}$ should agree with the corresponding values of z to at least 1 part in 300. Any (unlikely) larger deviations can be assumed to arise from the contribution of the imperfectly known internal gravity waves to z, through (4.57). As has been mentioned, should these modes ever be adequately calculated, the corresponding tidal contributions can easily be computed.

1) $\ell=2$ $m=1$ tides

These are the principal diurnal tides. The calculated response consists of

$$u + \overline{\Delta u} = \tau^{m=1}_{\ell=1} + \sigma^1_2 + \sigma^1_3 + \sigma^1_4 \tag{5.16}$$

The spheroidal σ^1_2 component represents the primary tidal response. The τ^1_1 component describes the corresponding forced nutations of the Earth. The other two components represent additional tidal deformation and are found to be at least 100 times smaller than σ^1_2 throughout the upper mantle.

There is considerable frequency structure in this tidal group. Both the NDFW and the TOM have eigenfrequencies within the diurnal tidal band and are higly excited by certain tidal lines. As a result, it is important to compute the response for many tidal frequencies. The first step in finding $u + \overline{\Delta u}$ is to find the truncated solution

$$u = \tau^1_1 + \sigma^1_2 + \tau^1_3 \tag{5.17}$$

For this, the eigenfunction expansion technique is used as follows: a base tide, 0_1, is computed using standard integration methods. In addition, nine truncated eigenfunctions are found:

6 seismic modes and 3 nutations (NDFW, TOM, CW). These are added to the 0_1 tide according to (4.58), to find the truncated response at any other frequency. In this manner, results are computed for a complete set of frequencies at a relatively inexpensive cost.

Once u is found, $\overline{\Delta u}$ is calculated from (5.15) without undue difficulty. $\overline{\Delta u}$ has the form:

(5.18) $$\overline{\Delta u} = \sigma_4^1$$

2) $\underline{\ell=2\ m=2\ \text{tides}}$

These are the principal semi-diurnal tides. The approximate response is taken to be:

(5.19) $$u + \overline{\Delta u} = \sigma_{\ell=2}^{m=2} + \tau_3^2 + \sigma_4^2$$

The primary component in (5.19) is σ_2^2. The other two components are reduced throughout the upper mantle by a factor of about 200.

There should be little significant frequency structure in $u + \overline{\Delta u}$. For this reason, calculations are done only for a small set of important tidal lines. The slight frequency structure then permits extrapolation to any other semi-diurnal frequency.

The truncated solution, u, consisting of

$$u = \sigma_2^2 + \tau_3^2 \tag{5.20}$$

is first calculated using the standard integration approach.

The correction

$$\Delta u = \sigma_4^2 \tag{5.21}$$

is found with little difficulty.

3) ℓ=2 m=0 tides

These are the principal long period tides. The calculated response is

$$u + \overline{\Delta u} = \sigma_{\ell=0}^{m=0} + \tau_1^0 + \sigma_2^0 + \tau_3^0 + \sigma_4^0 \tag{5.22}$$

The primary tidal response is σ_2^0. In addition, the τ_1^0 component represents an incremental rotation about the $\hat{z}$ axis and is responsible for long period changes in the Earth's rotation rate. The other three components are less than a percent of σ_2^0 through the upper mantle.

The only significant frequency dependence in (5.22) is found in the τ_1^0 component. It comes from near resonance excitation of the zero frequency axial spin modes. What is happening, as discussed in Chapter IV, is that the important tidal response, σ_2^0, serves to change the greatest moment of inertia, which by itself would alter the angular momentum. Since the tidal force cannot exert a torque about the spin axis on an axisymemtric Earth, the induced angular momentum change must be balanced by a corresponding change in the spin rate. The result is a large linear (in r) τ_1^0 component. Since the angular momentum from such a term is proportional to $\omega\tau_1^0$, with ω the tidal frequency, we would expect τ_1^0 to vary with frequency as $1/\omega$. This behavior can also be anticipated directly from the eigenfunction expansion expression (4.57).

The consequences are that although there is frequency dependence in (5.22), it is evidently predictable from just a few tides. As a result, calculations are done for only a few frequencies, and the results extended throughout the tidal band.

The truncated solution

$$u = \tau_1^0 + \sigma_2^0 + \tau_3^0 \tag{5.23}$$

is first found by direct integration. The correction:

$$\Delta u = \sigma_0^0 + \sigma_4^0 \tag{5.24}$$

may then be computed from (5.15). However, as described above, the real correction, u, should include a contribution from the axial spin mode, as well (i.e. a τ_1^0 component). What happens is that, like the σ_2^0 component, σ_0^0 affects the greatest moment of inertia. As a result, the axial spin mode must be additionally excited to offset the induced angular momentum. This second excitation will be about 300 times smaller than the primary ASM terms, since σ_0^0 is approximately 300 times smaller than σ_2^0. The extra contribution may be computed, once $\overline{\Delta u}$ is found from (5.15), by calculating the change in the angular momentum due to σ_0^0 and then absorbing this angular momentum into an excited ASM.

ℓ=3 m=3 and ℓ=3 m=2 tides

These are ter-diurnal and semi-diurnal tides, respectively. As for all ℓ=3 tides, the amplitudes here are smaller than the ℓ=2 amplitudes by at least a factor of 60. The assumed response is

$$u + \overline{\Delta u} = \sigma_{\ell=3}^{m=3} + \tau_4^3 + \tau_5^3 \qquad \text{for } m = 3 \tag{5.25}$$

$$u + \overline{\Delta u} = \tau_{\ell=2}^{m=2} + \sigma_3^2 + \sigma_4^2 + \sigma_5^2 \qquad \text{for } m=2 \tag{5.26}$$

The principal tidal response for both (5.25) and (5.26) is σ_3^m. The other components are reduced in size near the surface by about a factor of 100 or more.

Little significant frequency dependence is expected over these tidal bands. As a result, only three of the larger tides have been computed for each group, with the result assumed to be extendable, as usual. In both cases, standard integration is used to find the truncated solutions.

$$u = \sigma_3^3 + \tau_4^3 \qquad m=3 \tag{5.27}$$

$$u = \tau_2^2 + \sigma_3^2 + \tau_4^2 \qquad m=2 \tag{5.28}$$

The corrections

$$\overline{\Delta u} = \sigma_5^m \tag{5.29}$$

are easily computed, though of little importance.

ℓ=3 m=1 and ℓ=3 m=0 tides

These are diurnal and long period tides, respectively. As discussed in Section 2.2 both the ℓ=3 and the ℓ=3 m=0 potential terms exert a net force on the elliptical Earth. However, as shown in Section 2.2, the true tidal potential must include additional $Y_{\ell=1}^{m=1}$ and Y_1^0 terms, the sole effect of which will be to offset this center of mass motion. These latter terms may, in principle, be tacitly included when computing $\overline{\Delta u}$ by first solving (5.15) and then

subtracting off all net translational motion. However, since $\overline{\Delta u}$ is so unimportant for the $\ell=3$ tides we have not computed it here.

Instead, only the truncated solution, u, is found

$$u = \tau_2^m + \sigma_3^m + \tau_4^m \qquad m=0 \text{ or } 1 \tag{5.30}$$

As might be expected, u shows no anomalous frequency structure.

CHAPTER VI

RELATIONSHIPS BETWEEN TIDAL DISPLACEMENTS AND OBSERVATIONS

The tidal solution, described in Chapter V, consists of a scalar gravitational potential field, ϕ_1^E, a vector displacement field, $\underset{\sim}{s}$, and a second rank tensor stress field, $\underset{\sim}{T}$. Physical observations of these quantities are restricted to the outer surface of the Earth. In this Chapter we will develop the relations between the surface tidal solution and a variety of physical observables. The particular quantities modelled are: tilt, strain and gravity signals; variations in astronomical latitude and longitude of the instantaneous gravity normal (local vertical); perturbations in the free space gravitational potential due to the Earth's deformation; and inertial space vector displacements of the Earth's surface.

6.1) Gravity

Consider a fixed point, P, on the Earth's surface with undeformed (Lagrangian) position vector, $\underset{\sim}{x}$. The deformed (Eulerian) position of P at time t in the invariably rotating coordinate system, R is:

$$\underset{\sim}{r}(\underset{\sim}{x},t) = \underset{\sim}{x} + \underset{\sim}{s}(\underset{\sim}{x},t) \tag{6.1}$$

where $\underset{\sim}{s}(\underset{\sim}{x},t)$ is the incremental Lagrangian particle displacement described in Chapter II. The gravitational acceleration at P is the Eulerian acceleration at $\underset{\sim}{r}$:

$$\underset{\sim}{g}_E(\underset{\sim}{r}) = \underset{\sim}{g}_E(\underset{\sim}{x} + \underset{\sim}{s}) = \underset{\sim}{g}_E(\underset{\sim}{x}) + \underset{\sim}{s}\cdot\nabla\underset{\sim}{g}_E(\underset{\sim}{x}) \tag{6.2}$$

Expressing $\underset{\sim}{g}_E$ as the sum of the undeformed acceleration, $\underset{\sim}{g}_o$, and the negative gradient of the incremental Eulerian potential energy, ϕ_1^E, gives

$$\underset{\sim}{g}_E(\underset{\sim}{r}) = \underset{\sim}{g}_o(\underset{\sim}{x}) - \nabla\phi_1^E + \underset{\sim}{s}\cdot\nabla\underset{\sim}{g}_o \tag{6.3}$$

Suppose a test mass is dropped from P at time t_o. The position of the mass at a later time t may be represented as

$$\text{position} = \underset{\sim}{r}(t,\underset{\sim}{x}) + \underset{\sim}{d}(t,\underset{\sim}{x}) \tag{6.4}$$

where $\underset{\sim}{d}(t,\underset{\sim}{x})$ is the separation vector between P and the falling mass. The equation of motion for the mass is

$$\partial_t^2(\underset{\sim}{r}+\underset{\sim}{d}) + 2\underset{\sim}{\Omega} \times \partial_t(\underset{\sim}{r}+\underset{\sim}{d}) + \underset{\sim}{\Omega} \times (\underset{\sim}{\Omega}\times(\underset{\sim}{r}+\underset{\sim}{d})) \tag{6.5}$$

$$= \underset{\sim}{g}_o - \nabla\phi_1^E + \underset{\sim}{s}\cdot\nabla\underset{\sim}{g}_o$$

Or, since $\underset{\sim}{r} = \underset{\sim}{x} + \underset{\sim}{s}$:

$$\partial_t^2 \underset{\sim}{d} + 2\underset{\sim}{\Omega} \times \partial_t \underset{\sim}{d} + \underset{\sim}{\Omega} \times (\underset{\sim}{\Omega} \times \underset{\sim}{d}) = \underset{\sim}{g}_o - \underset{\sim}{\Omega} \times (\underset{\sim}{\Omega} \times \underset{\sim}{x}) + \delta \underset{\sim}{g} \tag{6.6}$$

where

$$\delta \underset{\sim}{g} = -\nabla \phi_1^E + \underset{\sim}{s} \cdot \nabla \underset{\sim}{g}_o - \partial_t^2 \underset{\sim}{s} - 2\underset{\sim}{\Omega} \times \partial_t \underset{\sim}{s} - \underset{\sim}{\Omega} \times (\underset{\sim}{\Omega} \times \underset{\sim}{s}) \tag{6.7}$$

is the tidal perturbation in the effective gravitational acceleration. $\delta \underset{\sim}{g}$ is thus affected by changes in the Lagrangian gravitational acceleration $(-\nabla \phi_1^E + \underset{\sim}{s} \cdot \nabla \underset{\sim}{g}_o)$ as well as by tidally induced inertial, Coriolis, and centripetal forces acting at the reference point, P.

The vector $\underset{\sim}{g}_o - \underset{\sim}{\Omega} x (\underset{\sim}{\Omega} x \underset{\sim}{x})$ is the apparent gravitational acceleration on an unperturbed Earth and may be written as $-A_o \hat{\underset{\sim}{n}}_o$ where $\hat{\underset{\sim}{n}}_o$ is the outward unit vector antiparallel to the acceleration, and A_o is the acceleration magnitude. We may analogously express the total perturbed acceleration as

$$\underset{\sim}{g}_o - \underset{\sim}{\Omega} \times (\underset{\sim}{\Omega} \times \underset{\sim}{x}) + \delta \underset{\sim}{g} = -A_g \hat{\underset{\sim}{n}}_g \tag{6.8}$$

where

$$A_g = A_o - \hat{\underset{\sim}{n}}_o \cdot \delta \underset{\sim}{g} \tag{6.9}$$

is the magnitude of acceleration and

$$(6.10) \qquad \hat{\underset{\sim}{n}}_g = \hat{\underset{\sim}{n}}_o - [\hat{\underset{\sim}{1}} - \hat{\underset{\sim}{n}}_o \hat{\underset{\sim}{n}}_o] \cdot \frac{\delta \underset{\sim}{g}}{A_o} = \hat{\underset{\sim}{n}}_o + \delta \underset{\sim}{n}_g$$

is (opposite to) its direction (1 is the 2nd rank identity tensor). Note that $\hat{\underset{\sim}{n}}_o$ and $\hat{\underset{\sim}{n}}_g$ will point towards the Earth's exterior and both have unit magnitude.

The simple picture of a test mass falling from an Earth fixed reference point may be applied to model many instruments. The most effective vertical gravimeters are conceptually just a falling mass with some additional non-gravitational force, $\underset{\sim}{f}$, applied to keep the mass continuously at the reference point. In this case $\underset{\sim}{d}(\underset{\sim}{x},t) = 0$ and the observed magnitude of $\underset{\sim}{f}$ will be (from (6.6)):

$$(6.11) \qquad |\underset{\sim}{f}| = |\underset{\sim}{g}_o - \underset{\sim}{\Omega} \times (\underset{\sim}{\Omega} \times \underset{\sim}{x}) + \delta \underset{\sim}{g}| = A_g$$

Consequently, the tidal perturbation in $|\underset{\sim}{f}|$ (and the instrument reading) is

$$(6.12) \qquad \delta f = - \hat{\underset{\sim}{n}}_o \cdot \delta \underset{\sim}{g}$$

with $\delta \underset{\sim}{g}$ given by (6.7).

This general dynamical relation between the gravimeter output and the tidal deformation may be compared to the simpler spherically symmetric, non-rotating expressions where $\hat{\underset{\sim}{n}}_o = \hat{\underset{\sim}{r}}$, $\underset{\sim}{\Omega} = 0$ and $\underset{\sim}{g}_o = -A_o \hat{\underset{\sim}{r}}$. In the spherical case, dropping the small $\partial_t^2 S$ term in $\underset{\sim}{\delta g}$ as is customary, gives:

$$\delta f = \partial_r \phi_1^E + \underset{\sim}{s} \cdot \hat{\underset{\sim}{r}}\, \partial_r A_o \qquad \text{(spherical case)} \tag{6.13}$$

which is proportional to the familiar combination of spherical Love numbers, $1 - \frac{3}{2} k + h$. The complete expression for δf (eq. 6.12) on a rotating, elliptical Earth is consequently modified for inertial, Coriolis and centrifugal effects acting on the reference point, P, for elliptical perturbations in the unperturbed gravitational acceleration, $\underset{\sim}{g}_o$, and for elliptical and centrifugal effects on the total unperturbed acceleration normal, $\hat{\underset{\sim}{n}}_o$. After some algebra, $-\hat{\underset{\sim}{n}}_o \cdot \underset{\sim}{\delta g}$ can be represented in terms of the computed solution scalars described in Chapter II. Numerical results are given in Chapter IX.

6.2) Tilt

Any point, $\underset{\sim}{x}$, on the outer geometric surface of the undeformed elliptical Earth will satisfy

$$T_o(\underset{\sim}{x}) = r - \frac{2}{3}\,\varepsilon(r) r\, D^2_{oo}(\theta,\phi) - r_o = 0 \tag{6.14}$$

where r_o is the mean radius of the surface, D^2_{oo} is a generalized spherical harmonic described in Appendix A, $\varepsilon(r)$ is the ellipticity of the surface, and the Lagrangian point, $\underset{\sim}{x}$, is described by the spherical coordinates (r,θ,ϕ). (T_o, defined by (6.14), is simply a utility function).

The local unit vector geometrically perpendicular to this surface is

$$\hat{\underset{\sim}{n}}_o = \underset{\sim}{\nabla} T_o / |\underset{\sim}{\nabla} T_o| \tag{6.15}$$

Because of the assumed hydrostatic equilibrium of the unperturbed Earth, this definition of $\hat{\underset{\sim}{n}}_o$ as the geometrical normal to the surface must coincide with the unperturbed gravitational normal, $\hat{\underset{\sim}{n}}_o$, defined in section 6.1.

When the Earth is deformed each Lagrangian point, $\underset{\sim}{x}$, is displaced to $\underset{\sim}{r} = \underset{\sim}{x} + \underset{\sim}{s}$. Since the surface particles of the

deformed Earth are the same as those of the undeformed Earth, we see that the Eulerian surface satisfies:

$$T_o(\underset{\sim}{r}-\underset{\sim}{s}) = T_o(\underset{\sim}{r}) - \underset{\sim}{s}\cdot\nabla T_o = 0 \tag{6.16}$$

Consequently, the geometrical normal to the deformed surface is

$$\hat{\underset{\sim}{n}}_s(\underset{\sim}{r}) = \nabla[T_o(\underset{\sim}{r}) - \underset{\sim}{s}\cdot\nabla T_o]/|\nabla[T_o(\underset{\sim}{r}) - \underset{\sim}{s}\cdot\nabla T_o]| \tag{6.17}$$

By writing $\underset{\sim}{r} = \underset{\sim}{x} + \underset{\sim}{s}$ we may express $\hat{\underset{\sim}{n}}_s$ in Lagrangian coordinates as

$$\hat{\underset{\sim}{n}}_s(\underset{\sim}{x}) = \hat{\underset{\sim}{n}}_o(\underset{\sim}{x}) - [1 - \hat{\underset{\sim}{n}}_o\hat{\underset{\sim}{n}}_o]\cdot\left[\frac{\nabla[\underset{\sim}{s}\cdot\nabla T_o]}{|\nabla T_o|} - \underset{\sim}{s}\cdot\nabla\hat{\underset{\sim}{n}}_o\right] \tag{6.18}$$

A tiltmeter measures horizontal components of the incremental spherical angle, $\underset{\sim}{\Delta}$, between the instantaneous geometrical normal, $\hat{\underset{\sim}{n}}_s$, and the instantaneous outward gravity normal $\hat{\underset{\sim}{n}}_g$ as given by (6.10).

$$\underset{\sim}{\Delta} = \hat{\underset{\sim}{n}}_s - \hat{\underset{\sim}{n}}_g = (1 - \hat{\underset{\sim}{n}}_o\hat{\underset{\sim}{n}}_o)\cdot[\delta\underset{\sim}{g}/A_o - \nabla(\underset{\sim}{s}\cdot\nabla T_o)/|\nabla T_o| + \underset{\sim}{s}\cdot\nabla\underset{\sim}{n}_o] \tag{6.19}$$

The tilt in the East (or ϕ) direction is

$$\Delta_E = \hat{\underset{\sim}{e}}_\phi \cdot \underset{\sim}{\Delta} \tag{6.20}$$

and that in the (approximately) north direction is

$$\Delta_N = (\hat{\underset{\sim}{e}}_\phi \times \hat{\underset{\sim}{n}}_o) \cdot \underset{\sim}{\Delta} \tag{6.21}$$

(Note that for an elliptical Earth the horizontal vector $\hat{\underset{\sim}{e}}_\phi \times \hat{\underset{\sim}{n}}_o$ is not quite equal to $\hat{\underset{\sim}{e}}_\theta$). For the spherically symmetric case, (6.19) reduces to

$$\underset{\sim}{\Delta} = [1 - \hat{\underset{\sim}{r}}\hat{\underset{\sim}{r}}] \cdot \left[-\underset{\sim}{\nabla} (\underset{\sim}{s} \cdot \hat{\underset{\sim}{r}}) - \frac{1}{A_o} \underset{\sim}{\nabla} \phi_1^E \right] \qquad \text{(spherical case)} \tag{6.22}$$

which is proportional to the spherical Love number combination: $1 + k - h$. Complete scalar representations for Δ_E and Δ_N on a rotating, elliptical Earth are given in Chapter IX.

6.3) Strain

Consider two closely spaced Lagrangian points, $\underset{\sim}{x}_1$ and $\underset{\sim}{x}_2$, on the Earth's surface. These points are tidally displaced to $\underset{\sim}{x}_1 + \underset{\sim}{s}(\underset{\sim}{x}_1, t)$ and $\underset{\sim}{x}_2 + \underset{\sim}{s}(\underset{\sim}{x}_2, t)$, respectively, with a separation of

$$L = |\underset{\sim}{x}_1 + \underset{\sim}{s}(\underset{\sim}{x}_1,t) - \underset{\sim}{x}_2 - \underset{\sim}{s}(\underset{\sim}{x}_2,t)| \tag{6.23}$$

Since

$$\underset{\sim}{s}(\underset{\sim}{x}_2,t) = \underset{\sim}{s}(\underset{\sim}{x}_1,t) + (\underset{\sim}{x}_2 - \underset{\sim}{x}_1)\cdot\nabla\underset{\sim}{s} \tag{6.24}$$

and defining the unperturbed baseline length as

$$L_o = |\underset{\sim}{x}_1 - \underset{\sim}{x}_2| \tag{6.25}$$

with direction

$$\hat{\underset{\sim}{\ell}}_o = \frac{\underset{\sim}{x}_1 - \underset{\sim}{x}_2}{L_o} \tag{6.26}$$

we find the strain:

$$L/L_o = 1 + \hat{\underset{\sim}{\ell}}_o \cdot \nabla\underset{\sim}{s} \cdot \hat{\underset{\sim}{\ell}}_o \tag{6.27}$$

Observed tidal variations in strain are represented by

$$\delta(L/L_o) = \hat{\underset{\sim}{\ell}}_o \cdot \nabla\underset{\sim}{s} \cdot \hat{\underset{\sim}{\ell}}_o \tag{6.28}$$

$\delta(L/L_o)$ is dependent on the choice of baseline orientation, $\hat{\ell}_o$, which is assumed tangent to the surface of the unperturbed Earth (or normal to $\hat{n}_o$). $\hat{\ell}_o$ may be expressed as

$$\hat{\ell}_o = \sin\theta_s \hat{e}_\phi - \cos\theta_s (\hat{e}_\phi \times \hat{n}_o) \tag{6.29}$$

where θ_s is the orientation angle of $\hat{\ell}_o$ measured clockwise from North. $(\hat{e}_\phi \times \hat{n}_o$ is tangent to the surface of the Earth but on an elliptical Earth is not quite equal to $\hat{e}_\theta$).

Using (6.29) and (6.28) gives

$$\delta\left(\frac{L}{L_o}\right) = \varepsilon_{NS}\cos^2\theta_s - \varepsilon_{NE}\cos\theta_s \sin\theta_s + \varepsilon_{EW}\sin^2\theta_s \tag{6.30}$$

where ε_{NS}, ε_{NE} and ε_{EW} are the three tangential components of strain and are independent of θ_s.

$$\varepsilon_{NS} = (\hat{e}_\phi \times \hat{n}_o)\cdot\nabla s\cdot(\hat{e}_\phi \times \hat{n}_o) \tag{6.31}$$

$$\varepsilon_{NE} = \hat{e}_\phi\cdot\nabla s\cdot(\hat{e}_\phi \times \hat{n}_o) + (\hat{e}_\phi \times \hat{n}_o)\cdot\nabla s\cdot\hat{e}_\phi \tag{6.32}$$

$$\varepsilon_{EW} = \hat{e}_\phi\cdot\nabla s\cdot\hat{e}_\phi \tag{6.33}$$

Scalar representations for ε_{NS}, ε_{NE} and ε_{EW} are given in Chapter IX.

6.4) Astronomical Co-Latitude and Longitude

Classical astronomical position measurements reflect changes in the inertial space orientation of $\hat{n}_g$, the outward instantaneous gravity normal as given by equation (6.10). At any surface point, P, the direction of $\hat{n}_g$ in the uniformly rotating frame, R, uniquely defines two angles, θ and λ, at P, by:

$$\cos\theta = \hat{n}_g \cdot \hat{z} \tag{6.34}$$

$$\sin\theta\cos\lambda = \hat{n}_g \cdot \hat{x} \tag{6.35}$$

where $\hat{x}$ and $\hat{z}$ are unit vectors with $\hat{z}$ in the direction of Ω and $\hat{x}$ along the equilibrium Greenwich meridian (see figures 3a and 3b). It is convenient to think of θ and λ as the instantaneous astronomical co-latitude and (eastward) longitude at P. By writing

$$\theta = \theta_o + \delta\theta \tag{6.36}$$

$$\lambda = \lambda_o + \delta\lambda \tag{6.37}$$

where the unperturbed angles θ_o and λ_o are defined by (6.34) and (6.35) with $\hat{n}_g$ replaced by $\hat{n}_o$, we find

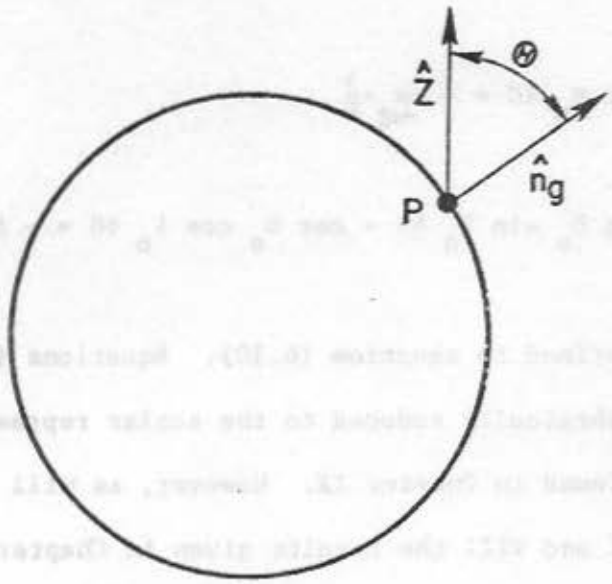

FIGURE 3a

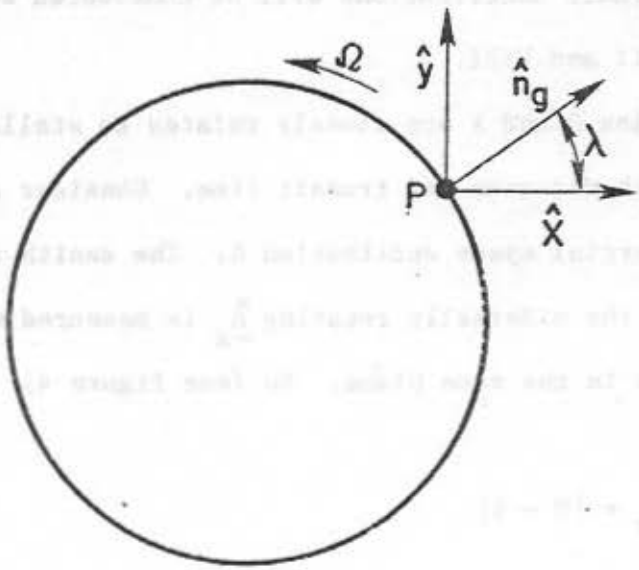

FIGURE 3b

Figure 3. The astronomical co-latitude, Θ, and longitude, λ, at the surface point, P. $\hat{n}_g$ is the instantaneous gravity normal. Figures 3a and 3b are, respectively, perpendicular to and coincident with the Earth's equator.

$$\sin \theta_o \, \delta\theta = - \delta \underset{\sim}{n}_g \cdot \hat{z} \tag{6.38}$$

$$\sin \theta_o \sin \lambda_o \, \delta\lambda - \cos \theta_o \cos \lambda_o \, \delta\theta = - \delta \underset{\sim}{n}_g \cdot \hat{x} \tag{6.39}$$

where $\delta \underset{\sim}{n}_g$ is defined in equation (6.10). Equations (6.38) and (6.39) are algebraically reduced to the scalar representation for $\delta\lambda$ and $\delta\theta$ found in Chapter IX. However, as will be described in Chapters VII and VIII the results given in Chapter IX do not include the effects of the diurnal $\tau^{m=1}_{\ell=1}$ or long period $\tau^{m=0}_{\ell=1}$ tidal components. Their contributions will be considered separately in Chapters VII and VIII.

The angles θ and λ are closely related to stellar observations of zenith distance and transit time. Consider a star, S, with known inertial space declination δ. The zenith angle, θ_z, between S and the sidereally rotating $\hat{\underset{\sim}{n}}_g$ is measured when S, $\underset{\sim}{\Omega}$ and $\hat{\underset{\sim}{n}}_g$ all lie in the same plane. So (see figure 4)

$$\theta_z = |\theta - \delta| \tag{6.40}$$

Let t_o be the atomic time at which S, $\underset{\sim}{\Omega}$ and $\hat{\underset{\sim}{n}}_g$ are coplanar; i.e. t_o is the observed time of transit of S. Let t_c be the time at which $\underset{\sim}{S}$, $\underset{\sim}{\Omega}$ and the unperturbed normal $\hat{\underset{\sim}{n}}_o$ are coplanar; t_c is

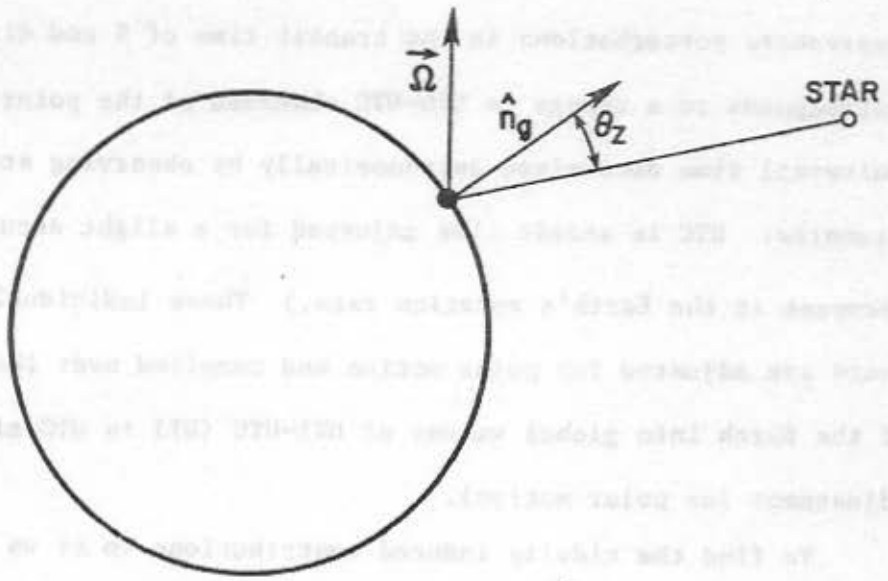

FIGURE 4. θ_z is the observed zenith angle of the star at transit. The plane of the figure is perpendicular to the equator.

the predicted time of transit of S on an unperturbed, sidereally rotating Earth. Then

$$\Delta t = t_o - t_c \tag{6.41}$$

represents perturbations in the transit time of S and directly corresponds to a change in UT0-UTC observed at the point, P. (UT0 is universal time determined astronomically by observing stellar transits. UTC is atomic time adjusted for a slight secular decrease in the Earth's rotation rate.) These individual measurements are adjusted for polar motion and compiled over the surface of the Earth into global values of UT1-UTC (UT1 is UT0 after adjustment for polar motion).

To find the tidally induced contributions to Δt we note that at time t_c the equatorial projection of the rotating normal, $\hat{\underset{\sim}{n}}_g$, is advanced relative to $\underset{\sim}{S}$ by the angle $\delta\lambda(t=t_c)$ (see figure 5). Consequently, the additional time needed for these two vectors to line up is

$$\Delta t = -\frac{1}{\Omega}\,\delta\lambda(t=t_c) \tag{6.42}$$

For an individual tidal harmonic where

$$\delta\lambda(t) = \delta\lambda e^{i(\omega t+\alpha)} \tag{6.43}$$

equation (6.42) becomes

$$\Delta t = -\frac{1}{\Omega}\,\delta\lambda e^{i(\omega t_c+\alpha)} \tag{6.44}$$

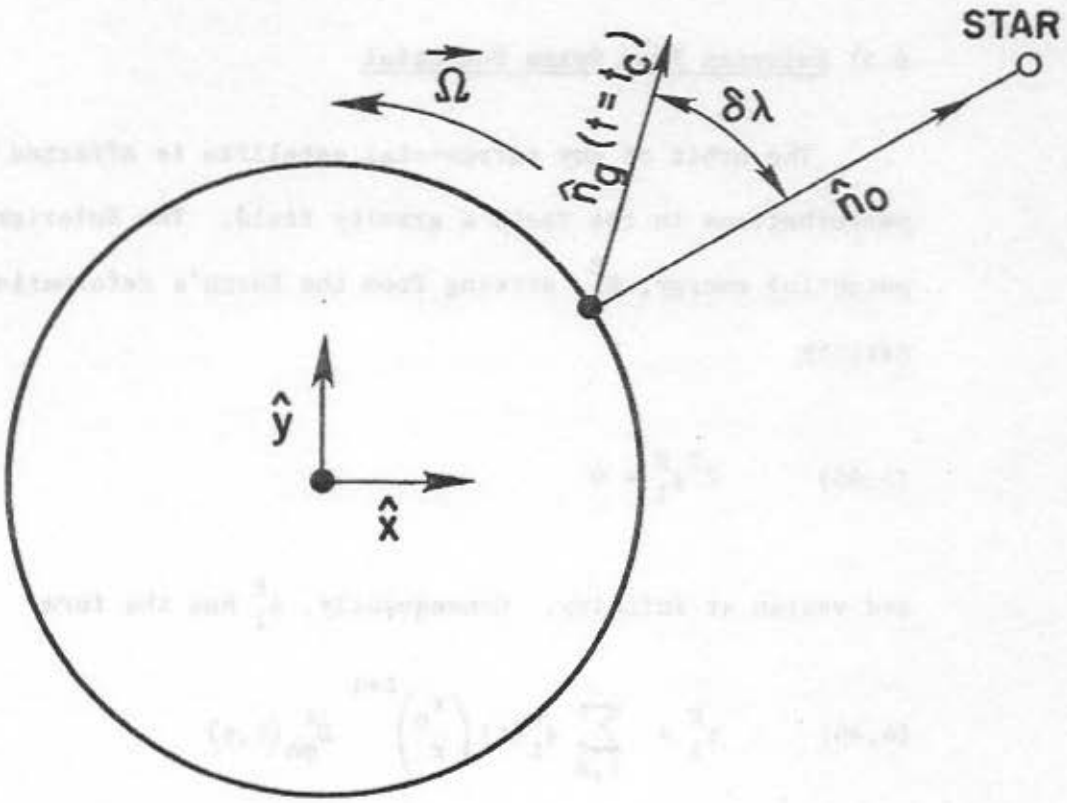

Figure 5. A variation in longitude, $\delta\lambda$, affects astronomical time. The time needed for $\hat{n}_g$ to line up with the star is $-\delta\lambda/\Omega$. The plane of the figure coincides with the equator.

6.5) Eulerian Free Space Potential

The orbit of any terrestrial satellite is affected by tidal perturbations in the Earth's gravity field. The Eulerian free space potential energy, ϕ_1^E, arising from the Earth's deformation must satisfy

$$\nabla^2 \phi_1^E = 0 \tag{6.45}$$

and vanish at infinity. Consequently, ϕ_1^E has the form

$$\phi_1^E = \sum_{\ell,m} \phi_\ell^m(t) \left(\frac{r_o}{r}\right)^{\ell+1} D_{mo}^{\ell}(\theta,\phi) \tag{6.46}$$

where r_o is the mean radius of the Earth, the D_{mo}^{ℓ} are generalized spherical harmonics discussed in Appendix A, and the $\phi_\ell^m(t)$, which completely characterize the deformation, are independent of position. The ϕ_ℓ^m are found for any tidal line by demanding continuity of ϕ_1^E across the outer surface. Scalar expressions are given in Chapter IX. For a spherical, non-rotating Earth perturbed by a luni-solar tidal potential component with angular orders ℓ_o and m_o, $\phi_{\ell_o}^{m_o}$ would be proportional to the spherical Love number k, and all other $\phi_\ell^m = 0$.

6.6) Surface Displacement

Absolute geocentric distance and position measurements of any object in space are affected by tidal displacements of the observing station. This motion is directly represented by the Lagrangian displacement, $\underset{\sim}{s}$. In Chapter IX, expressions for the scalar components of $\underset{\sim}{s}$ at the Lagrangian point described by (r,θ,ϕ) are given. These may be incorporated into experimental models, as needed.

CHAPTER VII

FORCED NUTATIONS

An understanding of the Earth's nutational behavior is valuable both for its own sake as an important physical phenomenon and for the potential constraints its observation can place on structural models of the Earth. Traditional conceptions of nutation (e.g. Woolard, 1953; Kinoshita, 1977) rely on rheologically rigid Earth models, for which the instantaneous response to an $\ell = 2$ diurnal tidal potential can be completely described by incremental rotation about a moving vector in the equatorial plane; i.e., the Earth 'nutates' about the celestial pole (the normal to the equatorial plane). Any such incremental rotation will perturb the inertial space orientation of the Earth's instantaneous rotation axis, instantaneous angular momentum axis and instantaneous axis of figure (all defined below). It is usual to identify the Earth's nutational motion with these changes in axis orientation, although this has led to some confusion concerning the axis to use (a problem considerably compounded when non-rigidity is later included). This difficulty was addressed by Atkinson (1975) who showed that for a rigid Earth the incremental rotation, itself, directly corresponds to perturbations of the figure axis. Relationships between the

three axes may be understood using either the geometrical Poinsot representation (see, e.g. Woolard, 1953) or its purely algebraic representation, the rigid Earth 'dynamical variation of latitude' (Oppolzer, 1880; Atkinson, 1973). Both approaches are straightforward variations of the operator equality $\frac{\partial}{\partial t} = \partial_t + \underset{\sim}{\Omega} x$ which holds in the sidereally rotating reference frame.

For a non-rigid Earth the diurnal tidal response is not simply rotational in character but also includes elastic deformation. The perturbed rotation, figure and angular momentum axes are affected by these terms to varying degrees, and their interrelationship may no longer be described with the simple Poinsot representation. In fact, knowledge of the differences between these axes provides some understanding of the elastic tidal response within the Earth.

Nutational motion need not be viewed as a separate tidal phenomenon, as it is necessarily included in the total diurnal Lagrangian displacement, $\underset{\sim}{s}$. Since the invariant observational equations of Chapter VI are represented as functionals of the complete displacement, $\underset{\sim}{s}$, any effects of nutation are automatically included there, as well. Consequently, a separate identification of nutational motion may appear an observationally unnecessary complication.

However, our results for $\underset{\sim}{s}$ are computed at any frequency assuming a unit harmonic potential at that frequency and must eventually be convolved with a luni-solar tidal potential theory (most accurate is probably that of Cartwright and Tayler (1971) and Cartwright and Edden (1973)). As will be seen, the rotational component of $\underset{\sim}{s}$ is highly resonant in the frequency domain at exactly one cycle per sidereal day. In fact, this component becomes so large at frequencies close to $\omega = \Omega$ that the inherent computational errors in existing tidal potential theories introduce errors in the Earth's rotation which lie above experimental precision. For this reason we choose to separate the rotational ($\underset{\sim}{\tau}_1^1$) component out of the diurnal tidal response (5.16) and treat it separately. We will uniquely identify the values of $\underset{\sim}{\tau}_1^1$ on the mean outer surface with the Earth's nutation and will introduce a related axis, $\underset{\sim}{B}$, whose nutational behavior matches this definition. $\underset{\sim}{B}$ will be computed by convolving $\underset{\sim}{\tau}_1^1$ with Kinoshita's (1977) nutational results for a rigid Earth.

The observational effects of the remaining elastic deformation in s is compiled analytically and numerically in Chapter IX. In this manner, after correcting astronomical latitude and longitude measurements for these 'body tide' results (which differ from terms proportional to $1 + k - \ell$ only by small elliptical effects) the observer is left with reduced observations which exactly reflect motion of the axis, $\underset{\sim}{B}$.

7.1) Identification of Nutational Motion

The tidal response to an $\ell = 2$, $m = 1$ (diurnal) applied potential can be adequately expanded into toroidal and spheroidal components

$$\underset{\sim}{s} = \underset{\sim}{\tau}_{\ell=1}^{m=1} + \underset{\sim}{\sigma}_2^1 + \underset{\sim}{\tau}_3^1 + \underset{\sim}{\sigma}_4^1 \tag{7.1}$$

as discussed in Section 5.4. Here, $\underset{\sim}{\sigma}_2^1$ and the smaller $\underset{\sim}{\tau}_3^1$ and $\underset{\sim}{\sigma}_4^1$ represent elastic deformation. The remaining toroidal component, $\underset{\sim}{\tau}_1^1$, is strongly excited in the diurnal band and has a more unique interpretation. Its (complex) displacement field has the form

$$\underset{\sim}{\tau}_1^1(r) = \underset{\sim}{\chi} \times r \tag{7.2}$$

where

$$\underset{\sim}{\chi} = \eta(r)(\hat{\underset{\sim}{x}} + i\hat{\underset{\sim}{y}})\, e^{i(\omega t+\alpha)} \tag{7.3}$$

Here, $\hat{\underset{\sim}{x}}$ and $\hat{\underset{\sim}{y}}$ are unit vectors and α and ω are the phase and positive angular frequency of the disturbance. For any spherical surface, $r=r_o$, (7.2) and (7.3) represent a rigid rotation of that surface around an axis perpendicular to the uniform sidereal rotation vector, $\underset{\sim}{\Omega}$. For positive ω the surface is said to 'nutate' about $\underset{\sim}{\Omega}$ in a retrograde (opposite to $\underset{\sim}{\Omega}$) sense.

The usual global concept of the Earth's nutation is rooted in traditional rigid body treatments, where $\underset{\sim}{\sigma}_2^1 = \underset{\sim}{\tau}_3^1 = \underset{\sim}{\sigma}_4^1 = 0$ and $\eta(r)$ in (7.3) is a constant (in r). This allows for an unambiguous identification of global nutational motion. For the realistic, deformable case the picture is complicated not only by $\underset{\sim}{\sigma}_2^1 + \underset{\sim}{\tau}_3^1 + \underset{\sim}{\sigma}_4^1$ in (7.1), but also by the possible radial variation in $\eta(r)$. We will choose, for reasons discussed below, to identify nutations solely with the $\underset{\sim}{\tau}_1^1$ component at the outer surface. The remaining terms in (7.1) will be hereafter referred to as the diurnal body tide.

7.2) Nutations and Gravitational Perturbations of a Rigid Earth

The rigid Earth responds to an $\ell = 2$, $m = 1$ tidal potential with a displacement field given by

$$\underset{\sim}{s}(r) = \underset{\sim}{\chi}_o \times r \tag{7.4}$$

where

$$\underset{\sim}{\chi}_o = \eta_o(\hat{\underset{\sim}{x}} + i\hat{\underset{\sim}{y}})\, e^{i(\omega t+\alpha)} \tag{7.5}$$

Here, η_o is a constant and ω, α are the frequency and phase of the disturbance. As shown above, (7.4) implies

$$(7.6) \qquad \underset{\sim}{s}(r) = \underset{\sim}{\tau}^{1}_{1}(r)$$

Given the tidally induced torque, $\underset{\sim}{N}$, it is possible to solve for η_o using conservation of angular momentum.

$$(7.7) \qquad \partial_t \underset{\sim}{H} + \underset{\sim}{\Omega} \times \underset{\sim}{H} = \underset{\sim}{N}$$

where $\underset{\sim}{H}$ is the angular momentum of the Earth.

However, to facilitate later comparison with the more general elastic results, we will instead compute η_o using the eigenfunction expansion technique detailed in Chapter IV. The only pertinent normal modes for a rigid Earth in a uniformly rotating frame are

1) the Tilt-Over-Mode (TOM) characterized by a displacement:

   $\underset{\sim}{s}_{TOM} = (\hat{\underset{\sim}{x}} + i\hat{\underset{\sim}{y}}) \times \underset{\sim}{r}$, and eigenfrequency $\omega_{TOM} = \Omega$

2) the rigid Earth Chandler Wobble (CW) with displacement

   $\underset{\sim}{s}_{CW} = (\hat{\underset{\sim}{x}} + i\hat{\underset{\sim}{y}}) \times \underset{\sim}{r}$, and eigenfrequency $\omega_{CW} = -((C-A)/A)\Omega$

   where C and A are the Earth's greatest and least moments of inertia.

Given any applied torque of the form

$$(7.8) \qquad \underset{\sim}{N} = N_o[\hat{\underset{\sim}{x}} + i\hat{\underset{\sim}{y}}]$$

we sum (4.57) over these two modes to find:

$$(7.9) \qquad \eta_o = \frac{N_o}{C\Omega}\left[\frac{1}{\Omega-\omega} + \frac{1}{\Omega\,\frac{C-A}{A} + \omega}\right]$$

Equation (7.9) shows η_o to be resonant in the retrograde direction at exactly one sidereal day and in the prograde direction at about 300 days ($C-A/A \cong 1/300$). Since the diurnal tides are closely grouped around $\omega = \Omega$, the sidereal resonance is clearly visible in the rigid Earth nutation series (after transforming to non-rotating, inertial space, this resonance is seen centered at zero frequency).

The rigid rotation, (7.4) and (7.5), perturbs the incremental Eulerian gravitational potential, ϕ_1^E. Since the potential rotates with the rigid Earth, the Lagrangian potential at any point must vanish. Consequently, within the Earth

$$(7.10) \qquad \phi_1^E = \phi_1^L - \underset{\sim}{s}\cdot\underset{\sim}{\nabla}\phi_o = -\underset{\sim}{s}\cdot\underset{\sim}{\nabla}\phi_o$$

where $-\underset{\sim}{\nabla}\phi_o$ is the unperturbed gravitational acceleration and $\underset{\sim}{s}$ the rigid rotation described by (7.4). By continuously extending ϕ_1^E into free space we find that at any interior or exterior point:

$$(7.11) \qquad \phi_1^E(r) = -(\underset{\sim}{\chi}_o \times \underset{\sim}{r})\cdot\underset{\sim}{\nabla}\phi_o$$

As (7.10) suggests, ϕ_1^E is non-zero only if the Earth is elliptical: $(\underset{\sim}{\chi}_o \times \underset{\sim}{r})\cdot\underset{\sim}{\nabla}\phi_o = 0$ if ϕ_o depends only on r. The reason is that after any rigid rotation a spherically symmetric body will not look any different to an observer fixed in space. Consequently, although $\phi_1^E/|\underset{\sim}{\nabla}\phi_o|$ is resonant along with $\underset{\sim}{s}$ at exactly one sidereal day this resonance is correspondingly less important by about a factor of ellipticity ($\sim 1/300$).

7.3) Relations Between Axes on a Rigid Earth

The instantaneous position of any particle, $\underset{\sim}{x}$, in a rigid, nutating Earth is

$$\underset{\sim}{r}(\underset{\sim}{x},t) = \underset{\sim}{x} + \underset{\sim}{\chi}_o \times \underset{\sim}{x} \tag{7.12}$$

with $\underset{\sim}{\chi}_o$ defined in (7.5). Since

$$\frac{d}{dt} = \partial_t + \underset{\sim}{\Omega}\times \tag{7.13}$$

we have

$$\frac{d\underset{\sim}{r}}{dt} = \partial_t \underset{\sim}{\chi}_o \times \underset{\sim}{x} + \underset{\sim}{\Omega} \times \underset{\sim}{r} = (\underset{\sim}{\Omega} + \partial_t \underset{\sim}{\chi}_o) \times \underset{\sim}{r} \tag{7.14}$$

The rotation vector, $\underset{\sim}{I}$, must satisfy

$$\frac{d\underset{\sim}{r}}{dt} = \underset{\sim}{I} \times \underset{\sim}{r} \tag{7.15}$$

so

$$\underset{\sim}{I} = \underset{\sim}{\Omega} + \partial_t \underset{\sim}{\chi}_o = \Omega \left[\hat{\underset{\sim}{z}} + i \frac{\omega}{\Omega} \underset{\sim}{\chi}_o \right] \tag{7.16}$$

The figure axis, $\underset{\sim}{F}$, can be found by noting that for a rigid body F will always point towards the geographic north pole. Since the inertial space orientation of the pole is

$$\underset{\sim}{r}(\hat{\underset{\sim}{z}},t) = \hat{\underset{\sim}{z}} + \underset{\sim}{\chi}_o(t) \times \hat{\underset{\sim}{z}} \tag{7.17}$$

we use (7.5) for $\underset{\sim}{\chi}_o$ to find

$$\underset{\sim}{F} = \underset{\sim}{r}(\underset{\sim}{z},t) = \hat{\underset{\sim}{z}} + i\underset{\sim}{\chi}_o \tag{7.18}$$

Polar motion is defined as the vector displacement between the figure axis and the rotation axis. By comparing (7.17) and (7.18) we can find the polar motion, $\underset{\sim}{P}$, as the offset of $\underset{\sim}{F}$ and $\underset{\sim}{I}$:

$$\underset{\sim}{P} = \underset{\sim}{I}/\Omega - \underset{\sim}{F} = \left(\frac{\omega}{\Omega} - 1 \right) i\underset{\sim}{\chi}_o \tag{7.19}$$

The unperturbed inertia tensor is

$$\underset{\sim}{I}_o = \begin{pmatrix} A & 0 & 0 \\ 0 & A & 0 \\ 0 & 0 & C \end{pmatrix} \tag{7.20}$$

and the perturbed inertia tensor, $\underset{\sim}{I}$, is found by rotating $\underset{\sim}{I}_o$ around $\underset{\sim}{\chi}_o$:

$$\underset{\sim}{I} = \underset{\sim}{R} \cdot \underset{\sim}{I}_o \cdot \underset{\sim}{R}^T \tag{7.21}$$

where the rotation tensor, $\underset{\sim}{R}$, is

$$\underset{\sim}{R} = \begin{pmatrix} 1 & 0 & \chi_o^y \\ 0 & 1 & -\chi_o^x \\ -\chi_o^y & \chi_o^x & 1 \end{pmatrix} \tag{7.22}$$

The angular momentum, $\underset{\sim}{H}$, is then given as the product of the inertia tensor with the rotation vector

$$\underset{\sim}{H} = \underset{\sim}{I} \cdot \underset{\sim}{I} = \underset{\sim}{R} \cdot \underset{\sim}{I}_o \cdot \underset{\sim}{R}^T \cdot \underset{\sim}{I} \tag{7.23}$$

After some algebra:

$$\underset{\sim}{H} = C\Omega \left[\underset{\sim}{\hat{z}} + \frac{A}{C\Omega} \left[\frac{C-A}{A} \Omega + \omega \right] i\underset{\sim}{\chi}_o \right] \tag{7.24}$$

The incremental parts of $\underset{\sim}{F}$, $\underset{\sim}{I}$, $\underset{\sim}{H}$ and $\underset{\sim}{P}$ scale linearly with $i\underset{\sim}{\chi}_o$. This permits the familiar Poinsot representation of the nutations (see, e.g. Woolard, 1953) which is to first order simply an inertial space, geometrical description of equations (7.16), (7.18), (7.19) and (7.24).

It is of some interest to examine polar motion and angular momentum in more detail. Using (7.9) in (7.19) and (7.24) gives

$$\underset{\sim}{P} = \frac{-iN_o}{A\Omega} \frac{1}{\Omega \frac{C-A}{A} + \omega} (x + i\,y)\, e^{i(\omega t + \alpha)} \tag{7.25}$$

$$\underset{\sim}{H} = C\Omega \left[\underset{\sim}{\hat{z}} + \frac{iN_o}{C\Omega} \frac{1}{\Omega - \omega} (x + iy)\, e^{i(\omega t + \alpha)} \right] \tag{7.26}$$

Equation (7.25) shows $\underset{\sim}{P}$ to be resonant only at the CW frequency. This is not surprising since of the two free modes, only the CW contains any polar motion. As a consequence of (7.25) the tidally induced diurnal polar motion, although non-vanishing, is not resonant across the diurnal band.

On the other hand, the angular momentum given by (7.26) is resonant only at one sidereal day. This, also, should be expected

since the TOM contains incremental angular momentum while the CW does not.

As a final point, the figure axis given by (7.18) is directly representative of the displacement angle, $\underset{\sim}{\chi}_o$. Consequently, on a rigid Earth, $\underset{\sim}{F}$ is observationally the most useful axis to consider. This is discussed in more detail by Atkinson (1973, 1975). If the rotation axis is used, allowance must be made for the factor ω/Ω in (7.16), responsible for the so-called 'dynamical variation of latitude' (see, e.g. Atkinson, 1973). Similar considerations will hold for the angular momentum axis.

7.4) Elastic Modifications to $\underset{\sim}{\tau}^1_1$

The inclusion of non-rigidity into the tidal problem has two distinct effects:

1) The introduction of other spheroidal and toroidal terms into the solution, as shown in (7.1).
2) The potential non-linearity in r of the $\underset{\sim}{\tau}^1_1$ nutation term, represented in (7.3) by an r-dependent $\eta(r)$.

The additional components in (7.1) have been labelled as body tide deformation and differentiated from the rotational $\underset{\sim}{\tau}^1_1$ term. Care must be exercised since these terms have non-negligible effects on many traditional axes (this will be discussed below).

However, $\underset{\sim}{\tau}{}^1_1$ serves at this stage as a clear and distinct representation of the Earth's nutation which will be placed on a firm observational footing, below.

To discuss the effects of non-rigidity on $\underset{\sim}{\tau}{}^1_1$ we consider the $\underset{\sim}{\tau}{}^1_1$ projection of the eigenfunction expansion equation, (4.57)

$$\underset{\sim}{\tau}{}^1_1 = \sum_n a_n (\underset{\sim}{\tau}{}^1_1)_n \tag{7.27}$$

where the sum is over all pertinent rotating, elliptical, elastic normal modes, a_n is given by (4.41), and $(\underset{\sim}{\tau}{}^1_1)_n$ represents the $\underset{\sim}{\tau}{}^1_1$ component of the nth mode. The necessary modes in the sum (7.27) consist of the seismic free oscillations of the Earth and the three nutational modes: the TOM, CW and NDFW, all discussed in Chapter III. The internal gravity waves of the fluid core are not included consistent with the discussion in Chapter V. Nutations of the solid inner core are similarly excluded. Neither of these omissions should sensibly affect $\underset{\sim}{\tau}{}^1_1$ in the mantle.

The applied force, in this case, consists of an $\ell=2$, $m=1$ tidal potential. Consequently, the non-resonant modes most excited in (7.27) are those with large $\underset{\sim}{\sigma}{}^1_2$ components. Since free oscillations with sizable $\underset{\sim}{\sigma}{}^1_2$ terms will contribute little to an aggregate $\underset{\sim}{\tau}{}^1_1$, their contribution to (7.27) is quite small. Instead, the most important contributions come from the three nutational modes.

The TOM for a non-rigid Earth has the same displacement and eigenfrequency as the TOM for a rigid Earth. Consequently, its contribution to $\underset{\sim}{\tau}^1_1$ is the same as in the rigid case, namely (from (7.9)):

$$a_{TOM}(\underset{\sim}{\tau}^1_1)_{TOM} = \frac{N_o}{C\Omega}\frac{1}{\Omega-\omega}(\underset{\sim}{\hat{x}} + i\underset{\sim}{\hat{y}}) \times \underset{\sim}{r}\, e^{i(\omega t+\alpha)} \tag{7.28}$$

As in the rigid case, the TOM provides the highly visible, exactly diurnal resonance in the nutation series.

The $\underset{\sim}{\tau}^1_1$ CW component is modified slightly by non-rigidity. It is nearly linear in r throughout the mantle, corresponding to a constant η in (7.3), but vanishes in the fluid core. Equally importantly, its eigenfrequency is correspondingly altered (see Smith, 1977). Consequently, the CW contribution to (7.27) is somewhat different than in the rigid case.

The Nearly Diurnal Free Wobble (NDFW) is due entirely to the presence of the fluid core. Its $\underset{\sim}{\tau}^1_1$ toroidal field consists of a nearly uniform rotation throughout the mantle and an opposite rotation throughout the fluid core. It is particularly important in (7.27) because its eigenfreqnecy lies very near one day and is consequently resonant within the diurnal tidal band.

The total tidally induced $\underset{\sim}{\tau}{}^1_1$ component is then seen as a nearly constant rotation in the mantle coupled with a different, nearly constant rotation in the outer core. Differences between the rigid and non-rigid results are due predominantly to near-resonant excitation of the NDFW, and, to a lesser extent, the elastic modifications in the CW.

7.5) Observational Uniqueness of $\underset{\sim}{\tau}{}^1_1$

We have taken pains, above, to distinguish between $\underset{\sim}{\tau}{}^1_1$ and the $\underset{\sim}{\sigma}{}^1_2 + \underset{\sim}{\tau}{}^1_3 + \underset{\sim}{\sigma}{}^1_4$ combination in the diurnal tidal solution. Such a separation is not merely a conceptual aid but is in fact suggested by practical considerations. The tidal observables modeled in Chapter VI are functionals of the total tidal surface displacement and associated gravitational potential. As discussed in Chapter II, the solution at any frequency is computed by assuming an appropriately normalized amplitude for the luni-solar potential. To compare with observation these results must be convolved with some reliable potential theory. Unfortunately, due to the resonant $\frac{1}{\Omega-\omega}$ excitation of the TOM discussed above, the diurnal surface $\underset{\sim}{\tau}{}^1_1$ component becomes so large that no published diurnal tidal tables are accurate enough: i.e., inherent errors in these tables, when convolved with the computed $\underset{\sim}{\tau}{}^1_1$, lie above the experimental precision of most present day astronomical techniques. For this reason we choose to

separate $\underset{\sim}{\tau}_1^1$ from the diurnal surface solution and identify it solely with the Earth's nutational motion. It will be convolved, below, not with the tidal potential but with accurate rigid body nutation results.

A corresponding problem is the diurnal resonance in the Eulerian potential, ϕ_1^E, which must accompany rotational $\underset{\sim}{\tau}_1^1$ motion. The TOM, with eigenfunction $\underset{\sim}{s}_{TOM} = \underset{\sim}{\chi}_{TOM} \times \underset{\sim}{r}$, perturbs ϕ_1^E according to

$$(\phi_1^E)_{TOM} = - (\underset{\sim}{\chi}_{TOM} \times \underset{\sim}{r}) \cdot \underset{\sim}{\nabla} \phi_o \tag{7.29}$$

(see the discussion preceding equation (7.10)). Consequently, a highly resonant TOM shows up in ϕ_1^E, as well as in s. This gives reason to also separate ϕ_1^E into nutational and body tide factors. The manner of separation is somewhat arbitrary, as long as the entire resonant TOM contribution is included in the nutational contribution, $(\phi_1^E)_{nut}$. By writing the $\underset{\sim}{\tau}_1^1$ component on the mean spherical surface, $r = r_o$, as

$$\underset{\sim}{\tau}_1^1(r = r_o) = \underset{\sim}{\chi}_s \times \underset{\sim}{r} \tag{7.30}$$

we choose to define

$$(\phi_1^E)_{nut} = -(\underset{\sim}{\chi}_s \times \underset{\sim}{r})\cdot\nabla\phi_o \qquad (7.31)$$

Equation (7.31) is similar to the simple rigid Earth and TOM relationsihps between $\underset{\sim}{\chi}_o$ and ϕ_1^E ((7.11) and (7.29)).

The result of this discussion is that when expanding the invariant expressions of Chapter VI into the diurnal scalar components described in Chapter IX, the resonant effects of $\underset{\sim}{\tau}_1^1$ and $(\phi_1^E)_{nut}$ are analytically removed. These effects can be visualized as the nutational contributions to the observable quantities and will now be discussed.

7.6) Observable Effects of $\underset{\sim}{\tau}_1^1$

The $\underset{\sim}{\tau}_1^1$ component at the mean outer surface for any diurnal tidal frequency, ω, is given by (7.30) with

$$\underset{\sim}{\chi}_s = \eta_s(\hat{\underset{\sim}{x}} + i\hat{\underset{\sim}{y}})\, e^{i(\omega t+\alpha)} \qquad (7.32)$$

where α is the phase associated with ω. The corresponding nutational contribution to ϕ_1^E is defined by (7.31). Using these expressions in the relevant Chapter VI equations gives:

gravity

$$\delta f = i\eta_s[\omega-\Omega]\, r\Omega \sin 2\theta\, e^{i(\phi+\omega t+\alpha)}$$

tilt

$$\Delta_E = -\frac{\eta_s}{A_o}\,[\omega-\Omega]^2\, r \cos\theta\, e^{i(\phi+\omega t+\alpha)}$$

$$\Delta_N = \frac{i\eta_s}{A_o}\,[\omega-\Omega]\, r\,[\omega-\Omega\cos 2\theta]\, e^{i(\phi+\omega t+\alpha)}$$

astronomical co-latitude and longitude

(7.33)

$$\delta\theta + i\eta_s\left[1 + \frac{r}{A_o}\,[\Omega-\omega][\omega-\Omega\cos 2\theta]\right] e^{i(\phi+\omega t+\alpha)}$$

$$\delta\lambda = \eta_s \cot\Theta_o\left[-1 + \frac{r}{A_o}\,[\Omega-\omega]^2\right] e^{i(\phi+\omega t+\alpha)}$$

free space potential

$$\phi_1^E = -(\underset{\sim}{\chi}_s \times \underset{\sim}{r})\cdot\nabla\phi_o$$

surface displacement

$$\underset{\sim}{s} = \underset{\sim}{\chi}_s \times \underset{\sim}{r}$$

where θ and ϕ are the geocentric co-latitude and longitude, Θ_o is the angle between the unperturbed outward gravity normal, $\hat{\underset{\sim}{n}}_o$, and the invariant rotation vector, (i.e., Θ_o is the unperturbed astronomical

co-latitude given by $\theta_o = \theta - \varepsilon \sin 2\theta$, with ε = surface ellipticity), and A_o is the equilibrium gravitational plus centripetal acceleration at the surface (see Section 6.1). There are no effects on strain.

Equation (7.33) represent the effects of nutational motion on observable quantities. Many terms contain the product $(\omega-\Omega)\,\eta_s$ which results from incremental inertial, Coriolis and/or centripetal forces. These terms are not resonant at one sidereal day; in fact they are notably smaller than the corresponding body tide contributions. For this reason, all $(\omega-\Omega)\,\eta_s$ contributions to (7.33) are included in the body tide results given in Chapter IX. Consequently, the only diurnal terms which are removed and must be treated separately are:

(7.34)

<u>astronomical co-latitude and longitude</u>

$$\delta\theta = i\eta_s\, e^{i(\phi+\omega t+\alpha)}$$

$$\delta\lambda = -\eta_s \cot\theta_o\, e^{i(\phi+\omega t+\alpha)}$$

<u>free space potential</u>

$$\phi_1^E = -(\underset{\sim}{\chi}_s \times \underset{\sim}{r})\cdot\underset{\sim}{\nabla}\phi_o$$

<u>surface displacement</u>

$$\underset{\sim}{s} = \underset{\sim}{\chi}_s \times \underset{\sim}{r}$$

Any observer wishing to completely model one of these observables must add (7.34) to the body tide results described in Chapter IX.

7.7) Convolution with Rigid Earth Results

In order to accurately include the rotational contributions, (7.34), values of η_s, the surface rotation angle, must be specified. The computational process described in Chapter V gives $\underset{\sim}{\tau}^1_1$, and consequently η_s, to desired accuracy assuming a unit amplitude tidal potential. As already discussed, it is convolution with inaccurate luni-solar potential theory which is troublesome. Fortunately, highly accurate tidal potential theories do exist, although in disguised form. Most useful is presently Kinoshita's (1977) investigation of the nutations of a rigid Earth. Kinoshita combined a very accurate potential theory with the simple dynamical response of a rigid Earth to produce a corresponding nutation series. To use his results we write η_s as

$$\eta_s = \eta_o \left[1 + \frac{\eta_s - \eta_o}{\eta_o} \right] \tag{7.35}$$

where $\eta_s - \eta_o$ is the perturbation in η_s due to effects of non-rigidity and η_o is the rigid rotational angle given by (7.9). A description of the elastic contributions to η_s using $\frac{\eta_s - \eta_o}{\eta_o}$ is particularly useful because it is independent of errors in the tidal theory: they cancel by division. Numerical results for $\frac{\eta_s - \eta_o}{\eta_o}$ will be described in Chapter IX.

7.8) Description of η_s Using Longitude and Obliquity Variations

It is not usual to find rigid body nutations expressed as diurnal variations in the angle, η_o. Instead, results usually describe long period variations in longitude and obliquity of some familiar physical axis. We show, here, how to connect these formulations.

First, three related coordinate systems must be described (see figure 6). The geocentric ecliptic system, E, is (nearly) inertial with origin at the Earth's instantaneous center of mass and is almost always used to describe nutational motion. The $\hat{x}$-$\hat{y}$ ecliptic plane is defined as the mean plane of the Earth's orbit about the Sun and Moon with the $\hat{x}$ axis oriented along the intersection with the Earth's equatorial plane (this intersecting line is called the equinox).

The Earth's rotating equatorial system, R, is the invariably rotating coordinate system defined in Section 2.1 and used for computation of the tidal response. In this system the $\hat{z}$ axis points along the time-averaged rotation vector, $\underset{\sim}{\Omega}$, and the $\hat{x}$ axis along the equilibrium Greenwich meridian. $\underset{\sim}{\Omega}$, and thus $\hat{z}$, are chosen to follow the Earth's 26,000 year precession through space.

The Earth's non-rotating equatorial system, X, is similar to R except that X is not sidereally rotating. The $\hat{z}$ axis in X

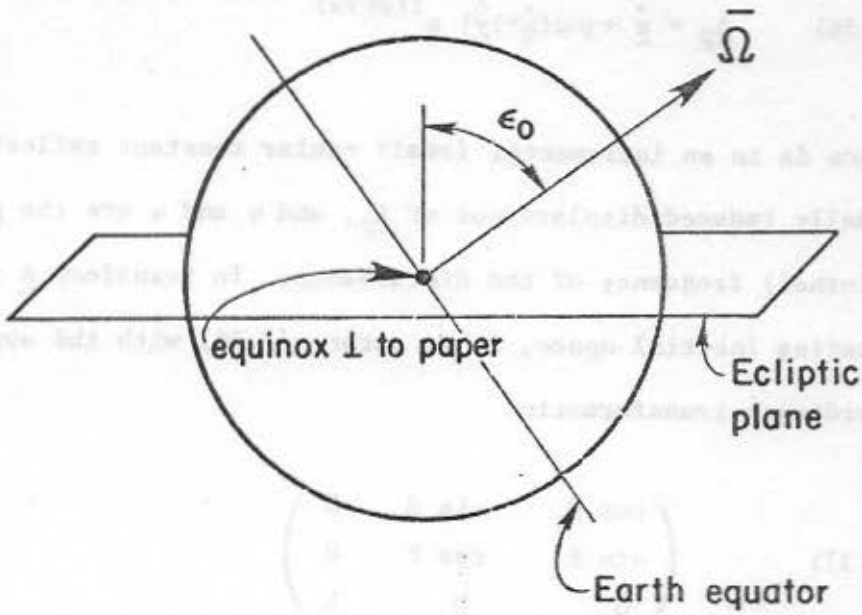

Figure 6. Relationship between the eliptic and equatorial planes.

points along the precessing rotation vector, $\underset{\sim}{\Omega}$, and the $\hat{\underset{\sim}{x}}$ axis points along the equinox.

Consider any unit vector, $\hat{\underset{\sim}{A}}$, in $\bar{R}$ with the form

$$\underset{\sim}{A}_{\bar{R}} = \hat{\underset{\sim}{z}} + i\delta a(\hat{\underset{\sim}{x}} + i\hat{\underset{\sim}{y}})\, e^{i(\omega t+\alpha)} \tag{7.36}$$

where δa is an incremental (real) scalar constant reflecting the tidally induced displacement of $\underset{\sim}{A}_{\bar{R}}$, and α and ω are the phase and (diurnal) frequency of the disturbance. To transform $\underset{\sim}{A}$ to non-rotating inertial space, X, we rotate (7.36) with the appropriate coordinate transformation

$$\begin{pmatrix} \cos\beta & -\sin\beta & 0 \\ \sin\beta & \cos\beta & 0 \\ 0 & 0 & 1 \end{pmatrix} \tag{7.37}$$

where β is Greenwich mean sidereal time (the angle between the equilibrium Greenwich meridian and the equinox)

$$\beta = \Omega t + \alpha_o \tag{7.38}$$

with α_o the phase at epoch. Then

$$\underset{\sim}{A}_{X} = \hat{\underset{\sim}{z}} + i\delta a(\hat{\underset{\sim}{x}} + i\hat{\underset{\sim}{y}})\, e^{i((\omega-\Omega) + \alpha-\alpha_o)} \tag{7.39}$$

As (7.39) shows, the nearly diurnal tidal frequency, ω, in R corresponds to a long period frequency, $\omega-\Omega$, in inertial space, X.

By a tedious but conceptually simple application of successive rotations, the orientation of $\underset{\sim}{A}$ relative to the ecliptic plane can be described by two angles: $\varepsilon = \varepsilon_o + \delta\varepsilon$ and $\psi = \delta\psi$ where

$$\begin{aligned} \delta\varepsilon &= -\delta a\, e^{i((\omega-\Omega)t + (\alpha-\alpha_o)} \\ \sin\varepsilon_o\, \delta\psi &= i\delta a\, e^{i((\omega-\Omega)t + \alpha-\alpha_o)} \end{aligned} \tag{7.40}$$

The obliquity, ε, describes the absolute angle between $\underset{\sim}{A}$ and the normal to the ecliptic, while the longitude, ψ, is defined as 90° minus the angle in the ecliptic plane between the projection of $\underset{\sim}{A}$ and the equinox (see Figure 7). For an unperturbed axis, where $\underset{\sim}{A}_R = \hat{\underset{\sim}{z}}$, we find $\varepsilon = \varepsilon_o$ and $\psi = 0$.

Every diurnal tidal harmonic with frequency $\omega_+ = \Omega + f$ and phase $\alpha_+ = \pi/2 + \alpha_o + \delta\alpha$ has a complementary term with frequency $\omega_- = \Omega - f$ and phase $\alpha_- = \pi/2 + \alpha_o - \delta\alpha$. Defining δa_+ and δa_- as the amplitudes of δa at these two complementary frequencies and combining perturbations in ε and ψ gives

$$\begin{aligned} \delta\varepsilon &= -(\delta a_+ + \delta a_-)\cos(ft + \delta\alpha) \\ \sin\varepsilon_o\, \delta\psi &= -(\delta a_+ - \delta a_-)\sin(ft + \delta\alpha) \end{aligned} \tag{7.41}$$

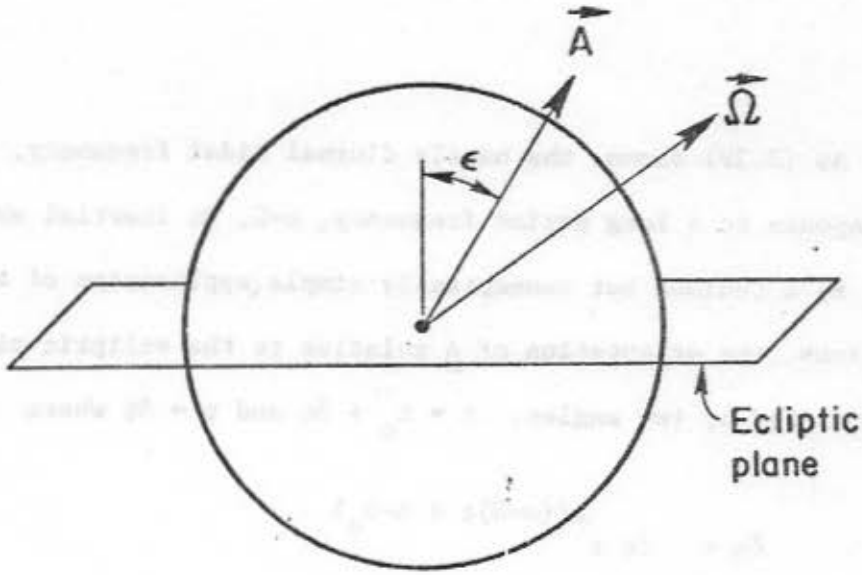

FIGURE 7a

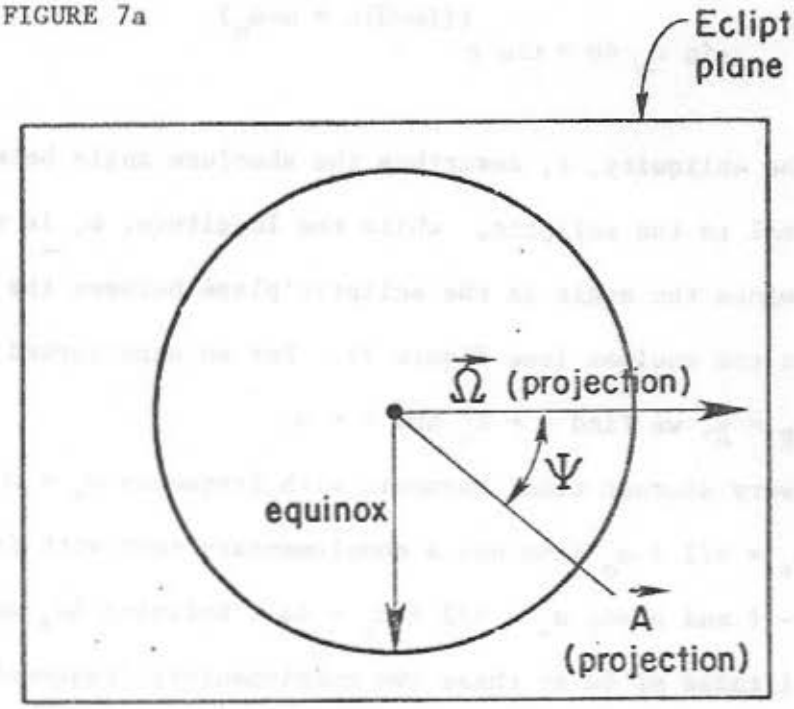

FIGURE 7b

Figure 7. The obliquity, ε, and longitude, ψ, of the vector $\underline{A}$ are shown. $\underline{A}$ is assumed to be very nearly coincident with $\underline{\Omega}$. Figures 7a and 7b are, respectively, perpendicular to and coincident with the ecliptic plane.

Equations (7.41) can be used, for example, to find η_o from published rigid body perturbations in $\delta\varepsilon$ and $\delta\psi$. As shown by equation (7.18), the figure axis, $\underset{\sim}{F}$, on a rigid Earth has an incremental component, $i\underset{\sim}{\chi}_o$, with $\underset{\sim}{\chi}_o$ given by (7.5). By using $\delta a = \eta_o$ in (7.41) we may relate η_o^+ and η_o^- (the two symmetric (about $\omega=\Omega$) tidal contributions to η_o) to $\delta\varepsilon_F$ and $\delta\psi_F$ (the Fourier transformed variations in obliquity and longitude for the rigid Earth figure axis) as:

$$\eta_o^+ = -\frac{1}{2}\left[\delta\varepsilon_F + \sin\varepsilon_o\ \delta\psi_F\right]$$

(7.42)

$$\eta_o^- = \frac{1}{2}\left[\sin\varepsilon_o\ \delta\psi_F - \delta\varepsilon_F\right]$$

and, conversely

$$\delta\varepsilon_F = -\left(\eta_o^+ + \eta_o^-\right)$$

(7.43)

$$\sin\varepsilon_o\ \delta\psi_F = \left(\eta_o^- - \eta_o^+\right)$$

We now use (7.41) in a similar manner for the non-rigid Earth. Consider the unit vector

$$\underset{\sim}{B} = \hat{\underset{\sim}{z}} + i\,\underset{\sim}{\chi}_s \qquad (7.44)$$

where $\underset{\sim}{\chi}_s$ is given by (7.32). Using $\delta a = \eta_s$ in (7.41) we find the Fourier transformed obliquity and longitude for the vector $\underset{\sim}{B}$:

$$\delta\varepsilon_\beta = -(\eta_s^+ + \eta_s^-)$$

$$\sin\varepsilon_o\ \delta\psi_\beta = (\eta_s^- - \eta_s^+) \tag{7.45}$$

Consequently, defining

$$B_{ratio} = \frac{\eta_s - \eta_o}{\eta_o} \tag{7.46}$$

as the ratio of the elastic components of $\underset{\sim}{B}$ to the rigid components of $\underset{\sim}{B}$, and using (7.42) and (7.35) gives

$$\delta\varepsilon_B = \delta\varepsilon_F\left[1 + \frac{1}{2}\,[B^+_{ratio} + B^-_{ratio}]\right]$$

$$+ \sin\varepsilon_o\ \delta\psi_F\ \frac{1}{2}\,[B^+_{ratio} - B^-_{ratio}] \tag{7.47}$$

$$\sin\varepsilon_o\ \delta\psi_B = \delta\varepsilon_F\ \frac{1}{2}\,[B^+_{ratio} - B^-_{ratio}]$$

$$+ \sin\varepsilon_o\ \delta\psi_F\left[1 + \frac{1}{2}\,[B^+_{ratio} + B^-_{ratio}]\right]$$

Thus, by combining the results for $B^{\pm}_{ratio}$ computed here with published results for $\delta\varepsilon_F$ and $\sin\varepsilon_o\ \delta\psi_F$, the angles $\delta\varepsilon_B$ and $\delta\psi_B$,

describing $\underset{\sim}{B}$, may be found. Results for $\delta\varepsilon_B$ and $\sin\varepsilon_o\,\delta\psi_B$ using Kinoshita's values for $\delta\psi_F$ and $\delta\varepsilon_F$ are discussed in Chapter IX. The rotational angles, $\eta_s^{\pm}$, may be recovered as desired by inverting (7.45) to find

$$\eta_s^+ = -\frac{1}{2}\left[\delta\varepsilon_B + \sin\varepsilon_o\,\delta\psi_B\right] \tag{7.48}$$

$$\eta_s^- = -\frac{1}{2}\left[\sin\varepsilon_o\,\delta\psi_B - \delta\varepsilon_B\right]$$

7.9) Nutations of Other Axes

We have been careful, above, to identify the Earth's nutational motion with the $\underset{\sim}{\tau}_1^1$ component in (7.1) and the corresponding vector $\underset{\sim}{B}$. Some such separation is necessary from a practical viewpoint because of the large TOM resonance near one day. Moreover, $\underset{\sim}{B}$ is an obvious choice for a nutation axis because its adoption allows for clear separation between the observational effects of nutation and those of the 'body tide'. Other axes, such as those described below, may be alternatively considered. However, particular care must be taken when relating nutations of these axes to observations.

Mean Rotation Vector

Let $\underset{\sim}{s}(\underset{\sim}{r})$ be the total tidally induced displacement vector at a point, $\underset{\sim}{r}$, in the Earth. Since a rigid change in rotation corresponds to a displacement of the form $\underset{\sim}{\chi}_o \times \underset{\sim}{r}$, we follow Jeffreys (1970) and define the mean rotation vector of the Earth as

$$\underset{\sim}{I}_E = \underset{\sim}{\Omega} + \partial_t \bar{\underset{\sim}{\chi}} \tag{7.49}$$

where $\underset{\sim}{\Omega}$ is the unperturbed uniform rotation vector of the Earth and $\bar{\underset{\sim}{\chi}}$ is the vector angle which minimizes

$$\int_{V_E} \rho \left| \underset{\sim}{s} - \bar{\underset{\sim}{\chi}} \times \underset{\sim}{r} \right|^2 dV \tag{7.50}$$

Here, V_E is the volume of the Earth and ρ its density. $\bar{\underset{\sim}{\chi}}$ is given by the solution to

$$\underset{\sim}{I}_o \cdot \bar{\underset{\sim}{\chi}} = \int_{V_E} \rho \, \underset{\sim}{r} \times \underset{\sim}{s} \, dV \tag{7.51}$$

where $\underset{\sim}{I}_o$ is the unperturbed inertia tensor of the Earth (see (7.20). This definition of $\bar{\underset{\sim}{\chi}}$ is slightly different than a global value of $\bar{\underset{\sim}{\chi}}$ derived solely from the $\underset{\sim}{\tau}_1^1$ component in $\underset{\sim}{s}$. This is

because the constant density surfaces in (7.50) and (7.51) are not spherical, but slightly elliptical, and consequently $\bar{\underset{\sim}{\chi}}$ is very slightly modified by $\underset{\sim}{\tau}_2^1$ in (7.1).

The mean rotation vector of any sub-region of the Earth may be similarly defined by changing the domain of integration in (7.50) and (7.51) accordingly. We have considered the mean rotation vector for the mantle ($\underset{\sim}{I}_M$) and for the outer elliptical surface ($\underset{\sim}{I}_s$) as well as for the entire Earth. Differences between these three axes are due predominantly to radial variations in the $\underset{\sim}{\tau}_1^1$ component through the Earth, particularly to its discontinuity across the core-mantle boundary. The nutational calculations of Molodensky (1961) refer to $\underset{\sim}{I}_M$.

Figure Axis

The Earth's figure axis is defined here as the instantaneous axis of greatest moment of inertia. For an axisymmetric Earth the unperturbed inertia tensor $\underset{\sim}{I}_o$, is given by (7.20). For the forced problem the total inertia tensor is

$$\underset{\sim}{I} = \underset{\sim}{I}_o + \delta\underset{\sim}{I} \tag{7.52}$$

where $\delta\underset{\sim}{I}$ is related in rectangular coordinates to the complete tidal deformation, $\underset{\sim}{s}$, by

$$(7.53) \qquad \delta I_{ij}(x) = \int_{V_E} \rho[2\underset{\sim}{s}\cdot\underset{\sim}{x}\,\delta_{ij} - (s_i x_j + s_j x_i)]$$

with δ_{ij} the Kroenecker delta function, ρ the density and V_E the volume of the Earth.

The instantaneous axis of figure, $\underset{\sim}{F}$, must satisfy

$$(7.54) \qquad \underset{\sim}{I}\cdot\underset{\sim}{F} = (C + \delta C)\underset{\sim}{F}$$

where $C + \delta C$ is the instantaneous moment of greatest inertia. It is not difficult to show that

$$(7.55) \qquad \underset{\sim}{F} = \underset{\sim}{\hat{z}} + \frac{1}{C-A}\,[\underset{\sim}{\hat{x}}\delta I_{xz} + \underset{\sim}{\hat{y}}\delta I_{yz}]$$

and

$$(7.56) \qquad \delta C = \delta I_{zz}$$

The diurnal tides do not contribute to δI_{zz}.

$\underset{\sim}{F}$ is highly sensitive to the 'body tide': $\underset{\sim}{\sigma}^1_2 + \underset{\sim}{\sigma}^1_3 + \underset{\sim}{\sigma}^1_4$. The reason is the small ellipticity of the Earth. A little thought will show that on a nearly spherical Earth it doesn't take much

deformation to shift the figure axis, since that axis is quite weakly constrained to begin with. This is reflected in (7.55) by the factor 1/(C-A). On the other hand, the effect of rigid body rotational motion on F is nearly independent of the ellipticity. As a result, the figure axis is usually more a reflection of the elastic behavior of the Earth than of its rotational motion. The figure axes have, however, been computed for the surface ($\underset{\sim}{F}_S$), the mantle ($\underset{\sim}{F}_M$) and the whole Earth.

Angular Momentum

The angular momentum of the Earth is the product of the instantaneous inertia tensor with the instantaneous rotation vector

$$\underset{\sim}{H}_E = \underset{\approx}{I}\cdot\underset{\sim}{I} = C\underset{\sim}{\Omega} + \delta\underset{\approx}{I}\cdot\underset{\sim}{\Omega} + \underset{\approx}{I}_o\cdot\partial_t\overline{\underset{\sim}{\chi}} \tag{7.57}$$

where C is the greatest moment of inertia, $\underset{\sim}{\Omega}$ and $\partial_t\overline{\underset{\sim}{\chi}}$ the unperturbed and incremental mean rotation vectors, and $\underset{\approx}{I}_o$ and $\delta\underset{\approx}{I}$ the unperturbed and incremental inertia tensors. Similar expressions describe the angular momentum of the mantle, $\underset{\sim}{H}_M$.

Equation (7.57) shows the angular momentum to be affected by changes in the rotation rate (through $\partial_t\overline{\underset{\sim}{\chi}}$) and by internal mass redistribution (through $\delta\underset{\approx}{I}$). For $\underset{\sim}{H}_E$ we expect all elastic contributions to cancel leaving a value identical to the rigid body result. This offers a means of testing for internal consistency.

Convolution with Rigid Results

Every one of the above axes has the form (7.36). The corresponding nutational amplitude, δa, may be conveniently separated into rigid and non-rigid parts

$$(7.58) \qquad \delta a = \delta a_{\text{rigid}} \left[1 + \delta a_{\text{non-rigid}}/\delta a_{\text{rigid}}\right]$$

By presenting results for the ratio

$$(7.59) \qquad \delta a_{\text{ratio}} = \delta a_{\text{non-rigid}}/\delta a_{\text{rigid}}$$

uncertainties in the luni-solar ephemeris and related constants will cancel. This procedure has been discussed above (Section 7.8) for the axis, $\underset{\sim}{B}$, where $\delta a_{\text{ratio}} = B_{\text{ratio}}$. From knowledge of δa_{ratio} for any axis, perturbations in longitude and obliquity may be found if desired, using equations identical in form to (7.47)

7.10) Interpretation of $\underset{\sim}{B}$

The vector $\underset{\sim}{B}$, described in Section 7.8, is the nutation axis adopted here because it is clearly and simply connected with observational quantities. Consequently, it is useful to discuss

the physical significance of $\underset{\sim}{B}$. For this purpose the concept of the Tisserand mean is presented.

Let $\underset{\sim}{I}_M$ be the mean rotation vector of the mantle

$$\underset{\sim}{I}_M = \underset{\sim}{\Omega} + \partial_t \underset{\sim}{\overline{\chi}}_M \tag{7.60}$$

as described in Section 7.9. The 'Tisserand mean mantle' is then conventionally defined by rigidly rotating the unperturbed mantle with an instantaneous angular velocity of $\underset{\sim}{I}_M$ (see Munk and McDonald, 1960). The axis of figure of the rigidly displaced Tisserand mean mantle is (see equation (7.18))

$$\underset{\sim}{F}_M^{Tiss} = \underset{\sim}{\hat{z}} + i\, \underset{\sim}{\overline{\chi}}_M \tag{7.61}$$

The desired effect of this definition is to rid the Tisserand mantle figure axis of contamination from the body tide deformation. It does not quite realize this objective on an elliptical Earth, since the elliptical density distribution used to define $\underset{\sim}{\overline{\chi}}_M$ slightly couples the body tide to $\underset{\sim}{\overline{\chi}}_M$.

The concept of Tisserand mean can be extended to the outer (elliptical) surface, S, where the axis of figure for the appropriately defined Tisserand mean outer surface is

$$\underset{\sim}{F}_S^{Tiss} = \hat{\underset{\sim}{z}} + i\,\bar{\underset{\sim}{\chi}}_s \tag{7.62}$$

with $\bar{\underset{\sim}{\chi}}_s$ given by expressions similar to (7.50) and (7.51) ($\int_{V_E}$ replaced by $\int_S$). Once again, $\underset{\sim}{F}_S^{Tiss}$ is not completely free from body tide effects, since S is slightly elliptical. However, from a conceptual viewpoint this small elliptical coupling can be ignored and $\bar{\underset{\sim}{\chi}}_s$ and $\underset{\sim}{\chi}_s$, the latter defining the axis $\underset{\sim}{B}$, can be accepted as equivalent. $\underset{\sim}{B}$ may then be perceived as essentially the axis of figure for the Tisserand mean outer surface, $\underset{\sim}{F}_S^{Tiss}$.

CHAPTER VIII

LONG PERIOD CHANGES IN THE LENGTH OF DAY

The $\ell=2$ $m=0$ (long period) tides excite the non-secular, zero-frequency axial spin mode (ASM) of the mantle (see Chapters III and IV). This mode consists solely of a $\underset{\sim}{\tau}^o_1$ toroidal component, representing

$$\underset{\sim}{s}_{ASM} = \eta(r)\, \hat{\underset{\sim}{z}} \times \underset{\sim}{r} \tag{8.1}$$

motion. Harmonic excitation of the ASM increments the angular velocity of the mantle, and thus conserves angular momentum by compensating for tidally induced changes in the greatest moment of inertia.

The mantle ASM is resonant at zero frequency. Consequently, many of the very long period tidal solutions have extremely large surface $\underset{\sim}{\tau}^o_1$ components. We choose to separate the observational effects of $\underset{\sim}{\tau}^o_1$ from those of the remaining 'body tide' components $\underset{\sim}{\sigma}^o_0 + \underset{\sim}{\sigma}^o_2 + \underset{\sim}{\tau}^o_3 + \underset{\sim}{\tau}^o_4$, in much the same way as the nutations are handled in Chapter VII.

8.1) Description of $\underset{\sim}{\tau}_1^o$

The computed ℓ=2 m=0 tidal solution at the outer mean spherical surface may be written

$$\underset{\sim}{s} = \underset{\sim}{g}_{\ell=0}^{m=0} + \underset{\sim}{\tau}_1^0 + \underset{\sim}{g}_2^0 + \underset{\sim}{\tau}_3^0 + \underset{\sim}{g}_4^0 \tag{8.2}$$

The $\underset{\sim}{\tau}_1^0$ component in (8.2) has the form

$$\underset{\sim}{\tau}_1^0 = \underset{\sim}{\chi}_s \times \underset{\sim}{r} \tag{8.3}$$

where

$$\underset{\sim}{\chi}_s = \eta_s \hat{\underset{\sim}{z}}\, e^{i(\omega t + \alpha)} \tag{8.4}$$

Here, η_s is a constant scalar angle and α and ω are the phase and frequency of the tidal disturbance. η_s is affected slightly by excitation of seismic free oscillations, but mostly comes from the large resonant ASM of the mantle.

8.2) Observable Effects of $\tau_{\underset{\sim}{1}}^{0}$

By using $\underset{\sim}{s} = \underset{\sim}{\chi}_s \times \underset{\sim}{r}$, with $\underset{\sim}{\chi}_s$ given by (8.4), in the pertinent Chapter VI equations, we find the following observable $\tau_{\underset{\sim}{1}}^{0}$ effects:

gravity

$$\delta f = - i\eta_s \, 2\omega\Omega r \sin^2\theta \, e^{i(\omega t + \alpha)}$$

tilt

$$\Delta_E = \eta_s \frac{\omega^2 r}{A_o} \sin\theta \, e^{i(\omega t + \alpha)}$$

$$\Delta_N = i\eta_s \frac{\omega\Omega r}{A_o} 2 \cos\theta \sin\theta \, e^{i(\omega t + \alpha)}$$

(8.5)

astronomical latitude and longitude

$$\delta\Theta = - i\eta_s \frac{\omega\Omega r}{A_o} \sin 2\theta \, e^{i(\omega t + \alpha)}$$

$$\delta\lambda = \eta_s \left(1 - \frac{\omega^2 r}{A_o}\right) e^{i(\omega t + \alpha)}$$

surface displacement

$$\underset{\sim}{s} = \underset{\sim}{\chi}_s \times \underset{\sim}{r}$$

where θ and ϕ are the geocentric co-latitude and longitude, and A_o is the equilibrium gravitational plus centripetal acceleration at the surface (see Section 6.1). There are no effects on strain

or free space gravity (assuming an axisymmetric zero order gravitational field).

Most effects shown in (8.5) contain the product $\omega\eta_s$. This factor is non-resonant at $\omega = 0$ since ω exactly cancels the $1/\omega$ ASM resonance in η_s. As a result, we choose to categorize all $\omega\eta_s$ contributions as 'body tide' effects and have included them in the analytical body tide expressions and the numerical results described in Chapter IX. The only long period terms which must then be treated separately are:

$$\underline{\text{astronomical longitude}}$$

$$\delta\lambda = \eta_s \, e^{i(\omega t + \alpha)}$$

(8.6)

$$\underline{\text{surface displacement}}$$

$$\underset{\sim}{s} = \underset{\sim}{\chi}_s \times \underset{\sim}{r}$$

8.3) Changes in the Length of Day

It is evident from (8.6) and the discussion in Section 6.4, that the surface rotation $\underset{\sim}{\chi}_s$ affects transit time observations (reflected in UT1-UTC) but not the apparent zenith distances. This phenomenon is often referred to in the geophysical literature as a long period change in the length of day.

Strictly speaking, a perturbation in the length of day is proportional to the incremental angular velocity, $\eta\omega_s$, which is non-resonant at $\omega = 0$. In fact, for a unit tidal disturbing potential both $\omega\eta_s$ and the accompanying 'body tide', $\underset{\sim}{\sigma}^0_0 + \underset{\sim}{\sigma}^0_2 + \underset{\sim}{\tau}^0_3 + \underset{\sim}{\sigma}^0_4$, are nearly constant across the long period band. Results for both $\omega\eta_s$ and η_s are presented in Chapter IX.

CHAPTER IX

NUMERICAL RESULTS

9.1 Earth Models

Adoption of a set of equilibrium values for $\lambda_o(r)$, $\mu_o(r)$ and $\rho_o(r)$ (see Section 2.1) is equivalent to choosing a model for the mechanical structure of the Earth. Here we use models PEM-C (Dziewonski et al., 1975), C2 (Anderson and Hart, 1976), 1066A (Gilbert and Dziewonski, 1975) and two variants of 1066A obtained by slightly modifying the stability of the fluid core. These models are constructed to accommodate a large volume of recent seismological data and probably represent the most reliable elastic global models currently available.

1066A

By applying powerful numerical techniques to two important sets of global seismic records, Gilbert and Dziewonski (1975) succeeded in observing 1064 free oscillation eigenfrequencies of the Earth. Using these frequencies as constraints in a linear inverse scheme, Gilbert and Dziewonski arrived at two distinct Earth models: 1066A, a perturbation of Model 508 (Gilbert and Dziewonski, 1973) and 1066B, derived from Model B1 (Jordan and Anderson, 1974). Differences between 1066A and 1066B are most

apparent in the upper 1000 km of the mantle, where 1066B has two sharp discontinuities in material properties and 1066A is continuous.

PEM-C

Dziewonski et al. (1975) used the 1064 free oscillation eigenfrequencies of Gilbert and Dziewonski (1975) together with recent body wave travel time and surface wave dispersion data to obtain models PEM-O, PEM-C and PEM-A. Model 1066B of Gilbert and Dziewonski (1975) was chosen as the starting model and its upper mantle discontinuities preserved. Most obvious differences between the PEM models and 1066A occur in the upper 1000 km and are associated with these discontinuities. Of the three PEM models, PEM-C is most appropriate for tidal calculations since it includes a solid crustal surface. A unique characteristic of the PEM models is their description of material properties as piecewise parameterized functions of radius.

C2

Starting from Model B1 (Jordan and Anderson, 1974), Anderson and Hart (1976) inverted 437 free oscillation frequencies and a large volume of body wave data to produce Model C2. Much of the free oscillation data is taken from Gilbert and Dziewonski (1975). Model C2 differs from the 1066 and PEM models most noticeably in the upper mantle. In addition, C2 has a significantly smaller inner core density than the other models. As presented, C2 includes

an oceanic surface. We have replaced this fluid layer with a continental crust taken from PEM-C.

Variants of 1066A

An important parameter summarizing the dynamical behavior of the fluid core is the squared Brunt-Väisälä frequency (see, e.g. Masters, 1978)

$$(9.1) \qquad N^2 = -g_o \left[\frac{\rho_o g_o}{\lambda_o} + \frac{\partial_r \rho_o}{\rho_o} \right]$$

N^2 is a measure of the stability of the core and could be particularly important in the dynamics of the core dynamo (see, e.g. Busse, 1975). The models discussed above are found to have values of N^2 which fluctuate rapidly about an approximately zero mean. Unfortunately, however, $\partial_r \rho$ and consequently N^2 are not well determined by any free oscillation of body wave data. Masters (1978) has made optimal use of free oscillation results to conclude the core is nearly neutrally stable (i.e. $N^2 = 0$) except possibly near the core-mantle boundary where it may be significantly stable ($N^2 > 0$).

We have generated and used two variants of 1066A, each obtained by modifying the core density structure to produce an outer core which is, respectively: 1) neutrally stable; 2) positively

stable with $N^2 = 8.1 \times 10^{-9}$ sec^{-2} throughout. Both cases are probably within the limits imposed by the seismological data (Masters, 1978). Our hope is that tidal and/or nutational results could be used to obtain information about N^2.

Expected Differences

As discussed in Chapter IV, the Earth's tidal response can be written as a sum of normal modes of which the free oscillations, 3 mantle nutations and wobbles (i.e. the CW, NDFW and TOM) and the mantle axial spin mode (ASM) are observationally of most importance. Since the lower frequency free oscillations must provide the larger tidal contributions and since all models considered here are constrained by the same low frequency free oscillation observations, we may anticipate few important model differences for the free oscillation tidal contributions. In addition, the TOM and ASM are completely model independent and so their tidal contributions should also not differ significantly between models. Consequently, it is the NDFW and CW contributions which are most likely to differ from one model to another. In particular, the NDFW contribution is most promising since it is highly resonant within the diurnal band and affects both the body tide and the nutations.

However, we have found no significant numerical differences in the results for 1066A and its two variants. We are forced to conclude that geodetic and astrometric observations cannot differentiate between these three models differing only in N^2 in the fluid core - at least not at our level of computational accuracy: one part in 300. Of course, by further increasing the stability parameter, N^2, we might begin to notice computational differences (as do Shen and Manshina, 1976). However, a value of N^2 much larger than 8.1×10^{-9} sec^{-2} throughout the core is probably incompatible with the free oscillation data (see Masters, 1978).

9.2 Body Tide Results

Invariant vector expressions for the tidal observables are given in Chapter VI. Using surface spherical harmonic expansion, these expressions yield the following scalar representations:

Gravity

$$\text{(9.2a)} \qquad \delta f = -\frac{2}{r_o} H_s \times 10^2 \, g_a \left[G_o Y^m_{\ell} + G_+ Y^m_{\ell+2} + G_- Y^m_{\ell-2} \right]$$

Tilt

$$\Delta_N = \frac{1}{r_o} H_s \times 10^2 \left[T_o^N \partial_\theta Y_\ell^m + T_1^N \partial_\theta Y_{\ell+2}^m + T_2^N \partial_\theta Y_{\ell-2}^m + T_3^N \frac{m}{\sin\theta} Y_{\ell+1}^m + T_4^N \frac{m}{\sin\theta} Y_{\ell-1}^m \right]$$

(9.2b)

$$\Delta_E = \frac{i}{r_o} H_s \times 10^2 \left[T_o^E \frac{m}{\sin\theta} Y_\ell^m + T_1^E \frac{m}{\sin\theta} Y_{\ell+2}^m + T_2^E \frac{m}{\sin\theta} Y_{\ell-2}^m + T_3^E \partial_\theta Y_{\ell+1}^m + T_4^E \partial_\theta Y_{\ell-1}^m \right]$$

Latitude and Longitude

$$\delta\theta = \frac{1}{R(\theta)} H_s \times 10^2 \left[LAT_o \partial_\theta Y_\ell^m + LAT_1 \partial_\theta Y_{\ell+2}^m + LAT_2 \partial_\theta Y_{\ell-2}^m + LAT_3 \frac{1}{\sin\theta} Y_{\ell+1}^m + LAT_4 \frac{1}{\sin\theta} Y_{\ell-1}^m \right]$$

(9.2c)

$$\sin\theta\, \dot{\delta\lambda} = \frac{1}{R(\theta)} H_s \times 10^2 \left[LONG_o \frac{m}{\sin\theta} Y_\ell^m + LONG_1 \frac{m}{\sin\theta} Y_{\ell+2}^m + LONG_2 \frac{m}{\sin\theta} Y_{\ell-2}^m + LONG_3 \partial_\theta Y_{\ell+1}^m + LONG_4 \partial_\theta Y_{\ell-1}^m \right]$$

Strain

$$\epsilon_{NS} = \frac{1}{R(\theta)} H_s \times 10^2 \left[S_1 Y_\ell^m + S_2 \partial_\theta^2 Y_\ell^m + S_3 \frac{m}{\sin\theta} [\partial_\theta - \cot\theta] Y_{\ell+1}^m + \right.$$

$$S_4 \frac{m}{\sin\theta} [\partial_\theta - \cot\theta] Y_{\ell-1}^m + S_5 Y_{\ell+2}^m + S_6 Y_{\ell-2}^m +$$

$$\left. S_7 \frac{1}{2} [3\cos^2\theta - 1] \partial_\theta^2 Y_\ell^m + S_8 \partial_\theta^2 Y_{\ell+2}^m + S_9 \partial_\theta^2 Y_{\ell-2}^m \right]$$

$$\epsilon_{EW} = \frac{1}{R(\theta)} H_s \times 10^2 \left[-S_2 \left[\frac{m^2}{\sin^2\theta} - \cot\theta \, \partial_\theta \right] Y_\ell^m + S_1 Y_\ell^m \right.$$

(9.2d)

$$- S_8 \left[\frac{m^2}{\sin^2\theta} - \cot\theta \, \partial_\theta \right] Y_{\ell+2}^m - S_3 \frac{m}{\sin\theta} [\partial_\theta - \cot\theta] Y_{\ell+1}^m$$

$$- S_4 \frac{m}{\sin\theta} [\partial_\theta - \cot\theta] Y_{\ell-1}^m - S_9 \left[\frac{m^2}{\sin^2\theta} - \cot\theta \, \partial_\theta \right] Y_{\ell-2}^m$$

$$\left. + S_5 Y_{\ell+2}^m + S_6 Y_{\ell-2}^m - S_7 \frac{1}{2} [3\cos^2\theta - 1] \left[\frac{m^2}{\sin^2\theta} - \cot\theta \, \partial_\theta \right] Y_\ell^m \right]$$

Strain (continued)

$$\epsilon_{NE} = 2\,\frac{i}{R(\theta)}\,H_s \times 10^2 \left[-S_2\,\frac{m}{\sin\theta}\,[\cot\theta - \partial_\theta]\,Y_\ell^m + S_3\left[\partial_\theta^2 + \frac{(\ell+1)(\ell+2)}{2}\right] Y_{\ell+1}^m + S_4\left[\partial_\theta^2 + \frac{(\ell-1)\ell}{2}\right] Y_{\ell-1}^m - S_7\,\frac{1}{2}\,[3\cos^2\theta - 1]\,\frac{m}{\sin}\,[\cot\theta - \partial_\theta]\,Y_\ell^m + S_8\,\frac{m}{\sin\theta}\,[\cot\theta - \partial_\theta]\,Y_{\ell+2}^m + S_9\,\frac{m}{\sin\theta}\,[\cot\theta - \partial_\theta]\,Y_{\ell-2}^m \right]$$

Free Space Potential

$$\phi_1^E = -\,g_a H_s \times 10^2\, k_o \left[\left(\frac{r_o}{r}\right)^{\ell+1} Y_\ell^m + k_+ \left(\frac{r_o}{r}\right)^{\ell+3} Y_{\ell+2}^m + k_- \left(\frac{r_o}{r}\right)^{\ell-1} Y_{\ell-2}^m \right]$$

(9.2e)

Surface Displacement

$$\underset{\sim}{s} = H_s \times 10^2 \left[\hat{\underset{\sim}{e}}_r h_o \left[1 + \frac{y}{2}\,[3\cos^2\theta - 1]\; Y_\ell^m + h_+ Y_{\ell+2}^m + h_- Y_{\ell-2}^m \right] + \hat{\underset{\sim}{e}}_\theta \ell_o \left[1 + \frac{z}{2}\,[3\cos^2\theta - 1]\;\partial_\theta Y_\ell^m + \ell_+ \partial_\theta Y_{\ell+2}^m + \ell_- \partial_\theta Y_{\ell-2}^m + w_-\,\frac{m}{\sin\theta}\,Y_{\ell-1}^m + w_+\,\frac{m}{\sin\theta}\,Y_{\ell+1}^m \right] + i\hat{\underset{\sim}{e}}_\phi \ell_o \left[\frac{m}{\sin\theta} \left[1 + \frac{z}{2}\,[3\cos^2\theta - 1]\; Y_\ell^m + \ell_+ Y_{\ell+2}^m + \ell_- Y_{\ell-2}^m \right] + w_-\partial_\theta Y_{\ell-1}^m + w_+\partial_\theta Y_{\ell+1}^m \right] \right] \qquad (9.2f)$$

Here, r_o is the Earth's mean radius (6371 km); $R(\theta)$ is the distance between the Earth's center of mass and a surface point at co-latitude = θ (i.e. $R(\theta) = r_o - \frac{1}{3} \varepsilon r_o [3 \cos^2\theta - 1]$ where $\varepsilon = .00334$ is the ellipticity of the surface); and $g_a = \frac{GM_E}{R_E^2} = 979.8259$ cm/sec^2 is the equatorial gravitational acceleration which would be observed were the Earth spherically symmetric (R_E is the Earth's equatorial radius). The coefficients $\{H_s\}$ in (9.2) represent the frequency dependent tidal potential amplitudes in meters observed at the equator - thus chosen to directly correspond to the amplitude coefficients used by Cartwright and Tayler (1971) and Cartwright and Edden (1973). The scalars:

$$\left\{ G_o, G_+, G_-, T_o^N, T_1^N, T_2^N, T_3^N, T_4^N, T_o^E, T_1^E, \right.$$
$$T_2^E, T_3^E, T_4^E, S_1, S_2, S_3, S_4, S_5, S_6, S_7, S_8, S_9,$$
$$\text{LAT}_o, \text{LAT}_1, \text{LAT}_2, \text{LAT}_3, \text{LAT}_4, \text{LONG}_o, \text{LONG}_1, \text{LONG}_2, \tag{9.3}$$
$$\text{LONG}_3, \text{LONG}_4, k_o, k_-, k_+, h_o, h_-, h_+, \ell_o, \ell_-, \ell_+,$$
$$\left. y, z, w_-, w_+ \right\}$$

are dimensionless linear combinations of the solution scalars described in Chapter V. Finally, the Y_ℓ^m in (9.2) are surface spherical harmonics with normalization as defined in Appendix A.

For a spherical Earth, the scalars (9.3) reduce to a particularly simple form. First, the only non-zero free space potential and displacement Love numbers are k_o, h_o and ℓ_o. Secondly, all other scalars are zero except:

$$G_o = \frac{\ell}{2} - \frac{\ell+1}{2} k_o + h_o \qquad \text{(gravimetric factor)}$$

$$T_o^N = T_o^E = 1 - h_o + k_o \qquad \text{(diminishing factor)}$$

(9.4)
$$S_1 = h_o$$

$$S_2 = \ell_o$$

$$LAT_o = LONG_o = -[1 + k_o - \ell_o]$$

To illustrate the cumulative effects of rotation and ellipticity, we consider the gravity signal. From (9.2a):

(9.5)
$$\delta f = -\frac{2}{r_o} H_s \times 10^2 \, g_a Y_\ell^m \, G$$

where, in the spherical case, $G = G_o$ with G_o given by (9.4). For an elliptical, rotating Earth:

(9.6)
$$G = G_o + G_+ \, Y_{\ell+2}^m / Y_\ell^m + G_- \, Y_{\ell-2}^m / Y_\ell^m$$

(9.6) describes a slightly latitude dependent gravimetric factor (G_+ and G_- are both <1% of G_o): not a surprising results since both rotation and ellipticity single out a preferred latitude in space. The kinematical relation between G_o and the tidal solution scalars, represented in (9.4) for the spherical case, is also altered by non-sphericity at about the 1% level. Finally, the tidal solution itself is affected by eliipticity and rotation, particularly in the ℓ=2 diurnal tidal band, as we shall see. Similar arguments can be applied to the other observables in (9.2).

The dynamical behavior of the Earth is reflected by the dimensionless scalars, (9.3). Results for these scalars are presented in Tables 1-18 for models PEM-C, C2 and neutrally stratified 1066A (the scalars T_2^N, T_2^E, S_9, LAT_2, $LONG_2$ and ℓ_- do not appear since they vanish identically for the tidal groups considered). As is evident, no significant frequency structure was ever found within the ℓ=2 m=2, ℓ=2 m=0, or any ℓ=3 tidal bands. Furthermore, the truncation corrections described in Chapter V were not performed for the small ℓ=3 m=1, or ℓ=3 m=0 tides, and these tides do not appear in Tables 1-18. In this case, the appropriate scalars in (9.3) are adequately represented by the ℓ=3, m=2 results.

Presentation of the ℓ=2 diurnal results are more of a problem. They show considerable frequency dependence near ψ_1, a consequence of near-resonance excitation of the NDFW. Results

TABLE 1

TIDAL GRAVITY SIGNAL FOR NEUTRAL 1066A

Tidal Line	G_0	G_+	G_-
1) l=2 m=1 (diurnal)			
125755 ($2Q_1$)	1.152	-.006	.0
127555 (σ_1)	1.152	-.006	.0
135655 (Q_1)	1.152	-.006	.0
137455 (ρ_1)	1.152	-.006	.0
145555 (O_1)	1.152	-.006	.0
147555 (τ_1)	1.152	-.006	.0
155655 (M_1)	1.152	-.006	.0
157455 (χ_1)	1.152	-.006	.0
162556 (π_1)	1.149	-.006	.0
163555 (P_1)	1.147	-.006	.0
164556 (S_1)	1.144	-.006	.0
165545	1.134	-.006	.0
165555 (K_1)	1.132	-.006	.0
165565	1.131	-.006	.0
165575	1.129	-.006	.0
166554 (ψ_1)	1.235	-.007	.0
167555 (ϕ_1)	1.167	-.006	.0
173655 (θ_1)	1.155	-.006	.0
175455 (J_1)	1.155	-.006	.0
183555 (SO_1)	1.154	-.006	.0
185555 (OO_1)	1.154	-.006	.0
195455 (ν_1)	1.154	-.006	.0
2) any l=2 m=2 (semi-diurnal)	1.160	-.005	.0
3) any l=2 m=0 (long period)	1.155	-.007	.005
4) any l=3 m=3 (ter-diurnal)	1.606	-.005	.0
5) any l=3 m=2 (semi-diurnal)	1.602	-.008	.0

TABLE 2

TIDAL GRAVITY SIGNAL FOR PEM-C

Tidal Line	G_0	G_+	G_-
1) l=2 m=1 (diurnal)			
125755 ($2Q_1$)	1.152	-.007	.0
127555 (σ_1)	1.152	-.007	.0
135655 (Q_1)	1.152	-.007	.0
137455 (ρ_1)	1.152	-.007	.0
145555 (O_1)	1.152	-.007	.0
147555 (τ_1)	1.152	-.007	.0
155655 (M_1)	1.152	-.007	.0
157455 (χ_1)	1.152	-.007	.0
162556 (π_1)	1.149	-.007	.0
163555 (P_1)	1.147	-.007	.0
164556 (S_1)	1.144	-.007	.0
165545	1.134	-.006	.0
165555 (K_1)	1.132	-.006	.0
165565	1.131	-.006	.0
165575	1.129	-.006	.0
166554 (ψ_1)	1.235	-.007	.0
167555 (ϕ_1)	1.167	-.007	.0
173655 (θ_1)	1.155	-.007	.0
175455 (J_1)	1.155	-.007	.0
183555 (SO_1)	1.154	-.007	.0
185555 (OO_1)	1.154	-.007	.0
195455 (ν_1)	1.154	-.007	.0
2) any l=2 m=2 (semi-diurnal)	1.160	-.005	.0
3) any l=2 m=0 (long period)	1.155	-.007	.005
4) any l=3 m=3 (ter-diurnal)	1.606	-.005	.0
5) any l=3 m=2 (semi-diurnal)	1.602	-.008	.0

TABLE 3

TIDAL GRAVITY SIGNAL FOR C2

Tidal Line	G_0	G_+	G_-
1) l=2 m=1 (diurnal)			
125755 ($2Q_1$)	1.151	-.007	.0
127555 (σ_1)	1.151	-.007	.0
135655 (Q_1)	1.151	-.007	.0
137455 (ρ_1)	1.151	-.007	.0
145555 (O_1)	1.151	-.007	.0
147555 (τ_1)	1.151	-.007	.0
155655 (M_1)	1.151	-.007	.0
157455 (χ_1)	1.151	-.007	.0
162556 (π_1)	1.148	-.007	.0
163555 (P_1)	1.147	-.006	.0
164556 (S_1)	1.143	-.006	.0
165545	1.133	-.006	.0
165555 (K_1)	1.132	-.006	.0
165565	1.130	-.006	.0
165575	1.129	-.006	.0
166554 (ψ_1)	1.235	-.007	.0
167555 (ϕ_1)	1.166	-.007	.0
173655 (θ_1)	1.154	-.007	.0
175455 (J_1)	1.154	-.007	.0
183555 (SO_1)	1.153	-.007	.0
185555 (OO_1)	1.153	-.007	.0
195455 (ν_1)	1.153	-.007	.0
2) any l=2 m=2 (semi-diurnal)	1.159	-.005	.0
3) any l=2 m=0 (long period)	1.154	-.007	.005
4) any l=3 m=3 (ter-diurnal)	1.606	-.005	.0
5) any l=3 m=2 (semi-diurnal)	1.602	-.008	.0

TABLE 4

TIDAL TILT SIGNAL FOR NEUTRAL 1066A

Tidal Line	T_0^N	T_1^N	T_3^N	T_4^N	T_0^E	T_1^E	T_3^E	T_4^E
1) l=2 m=1 (diurnal)								
125755 ($2Q_1$)	.688	-.001	-.001	.004	.688	.0	-.001	.002
127555 (σ_1)	.688	-.001	-.001	.004	.688	.0	-.001	.002
135655 (Q_1)	.689	-.001	-.001	.004	.688	.0	-.001	.002
137455 (ρ_1)	.689	-.001	-.001	.004	.688	.0	-.001	.002
145555 (O_1)	.689	-.001	-.001	.004	.689	.0	-.001	.002
147555 (τ_1)	.689	-.001	-.001	.004	.689	.0	-.001	.002
155655 (M_1)	.690	-.001	-.001	.004	.690	.0	-.001	.002
157455 (χ_1)	.691	-.001	-.001	.004	.690	.0	-.001	.002
162556 (π_1)	.697	-.001	-.001	.004	.696	.0	-.001	.002
163555 (P_1)	.700	-.001	-.001	.004	.700	.0	-.001	.002
164556 (S_1)	.707	-.001	-.001	.004	.706	.0	-.001	.002
165545	.728	-.001	-.001	.004	.727	.0	-.001	.002
165555 (K_1)	.730	-.001	-.001	.004	.730	.0	-.001	.002
165565	.733	-.001	-.001	.004	.733	.0	-.001	.002
165575	.737	-.001	-.001	.004	.737	.0	-.001	.002
166554 (ψ_1)	.523	-.001	-.001	.006	.522	.0	-.001	.003
167555 (ϕ_1)	.660	-.001	-.001	.004	.659	.0	-.001	.002
173655 (θ_1)	.685	-.001	-.001	.004	.684	.0	-.001	.002
175455 (J_1)	.685	-.001	-.001	.004	.685	.0	-.001	.002
183555 (SO_1)	.687	-.001	-.001	.004	.686	.0	-.001	.002
185555 (OO_1)	.687	-.001	-.001	.004	.686	.0	-.001	.002
195455 (ν_1)	.687	-.001	-.001	.004	.687	.0	-.001	.002
2) any l=2 m=2 (semi-diurnal)	.692	-.001	-.001	.0	.689	.0	-.002	.0
3) any l=2 m=0 (long period)	.689	-.001	.0	.0	.0	.0	.0	.0
4) any l=3 m=3 (ter-diurnal)	.801	-.001	-.001	.0	.799	.0	-.001	.0
5) any l=3 m=2 (semi-diurnal)	.799	-.001	.0	-.001	.799	-.001	-.001	-.004

TABLE 5

TIDAL TILT SIGNAL FOR PEM-C

Tidal Line	T_0^N	T_1^N	T_3^N	T_4^N	T_0^E	T_1^E	T_3^E	T_4^E
1) l=2 m=1 (diurnal)								
125755 ($2Q_1$)	.688	-.001	-.001	.004	.688	.0	-.001	.002
127555 (σ_1)	.689	-.001	-.001	.004	.688	.0	-.001	.002
135655 (Q_1)	.689	-.001	-.001	.004	.688	.0	-.001	.002
137455 (ρ_1)	.689	-.001	-.001	.004	.688	.0	-.001	.002
145555 (O_1)	.689	-.001	-.001	.004	.689	.0	-.001	.002
147555 (τ_1)	.689	-.001	-.001	.004	.689	.0	-.001	.002
155655 (M_1)	.690	-.001	-.001	.004	.690	.0	-.001	.002
157455 (χ_1)	.691	-.001	-.001	.004	.690	.0	-.001	.002
162556 (π_1)	.697	-.001	-.001	.004	.697	.0	-.001	.002
163555 (P_1)	.700	-.001	-.001	.004	.700	.0	-.001	.002
164556 (S_1)	.707	-.001	-.001	.004	.706	.0	-.001	.002
165545	.728	-.001	-.001	.003	.727	.0	-.001	.002
165555 (K_1)	.730	-.001	-.001	.003	.730	.0	-.001	.002
165565	.733	-.001	-.001	.003	.733	.0	-.001	.002
165575	.737	-.001	-.001	.003	.736	.0	-.001	.002
166554 (ψ_1)	.522	-.001	-.001	.005	.521	.0	-.001	.003
167555 (ϕ_1)	.660	-.001	-.001	.004	.660	.0	-.001	.002
173655 (θ_1)	.685	-.001	-.001	.004	.684	.0	-.001	.002
175455 (J_1)	.686	-.001	-.001	.004	.685	.0	-.001	.002
183555 (SO_1)	.687	-.001	-.001	.004	.686	.0	-.001	.002
185555 (OO_1)	.687	-.001	-.001	.004	.686	.0	-.001	.002
195455 (ν_1)	.687	-.001	-.001	.004	.687	.0	-.001	.002
2) any l=2 m=2 (semi-diurnal)	.693	.0	-.001	.0	.689	.0	-.002	.0
3) any l=2 m=0 (long period)	.689	-.001	.0	.0	.0	.0	.0	.0
4) any l=3 m=3 (ter-diurnal)	.802	-.001	-.001	.0	.800	.0	-.001	.0
5) any l=3 m=2 (semi-diurnal)	.799	-.001	-.001	-.001	.799	-.001	-.001	-.004

TABLE 6

TIDAL TILT SIGNAL FOR C2

Tidal Line	T_0^N	T_1^N	T_3^N	T_4^N	T_0^E	T_1^E	T_3^E	T_4^E
1) l=2 m=1 (diurnal)								
125755 ($2Q_1$)	.689	-.001	-.001	.004	.689	.0	-.001	.002
127555 (σ_1)	.689	-.001	-.001	.004	.689	.0	-.001	.002
135655 (Q_1)	.689	-.001	-.001	.004	.689	.0	-.001	.002
137455 (ρ_1)	.689	-.001	-.001	.004	.689	.0	-.001	.002
145555 (O_1)	.690	-.001	-.001	.004	.689	.0	-.001	.002
147555 (τ_1)	.690	-.001	-.001	.004	.689	.0	-.001	.002
155655 (M_1)	.691	-.001	-.001	.004	.690	.0	-.001	.002
157455 (χ_1)	.691	-.001	-.001	.004	.691	.0	-.001	.002
162556 (π_1)	.697	-.001	-.001	.004	.697	.0	-.001	.002
163555 (P_1)	.701	-.001	-.001	.004	.700	.0	-.001	.002
164556 (S_1)	.707	-.001	-.001	.004	.707	.0	-.001	.002
165545	.728	-.001	-.001	.003	.727	.0	-.001	.002
165555 (K_1)	.730	-.001	-.001	.003	.730	.0	-.001	.002
165565	.733	-.001	-.001	.003	.733	.0	-.001	.002
165575	.737	-.001	-.001	.003	.736	.0	-.001	.002
166554 (ψ_1)	.521	-.001	-.001	.006	.521	.0	-.001	.003
167555 (ϕ_1)	.661	-.001	-.001	.004	.660	.0	-.001	.002
173655 (θ_1)	.686	-.001	-.001	.004	.685	.0	-.001	.002
175455 (J_1)	.686	-.001	-.001	.004	.685	.0	-.001	.002
183555 (SO_1)	.687	-.001	-.001	.004	.687	.0	-.001	.002
185555 (OO_1)	.687	-.001	-.001	.004	.687	.0	-.001	.002
195455 (ν_1)	.688	-.001	-.001	.004	.687	.0	-.001	.002
2) any l=2 m=2 (semi-diurnal)	.693	.0	-.001	.0	.690	.0	-.002	.0
3) any l=2 m=0 (long period)	.689	-.001	.0	.0	.0	.0	.0	.0
4) any l=3 m=3 (ter-diurnal)	.802	-.001	-.001	.0	.800	.0	-.001	.0
5) any l=3 m=2 (semi-diurnal)	.799	-.001	-.001	-.001	.799	-.001	-.001	-.004

TABLE 7

TIDAL EFFECTS ON LATITUDE AND LONGITUDE FOR NEUTRAL 1066A

Tidal Line	LAT_0	LAT_1	LAT_3	LAT_4	$LONG_0$	$LONG_1$	$LONG_3$	$LONG_4$
1) l=2 m=1 (diurnal)								
125755 ($2Q_1$)	-1.212	.001	.005	-.008	-1.211	.0	.0	-.005
127555 (σ_1)	-1.212	.001	.005	-.008	-1.211	.0	.0	-.005
135655 (Q_1)	-1.212	.001	.005	-.008	-1.211	.0	.0	-.005
137455 (ρ_1)	-1.212	.001	.005	-.008	-1.211	.0	.0	-.005
145555 (O_1)	-1.211	.001	.005	-.008	-1.210	.0	.0	-.005
147555 (τ_1)	-1.211	.001	.005	-.008	-1.210	.0	.0	-.005
155655 (M_1)	-1.210	.001	.005	-.009	-1.209	.0	.0	-.005
157455 (χ_1)	-1.210	.001	.005	-.009	-1.209	.0	.0	-.005
162556 (π_1)	-1.203	.001	.005	-.009	-1.202	.0	.0	-.005
163555 (P_1)	-1.200	.001	.005	-.009	-1.199	.0	.0	-.005
164556 (S_1)	-1.193	.001	.005	-.008	-1.192	.0	.0	-.005
165545	-1.170	.001	.005	-.008	-1.169	.0	.0	-.005
165555 (K_1)	-1.167	.001	.005	-.008	-1.166	.0	.0	-.005
165565	-1.164	.001	.005	-.008	-1.163	.0	.0	-.005
165575	-1.160	.001	.005	-.008	-1.159	.0	.0	-.005
166554 (ψ_1)	-1.390	.001	.004	-.010	-1.388	.0	-.001	-.006
167555 (ϕ_1)	-1.243	.001	.005	-.009	-1.242	.0	.0	-.005
173655 (θ_1)	-1.216	.001	.005	-.009	-1.215	.0	.0	-.005
175455 (J_1)	-1.216	.001	.005	-.009	-1.215	.0	.0	-.005
183555 (SO_1)	-1.215	.001	.005	-.009	-1.214	.0	.0	-.005
185555 (OO_1)	-1.215	.001	.005	-.009	-1.213	.0	.0	-.005
195455 (ν_1)	-1.214	.001	.005	-.009	-1.213	.0	.0	-.005
2) any l=2 m=2 (semi-diurnal)	-1.217	.001	.004	.0	-1.216	.0	.0	.0
3) any l=2 m=0 (long period)	-1.215	.001	.005	-.008	.0	.0	.0	.0
4) any l=3 m=3 (ter-diurnal)	-1.079	.001	.003	.0	-1.078	.001	.0	.0
5) any l=3 m=2 (semi-diurnal)	-1.077	.002	.004	-.002	-1.077	.001	.0	-.001

TABLE 8

TIDAL EFFECTS ON LATITUDE AND LONGITUDE FOR PEM-C

Tidal Line	LAT_0	LAT_1	LAT_3	LAT_4	$LONG_0$	$LONG_1$	$LONG_3$	$LONG_4$
1) l=2 m=1 (diurnal)								
125755 ($2Q_1$)	-1.212	.001	.005	-.008	-1.211	.0	.0	-.005
127555 (σ_1)	-1.212	.001	.005	-.008	-1.211	.0	.0	-.005
135655 (Q_1)	-1.212	.001	.005	-.008	-1.211	.0	.0	-.005
137455 (ρ_1)	-1.212	.001	.005	-.008	-1.211	.0	.0	-.005
145555 (O_1)	-1.211	.001	.005	-.008	-1.210	.0	.0	-.005
147555 (τ_1)	-1.211	.001	.005	-.008	-1.210	.0	.0	-.005
155655 (M_1)	-1.210	.001	.005	-.008	-1.209	.0	.0	-.005
157455 (χ_1)	-1.210	.001	.005	-.008	-1.209	.0	.0	-.005
162556 (π_1)	-1.203	.001	.005	-.008	-1.202	.0	.0	-.005
163555 (P_1)	-1.200	.001	.005	-.008	-1.199	.0	.0	-.005
164556 (S_1)	-1.193	.001	.005	-.008	-1.192	.0	.0	-.005
165545	-1.171	.001	.005	-.008	-1.170	.0	.0	-.005
165555 (K_1)	-1.168	.001	.005	-.008	-1.167	.0	.0	-.005
165565	-1.164	.001	.005	-.008	-1.163	.0	.0	-.005
165575	-1.161	.001	.005	-.008	-1.160	.0	.0	-.005
166554 (ψ_1)	-1.391	.001	.004	-.010	-1.390	.0	-.001	-.006
167555 (ϕ_1)	-1.243	.001	.005	-.009	-1.242	.0	.0	-.005
173655 (θ_1)	-1.217	.001	.005	-.008	-1.215	.0	.0	-.005
175455 (J_1)	-1.216	.001	.005	-.008	-1.215	.0	.0	-.005
183555 (SO_1)	-1.215	.001	.005	-.008	-1.214	.0	.0	-.005
185555 (OO_1)	-1.215	.001	.005	-.008	-1.214	.0	.0	-.005
195455 (ν_1)	-1.214	.001	.005	-.009	-1.213	.0	.0	-.005
2) any l=2 m=2 (semi-diurnal)	-1.217	.001	.004	.0	-1.216	.0	.0	.0
3) any l=2 m=0 (long period)	-1.215	.001	.005	-.008	.0	.0	.0	.0
4) any l=3 m=3 (ter-diurnal)	-1.079	.001	.003	.0	-1.079	.001	.0	.0
5) any l=3 m=2 (semi-diurnal)	-1.078	.002	.005	-.002	-1.077	.001	.0	.0

TABLE 9

TIDAL EFFECTS ON LATITUDE AND LONGITUDE FOR C2

Tidal Line	LAT_0	LAT_1	LAT_3	LAT_4	$LONG_0$	$LONG_1$	$LONG_3$	$LONG_4$
1) l=2 m=1 (diurnal)								
125755 ($2Q_1$)	-1.211	.001	.005	-.008	-1.210	.0	.0	-.005
127555 (σ_1)	-1.211	.001	.005	-.008	-1.210	.0	.0	-.005
135655 (Q_1)	-1.211	.001	.005	-.008	-1.210	.0	.0	-.005
137455 (ρ_1)	-1.211	.001	.005	-.008	-1.210	.0	.0	-.005
145555 (O_1)	-1.211	.001	.005	-.008	-1.210	.0	.0	-.005
147555 (τ_1)	-1.211	.001	.005	-.008	-1.210	.0	.0	-.005
155655 (M_1)	-1.210	.001	.005	-.008	-1.209	.0	.0	-.005
157455 (χ_1)	-1.210	.001	.005	-.008	-1.209	.0	.0	-.005
162556 (π_1)	-1.203	.001	.005	-.008	-1.202	.0	.0	-.005
163555 (P_1)	-1.200	.001	.005	-.008	-1.199	.0	.0	-.005
164556 (S_1)	-1.193	.001	.005	-.008	-1.192	.0	.0	-.005
165545	-1.171	.001	.005	-.008	-1.170	.0	.0	-.005
165555 (K_1)	-1.168	.001	.005	-.008	-1.167	.0	.0	-.005
165565	-1.164	.001	.005	-.008	-1.163	.0	.0	-.005
165575	-1.161	.001	.005	-.008	-1.160	.0	.0	-.005
166554 (ψ_1)	-1.392	.001	.004	-.010	-1.391	.0	-.001	-.006
167555 (ϕ_1)	-1.243	.001	.005	-.009	-1.242	.0	.0	-.005
173655 (θ_1)	-1.216	.001	.005	-.008	-1.215	.0	.0	-.005
175455 (J_1)	-1.216	.001	.005	-.008	-1.215	.0	.0	-.005
183555 (SO_1)	-1.215	.001	.005	-.008	-1.213	.0	.0	-.005
185555 (OO_1)	-1.214	.001	.005	-.009	-1.213	.0	.0	-.005
195455 (ν_1)	-1.214	.001	.005	-.009	-1.213	.0	.0	-.005
2) any l=2 m=2 (semi-diurnal)	-1.217	.001	.004	.0	-1.216	.0	.0	.0
3) any l=2 m=0 (long period)	-1.215	.001	.005	-.008	.0	.0	.0	.0
4) any l=3 m=3 (ter-diurnal)	-1.079	.001	.003	.0	-1.078	.001	.0	.0
5) any l=3 m=2 (semi-diurnal)	-1.077	.002	.005	-.002	-1.077	.001	.0	.0

TABLE 10

TIDAL STRAIN SIGNAL FOR NEUTRAL 1066A

Tidal Line	S_1	S_2	S_3	S_4	S_5	S_6	S_7	S_8
1) l=2 m=1 (diurnal)								
125755 ($2Q_1$)	.604	.084	.0	.0	.0	.0	.001	.0
127555 (σ_1)	.604	.084	.0	.0	.0	.0	.001	.0
135655 (Q_1)	.604	.084	.0	.0	.0	.0	.001	.0
137455 (ρ_1)	.603	.084	.0	.0	.0	.0	.001	.0
145555 (O_1)	.603	.084	.0	.0	.0	.0	.001	.0
147555 (τ_1)	.603	.084	.0	.0	.0	.0	.001	.0
155655 (M_1)	.601	.084	.0	.0	.0	.0	.001	.0
157455 (χ_1)	.600	.084	.0	.0	.0	.0	.001	.0
162556 (π_1)	.587	.085	.0	.0	.0	.0	.001	.0
163555 (P_1)	.581	.085	.0	.0	.0	.0	.001	.0
164556 (S_1)	.568	.085	.0	.0	.0	.0	.001	.0
165545	.526	.087	.0	.0	.0	.0	.001	.0
165555 (K_1)	.520	.087	.0	.0	.0	.0	.001	.0
165565	.514	.087	.0	.0	.0	.0	.001	.0
165575	.507	.087	.0	.0	.0	.0	.001	.0
166554 (ψ_1)	.937	.074	.0	.0	.0	.0	.002	.0
167555 (ϕ_1)	.662	.082	.0	.0	.0	.0	.001	.0
173655 (θ_1)	.612	.084	.0	.0	.0	.0	.001	.0
175455 (J_1)	.611	.084	.0	.0	.0	.0	.001	.0
183555 (SO_1)	.608	.084	.0	.0	.0	.0	.001	.0
185555 (OO_1)	.608	.084	.0	.0	.0	.0	.001	.0
195455 (ν_1)	.607	.084	.0	.0	.0	.0	.001	.0
2) any l=2 m=2 (semi-diurnal)	.609	.085	.0	.0	.0	.0	.001	.0
3) any l=2 m=0 (long period)	.606	.084	.0	.0	.0	.0	.001	.0
4) any l=3 m=3 (ter-diurnal)	.292	.015	.0	.0	.0	.0	.001	.0
5) any l=3 m=2 (semi-diurnal)	.290	.015	.0	-.001	.0	.0	.001	.0

TABLE 11

TIDAL STRAIN SIGNAL FOR PEM-C

Tidal Line	S_1	S_2	S_3	S_4	S_5	S_6	S_7	S_8
1) l=2 m=1 (diurnal)								
125755 ($2Q_1$)	.604	.084	.0	.0	.0	.0	.001	.0
127555 (σ_1)	.604	.084	.0	.0	.0	.0	.001	.0
135655 (Q_1)	.603	.084	.0	.0	.0	.0	.001	.0
137455 (ρ_1)	.603	.084	.0	.0	.0	.0	.001	.0
145555 (O_1)	.602	.084	.0	.0	.0	.0	.001	.0
147555 (τ_1)	.602	.084	.0	.0	.0	.0	.001	.0
155655 (M_1)	.600	.084	.0	.0	.0	.0	.001	.0
157455 (χ_1)	.600	.084	.0	.0	.0	.0	.001	.0
162556 (π_1)	.587	.084	.0	.0	.0	.0	.001	.0
163555 (P_1)	.581	.085	.0	.0	.0	.0	.001	.0
164556 (S_1)	.567	.085	.0	.0	.0	.0	.001	.0
165545	.526	.086	.0	.0	.0	.0	.001	.0
165555 (K_1)	.520	.087	.0	.0	.0	.0	.001	.0
165565	.514	.087	.0	.0	.0	.0	.001	.0
165575	.507	.087	.0	.0	.0	.0	.001	.0
166554 (ψ_1)	.939	.073	.0	.0	.0	.0	.002	.0
167555 (ϕ_1)	.662	.082	.0	.0	.0	.0	.001	.0
173655 (θ_1)	.612	.084	.0	.0	.0	.0	.001	.0
175455 (J_1)	.611	.084	.0	.0	.0	.0	.001	.0
183555 (SO_1)	.608	.084	.0	.0	.0	.0	.001	.0
185555 (OO_1)	.608	.084	.0	.0	.0	.0	.001	.0
195455 (ν_1)	.607	.084	.0	.0	.0	.0	.001	.0
2) any l=2 m=2 (semi-diurnal)	.609	.085	.0	.0	.0	.0	.001	.0
3) any l=2 m=0 (long period)	.606	.084	.0	.0	.0	.0	.001	.0
4) any l=3 m=3 (ter-diurnal)	.291	.015	.0	.0	.0	.0	.001	.0
5) any l=3 m=2 (semi-diurnal)	.290	.015	.0	-.001	.0	.0	.001	.0

TABLE 12

TIDAL STRAIN SIGNAL FOR C2

Tidal Line	S_1	S_2	S_3	S_4	S_5	S_6	S_7	S_8
1) l=2 m=1 (diurnal)								
125755 ($2Q_1$)	.604	.085	.0	.0	.0	.0	.001	.0
127555 (σ_1)	.604	.085	.0	.0	.0	.0	.001	.0
135655 (Q_1)	.603	.085	.0	.0	.0	.0	.001	.0
137455 (ρ_1)	.603	.085	.0	.0	.0	.0	.001	.0
145555 (O_1)	.602	.085	.0	.0	.0	.0	.001	.0
147555 (τ_1)	.602	.085	.0	.0	.0	.0	.001	.0
155655 (M_1)	.600	.085	.0	.0	.0	.0	.001	.0
157455 (χ_1)	.599	.085	.0	.0	.0	.0	.001	.0
162556 (π_1)	.587	.085	.0	.0	.0	.0	.001	.0
163555 (P_1)	.581	.085	.0	.0	.0	.0	.001	.0
164556 (S_1)	.568	.086	.0	.0	.0	.0	.001	.0
165545	.526	.087	.0	.0	.0	.0	.001	.0
165555 (K_1)	.521	.087	.0	.0	.0	.0	.001	.0
165565	.515	.087	.0	.0	.0	.0	.001	.0
165575	.508	.088	.0	.0	.0	.0	.001	.0
166554 (ψ_1)	.942	.074	.0	.0	.0	.0	.002	.0
167555 (ϕ_1)	.661	.083	.0	.0	.0	.0	.001	.0
173655 (θ_1)	.611	.084	.0	.0	.0	.0	.001	.0
175455 (J_1)	.610	.084	.0	.0	.0	.0	.001	.0
183555 (SO_1)	.608	.084	.0	.0	.0	.0	.001	.0
185555 (OO_1)	.608	.084	.0	.0	.0	.0	.001	.0
195455 (ν_1)	.607	.084	.0	.0	.0	.0	.001	.0
2) any l=2 m=2 (semi-diurnal)	.609	.086	.0	.0	.0	.0	.001	.0
3) any l=2 m=0 (long period)	.606	.084	.0	.0	.0	.0	.001	.0
4) any l=3 m=3 (ter-diurnal)	.292	.015	.0	.0	.0	.0	.001	.0
5) any l=3 m=2 (semi-diurnal)	.290	.015	.0	-.001	.0	.0	.001	.0

TABLE 13

INDUCED FREE SPACE POTENTIAL FOR NEUTRAL 1066A

Tidal Line	k_0	k_+	k_-
1) l=2 m=1 (diurnal)			
125755($2Q_1$)	.298	-.005	.0
127555(σ_1)	.298	-.005	.0
135655(Q_1)	.298	-.005	.0
137455(ρ_1)	.298	-.005	.0
145555(O_1)	.298	-.005	.0
147555(τ_1)	.298	-.005	.0
155655(M_1)	.297	-.005	.0
157455(χ_1)	.296	-.005	.0
162556(π_1)	.290	-.005	.0
163555(P_1)	.287	-.005	.0
164556(S_1)	.280	-.005	.0
165545	.259	-.005	.0
165555(K_1)	.256	-.006	.0
165565	.253	-.005	.0
165575	.250	-.005	.0
166554(ψ_1)	.466	-.004	.0
167555(ϕ_1)	.328	-.005	.0
173655(θ_1)	.302	-.005	.0
175455(J_1)	.302	-.005	.0
183555(SO_1)	.301	-.005	.0
185555(OO_1)	.301	-.005	.0
195455(ν_1)	.300	-.005	.0
2) any l=2 m=2 (semi-diurnal)	.302	-.003	.0
3) any l=2 m=0 (long period)	.299	-.005	.0
4) any l=3 m=3 (ter-diurnal)	.094	-.008	.0
5) any l=3 m=2 (semi-diurnal)	.093	-.011	.0

TABLE 14

INDUCED FREE SPACE POTENTIAL FOR PEM-C

Tidal Line	k_0	k_+	k_-
1) l=2 m=1 (diurnal)			
125755 ($2Q_1$)	.298	-.005	.0
127555 (σ_1)	.298	-.005	.0
135655 (Q_1)	.298	-.005	.0
137455 (ρ_1)	.298	-.005	.0
145555 (O_1)	.298	-.005	.0
147555 (τ_1)	.298	-.005	.0
155655 (M_1)	.297	-.005	.0
157455 (χ_1)	.296	-.005	.0
162556 (π_1)	.290	-.005	.0
163555 (P_1)	.287	-.005	.0
164556 (S_1)	.280	-.005	.0
165545	.259	-.005	.0
165555 (K_1)	.256	-.006	.0
165565	.253	-.005	.0
165575	.250	-.005	.0
166554 (ψ_1)	.467	-.004	.0
167555 (ϕ_1)	.327	-.005	.0
173655 (θ_1)	.302	-.005	.0
175455 (J_1)	.302	-.005	.0
183555 (SO_1)	.301	-.005	.0
185555 (OO_1)	.301	-.005	.0
195455 (ν_1)	.300	-.005	.0
2) any l=2 m=2 (semi-diurnal)	.302	-.003	.0
3) any l=2 m=0 (long period)	.299	-.005	.0
4) any l=3 m=3 (ter-diurnal)	.094	-.008	.0
5) any l=3 m=2 (semi-diurnal)	.093	-.011	.0

TABLE 15

INDUCED FREE SPACE POTENTIAL FOR C2

Tidal Line	k_0	k_+	k_-
1) l=2 m=1 (diurnal)			
125755 ($2Q_1$)	.299	-.005	.0
127555 (σ_1)	.299	-.005	.0
135655 (Q_1)	.299	-.005	.0
137455 (ρ_1)	.299	-.005	.0
145555 (O_1)	.298	-.005	.0
147555 (τ_1)	.298	-.005	.0
155655 (M_1)	.297	-.005	.0
157455 (χ_1)	.297	-.005	.0
162556 (π_1)	.291	-.005	.0
163555 (P_1)	.287	-.005	.0
164556 (S_1)	.281	-.005	.0
165545	.260	-.005	.0
165555 (K_1)	.257	-.006	.0
165565	.254	-.006	.0
165575	.251	-.006	.0
166554 (ψ_1)	.469	-.004	.0
167555 (ϕ_1)	.328	-.005	.0
173655 (θ_1)	.303	-.005	.0
175455 (J_1)	.302	-.005	.0
183555 (SO_1)	.301	-.005	.0
185555 (OO_1)	.301	-.005	.0
195455 (ν_1)	.300	-.005	.0
2) any l=2 m=2 (semi-diurnal)	.302	-.004	.0
3) any l=2 m=0 (long period)	.299	-.006	.0
4) any l=3 m=3 (ter-diurnal)	.094	-.008	.0
5) any l=3 m=2 (semi-diurnal)	.093	-.011	.0

TABLE 16

DISPLACEMENT LOVE NUMBERS FOR NEUTRAL 1066A

Tidal Line	h_o	y	h_+	h_-	l_o	z	l_+	w	w_-
1) l=2 m=1 (diurnal)									
125755 ($2Q_1$)	.604	.001	.0	.0	.0841	.014	-.002	.0	.0
127555 (σ_1)	.604	.001	.0	.0	.0841	.014	-.002	.0	.0
135655 (Q_1)	.603	.001	.0	.0	.0841	.014	-.002	.0	.0
137455 (ρ_1)	.603	.001	.0	.0	.0841	.014	-.002	.0	.0
145555 (O_1)	.603	.001	.0	.0	.0841	.014	-.002	.0	.0
147555 (τ_1)	.603	.001	.0	.0	.0842	.014	-.002	.0	.0
155655 (M_1)	.600	.001	.0	.0	.0842	.014	-.002	.0	.0
157455 (χ_1)	.600	.001	.0	.0	.0843	.014	-.002	.0	.0
162556 (π_1)	.587	.001	.0	.0	.0847	.013	-.002	.0	.0
163555 (P_1)	.581	.001	.0	.0	.0849	.013	-.002	.0	.0
164556 (S_1)	.568	.001	.0	.0	.0853	.013	-.002	.0	.0
165545	.526	.001	.0	.0	.0866	.011	-.001	.0	.0
165555 (K_1)	.520	.001	.0	.0	.0868	.011	-.001	.0	.0
165565	.514	.001	.0	.0	.0870	.011	-.001	.0	.0
165575	.507	.001	.0	.0	.0872	.011	-.001	.0	.0
166554 (ψ_1)	.937	.001	.0	.0	.0736	.026	-.004	.001	.0
167555 (ϕ_1)	.662	.001	.0	.0	.0823	.016	-.002	.0	.0
173655 (θ_1)	.612	.001	.0	.0	.0839	.014	-.002	.0	.0
175455 (J_1)	.611	.001	.0	.0	.0839	.014	-.002	.0	.0
183555 (SO_1)	.608	.001	.0	.0	.0840	.014	-.002	.0	.0
185555 (OO_1)	.608	.001	.0	.0	.0840	.014	-.002	.0	.0
195455 (ν_1)	.607	.001	.0	.0	.0840	.014	-.002	.0	.0
2) any l=2 m=2 (semi-diurnal)	.609	.001	.0	.0	.0852	.014	-.001	.001	.0
3) any l=2 m=0 (long period)	.606	.001	.0	.0	.0840	.014	-.002	.0	.0
4) any l=3 m=3 (ter-diurnal)	.292	.001	.0	.0	.0151	.041	-.007	-.007	.0
5) any l=3 m=2 (semi-diurnal)	.291	.001	-.001	.0	.0149	.041	-.007	-.007	-.083

TABLE 17

DISPLACEMENT LOVE NUMBERS FOR PEM-C

Tidal Line	h_o	y	h_+	h_-	l_o	z	l_+	w_+	w_-
1) l=2 m=1 (diurnal)									
125755 ($2Q_1$)	.604	.001	.0	.0	.0839	.014	-.002	.0	.0
127555 (σ_1)	.604	.001	.0	.0	.0839	.014	-.002	.0	.0
135655 (Q_1)	.603	.001	.0	.0	.0839	.014	-.002	.0	.0
137455 (ρ_1)	.603	.001	.0	.0	.0839	.014	-.002	.0	.0
145555 (O_1)	.603	.001	.0	.0	.0839	.014	-.002	.0	.0
147555 (τ_1)	.602	.001	.0	.0	.0839	.014	-.002	.0	.0
155655 (M_1)	.600	.001	.0	.0	.0840	.014	-.002	.0	.0
157455 (χ_1)	.600	.001	.0	.0	.0840	.014	-.002	.0	.0
162556 (π_1)	.587	.001	.0	.0	.0844	.013	-.002	.0	.0
163555 (P_1)	.581	.001	.0	.0	.0846	.013	-.002	.0	.0
164556 (S_1)	.567	.001	.0	.0	.0850	.013	-.002	.0	.0
165545	.526	.001	.0	.0	.0864	.011	-.001	.0	.0
165555 (K_1)	.520	.001	.0	.0	.0865	.011	-.001	.0	.0
165565	.514	.001	.0	.0	.0867	.011	-.001	.0	.0
165575	.507	.001	.0	.0	.0869	.011	-.001	.0	.0
166554 (ψ_1)	.939	.001	.0	.0	.0735	.026	-.004	.001	.0
167555 (ϕ_1)	.661	.001	.0	.0	.0821	.016	-.002	.0	.0
173655 (θ_1)	.612	.001	.0	.0	.0837	.014	-.002	.0	.0
175455 (J_1)	.611	.001	.0	.0	.0837	.014	-.002	.0	.0
183555 (SO_1)	.608	.001	.0	.0	.0838	.014	-.002	.0	.0
185555 (OO_1)	.608	.001	.0	.0	.0838	.014	-.002	.0	.0
195455 (ν_1)	.607	.001	.0	.0	.0838	.014	-.002	.0	.0
2) any l=2 m=2 (semi-diurnal)	.609	.001	.0	.0	.0850	.014	-.001	.001	.0
3) any l=2 m=0 (long period)	.606	.001	.0	.0	.0838	.014	-.002	.0	.0
4) any l=3 m=3 (ter-diurnal)	.291	.001	.0	.0	.0148	.042	-.007	-.007	.0
5) any l=3 m=2 (semi-diurnal)	.290	.001	-.001	.0	.0147	.042	-.007	-.007	-.084

TABLE 18

DISPLACEMENT LOVE NUMBERS FOR C2

Tidal Line	h_o	y	h_+	h_-	l_o	z	l_+	w_+	w_-
1) l=2 m=1 (diurnal)									
125755 ($2Q_1$)	.603	.001	.0	.0	.0846	.014	-.002	.0	.0
127555 (σ_1)	.603	.001	.0	.0	.0846	.014	-.002	.0	.0
135655 (Q_1)	.603	.001	.0	.0	.0846	.014	-.002	.0	.0
137455 (ρ_1)	.603	.001	.0	.0	.0846	.014	-.002	.0	.0
145555 (O_1)	.602	.001	.0	.0	.0846	.014	-.002	.0	.0
147555 (τ_1)	.602	.001	.0	.0	.0846	.014	-.002	.0	.0
155655 (M_1)	.600	.001	.0	.0	.0847	.014	-.002	.0	.0
157455 (χ_1)	.599	.001	.0	.0	.0847	.014	-.002	.0	.0
162556 (π_1)	.587	.001	.0	.0	.0851	.013	-.002	.0	.0
163555 (P_1)	.581	.001	.0	.0	.0853	.013	-.002	.0	.0
164556 (S_1)	.568	.001	.0	.0	.0857	.013	-.002	.0	.0
165545	.526	.001	.0	.0	.0870	.011	-.001	.0	.0
165555 (K_1)	.521	.001	.0	.0	.0872	.011	-.001	.0	.0
165565	.515	.001	.0	.0	.0873	.011	-.001	.0	.0
165575	.508	.001	.0	.0	.0876	.011	-.001	.0	.0
166554 (ψ_1)	.942	.001	.0	.0	.0742	.026	-.004	.001	.0
167555 (ϕ_1)	.661	.001	.0	.0	.0828	.016	-.002	.0	.0
173655 (θ_1)	.611	.001	.0	.0	.0843	.014	-.002	.0	.0
175455 (J_1)	.610	.001	.0	.0	.0844	.014	-.002	.0	.0
183555 (SO_1)	.608	.001	.0	.0	.0845	.014	-.002	.0	.0
185555 (OO_1)	.608	.001	.0	.0	.0845	.014	-.002	.0	.0
195455 (ν_1)	.607	.001	.0	.0	.0845	.014	-.002	.0	.0
2) any l=2 m=2 (semi-diurnal)	.609	.001	.0	.0	.0857	.014	-.001	.001	.0
3) any l=2 m=0 (long period)	.606	.001	.0	.0	.0844	.014	-.002	.0	.0
4) any l=3 m=3 (ter-diurnal)	.292	.001	.0	.0	.0154	.040	-.006	-.006	.0
5) any l=3 m=2 (semi-diurnal)	.290	.001	-.001	.0	.0152	.040	-.007	-.007	-.082

are given in Tables 1-18 for a set of 22 important diurnal frequencies. It is possible to generate results for larger sets of frequencies by using the eigenfunction expansion, (4.58). In particular any scalar, α, in (9.3) is written as

$$(9.7) \qquad \alpha = \alpha_{o_1} + \frac{1}{2} \sum_n \left[\frac{(\underset{\sim}{f}, \underset{\sim}{s}_n)}{\omega_n (\underset{\sim}{s}_n, \underset{\sim}{s}_n) - (\underset{\sim}{s}_n, i\underset{\sim}{\Omega} \times \underset{\sim}{s}_n)} \frac{\omega - \omega_{o_1}}{(\omega_n - \omega)(\omega_n - \omega_{o_1})} \right] \alpha_n$$

where α_{o_1} and α_n are the computed values of α for the non-resonant base tide (o_1) and the nth normal mode, respectively. We rewrite (9.7) as

$$(9.8) \qquad \alpha = \alpha_{o_1} + \sum_n A_n(\alpha) \frac{\omega - \omega_{o_1}}{\omega_n - \omega}$$

where

$$(9.9) \qquad A_n = \frac{1}{2} \frac{(\underset{\sim}{f}, \underset{\sim}{s}_n)}{\omega_n (\underset{\sim}{s}_n, \underset{\sim}{s}_n) - (\underset{\sim}{s}_n, i\underset{\sim}{\Omega} \times \underset{\sim}{s}_n)} \frac{\alpha_n}{\omega_n - \omega_{o_1}}$$

If we give $A_n(\alpha)$ for each pertinent normal mode, s_n, and each scalar, α, then we have prescribed frequency dependent analytical expressions for the $\{\alpha\}$. To keep confusion to a minimum we choose to use (9.8) in an approximate sense. First, the $A_n(\alpha)$ and α_o are given only for the scalars k_o, h_o and ℓ_o. These correspond roughly to the familiar spherical Love numbers.

Approximate results for any other scalar in (9.3) can then be found using the spherical correspondence presented in (9.4). Second, the $A_n(\alpha)$ are found only for the resonant NDFW.

Consequently,

$$k_o = k_{o_1} + k_{NDFW} \frac{\lambda - \lambda_{o_1}}{\lambda_{NDFW} - \lambda} \tag{9.10}$$

$$h_o = h_{o_1} + h_{NDFW} \frac{\lambda - \lambda_{o_1}}{\lambda_{NDFW} - \lambda}$$

$$\ell_o = \ell_{o_1} + \ell_{NDFW} \frac{\lambda - \lambda_{o_1}}{\lambda_{NDFW} - \lambda}$$

where $\lambda_{o_1} = \frac{\omega_{o_1}}{\Omega}$ and $\lambda_{NDFW} = \frac{\omega_{NDFW}}{\Omega}$ are the frequencies of the 0_1 tide and NDFW in cycles per sidereal day. The coefficients k_{o_1}, k_{NDFW}, ℓ_{o_1}, ℓ_{NDFW}, h_{o_1}, h_{NDFW}, λ_{o_1} and λ_{NDFW} are listed in Tables 19-23 for all five Earth models. Tables 19-23 also allow us to compare the NDFW eigenfrequency, λ_{NDFW}, between structural models. The maximum difference in period is between C2 and stable 1066A and amounts to only about three days as seen in inertial space. Such a slight offset may not be numerically significant.

The results, (9.10), for h_o, k_o and ℓ_o appear accurate to within the .3% level suggested as the computational accuracy in Chapter V. Of course, the relationships, (9.4), between h_o, k_o and ℓ_o and the other scalars on a spherical Earth necessarily contain small errors of the order of ellipticity. Results for k_o, ℓ_o and h_o are presented in Figures 8-10 as functions of

TABLE 19

EXPANSION COEFFICIENTS FOR 1066A

	h	l	k	B	λ
O_1 Tide	.603	.0842	.298	.416	.92700
NDFW	-2.46×10^{-3}	7.81×10^{-5}	-1.23×10^{-3}	.665	1.0021714
CW				.810	-2.48×10^{-3}
Rigid CW				1.06	-3.28×10^{-3}

TABLE 20

EXPANSION COEFFICIENTS FOR NEUTRAL 1066A

	h	l	k	B	λ
O_1 Tide	.603	.0842	.298	.418	.92700
NDFW	-2.46×10^{-3}	7.82×10^{-5}	-1.24×10^{-3}	.667	1.0021716
CW				.810	-2.48×10^{-3}
Rigid CW				1.06	-3.28×10^{-3}

TABLE 21

EXPANSION COEFFICIENTS FOR STABLE 1066A

	h	l	k	B	λ
O_1 Tide	.603	.0842	.298	.418	.92700
NDFW	-2.46×10^{-3}	7.83×10^{-5}	-1.24×10^{-3}	.667	1.0021708
CW				.810	-2.48×10^{-3}
Rigid CW				1.06	-3.28×10^{-3}

TABLE 22

EXPANSION COEFFICIENTS FOR PEM-C

	h	l	k	B	λ
O_1 Tide	.602	.0839	.298	.417	.92700
NDFW	-2.46×10^{-3}	7.69×10^{-5}	-1.24×10^{-3}	.666	1.0021771
CW				.814	-2.48×10^{-3}
Rigid CW				1.06	-3.28×10^{-3}

TABLE 23

EXPANSION COEFFICIENTS FOR C2

	h	l	k	B	λ
O_1 Tide	.602	.0846	.298	.397	.92700
NDFW	-2.45×10^{-3}	7.58×10^{-5}	-1.23×10^{-3}	.661	1.0021844
CW				.608	-2.48×10^{-3}
Rigid CW				1.06	-3.28×10^{-3}

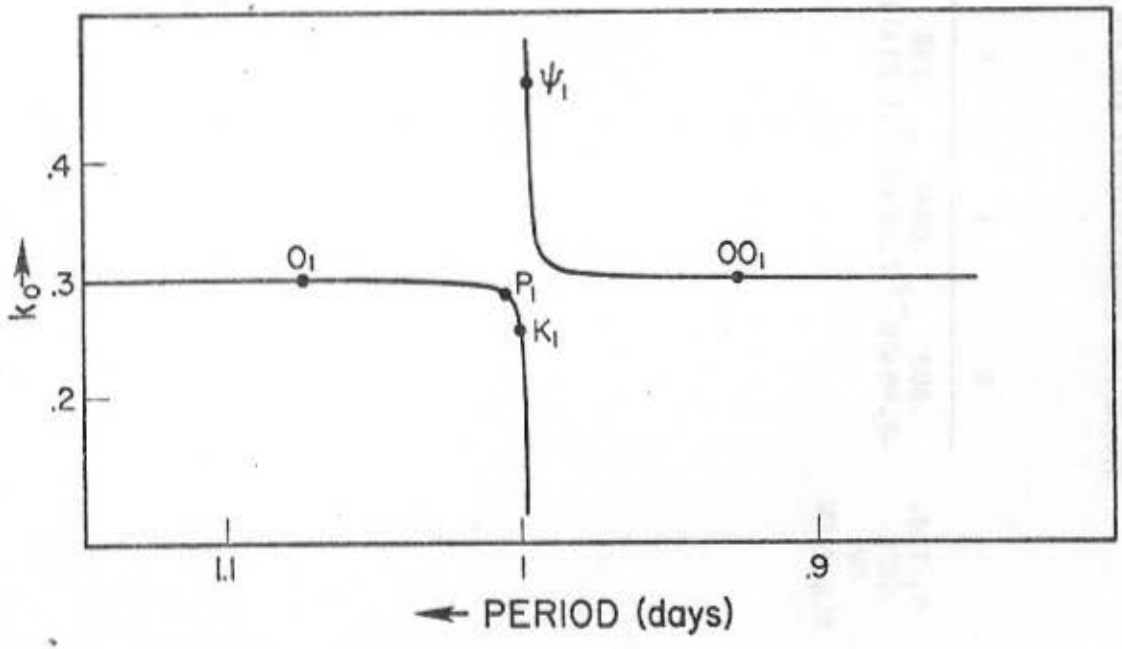

Figure 8. Diurnal frequency dependence of the Love number, k_o.

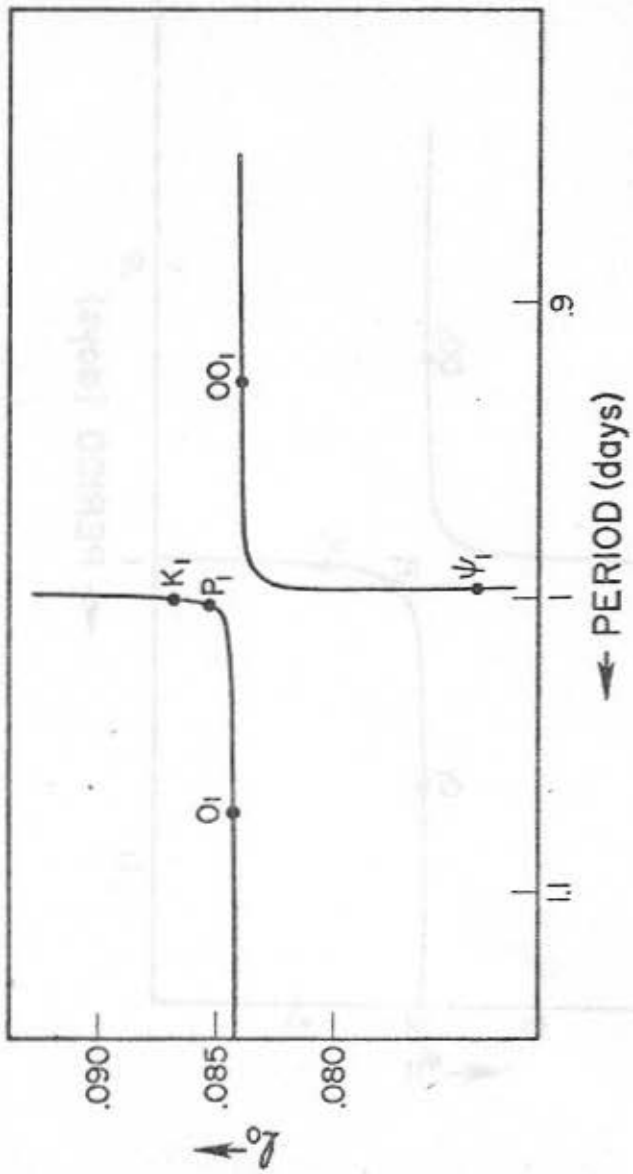

Figure 9. Diurnal frequency dependence of the Love number, ℓ_o.

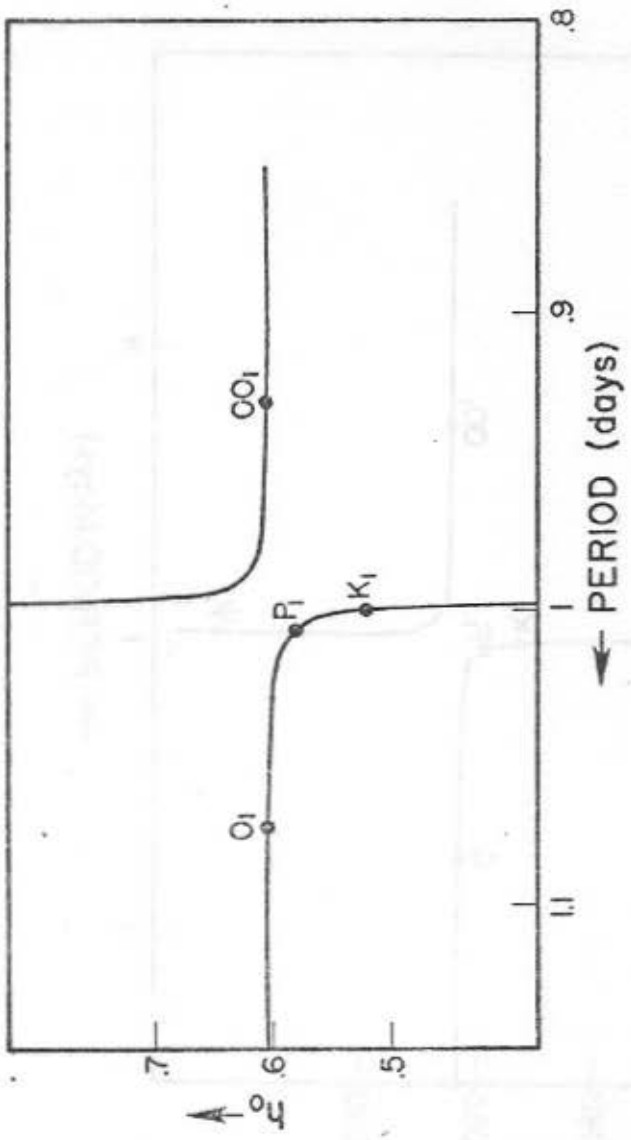

Figure 10. Diurnal frequency dependence of the Love number, h_o.

frequency over the diurnal band for model 1066A. In each case, the NDFW resonance is superimposed on the nearly frequency independent free oscillation contributions. It is instructive to compare these diurnal tidal results with the results of other theories. A precise, absolute comparison is difficult because of the more complex latitude dependence predicted here for the tides. However, we can get a general idea of the differences by examining the shape of the NDFW resonance. This is effectively accomplished by comparing changes in the Love numbers as we progress across the diurnal band. Tables 24-26 compare the results for k_o, h_o and ℓ_o computed here for models neutral 1066A, PEM-C and C2 with the corresponding results of Molodensky's (1961) Model II and the neutrally stable (i.e. $\beta = 0$) model of Shen and Mansinha (1976). The numbers in Tables 24-26 are ratios of the appropriate Love numbers at the given frequency to the corresponding value at the 0_1 frequency. In general, differences between our three structural models are noticeably smaller than our general disagreement with Molodensky (1961). Agreement with Shen and Mansinha (1976) is quite good except for ℓ_o, where their results exhibit some very peculiar frequency dependence.

TABLE 24

RATIOS OF THE LOVE NUMBER, k_o, TO ITS VALUE AT 0_1

	Neutral 1066A	PEM-C	C2	Molodensky Model II	Shen & Mansinha $\beta = 0$
M_1	.997	.997	.997	.997	.996
P_1	.963	.963	.963	.967	.962
K_1	.859	.859	.862	.870	.854
ψ_1	1.564	1.567	1.574	1.517	1.566
ϕ_1	1.101	1.097	1.101	1.093	1.102
J_1	1.013	1.013	1.013	1.013	1.014

TABLE 25

RATIOS OF THE LOVE NUMBER, h_o, TO ITS VALUE AT 0_1

	Neutral 1066A	PEM-C	C2	Molodensky Model II	Shen & Mansinha $\beta = 0$
M_1	.995	.995	.997	.997	.996
P_1	.964	.964	.965	.966	.963
K_1	.862	.862	.865	.871	.867
ψ_1	1.554	1.557	1.565	1.511	1.557
ϕ_1	1.098	1.096	1.098	1.091	1.101
J_1	1.013	1.013	1.013	1.011	1.014

TABLE 26

RATIOS OF THE LOVE NUMBER, ℓ_o, TO ITS VALUE AT 0_1

	Neutral 1066A	PEM-C	C2	Molodensky Model II	Shen & Mansinha $\beta = 0$
M_1	1.001	1.001	1.001	1.001	1.001
P_1	1.010	1.008	1.008	1.009	.902
K_1	1.032	1.031	1.031	1.035	.924
ψ_1	.875	.876	.877	.862	.777
ϕ_1	.979	.979	.979	.975	.873
J_1	.998	.998	.998	.996	.891

9.3 Nutation Results

The complete diurnal tidal motion comprises both body tide and nutational components. Separation of these two phenomena is discussed at some length in Chapter VII, where the Tisserand mean figure axis of the surface, $\underset{\sim}{B}$, is defined as the axis most naturally representing the observational consequences of nutation.

The most important normal mode contributions to $\underset{\sim}{B}$ come from the TOM, the CW and the NDFW. Free oscillation effects on $\underset{\sim}{B}$ are minor and essentially frequency independent over the diurnal band. Consequently, the eigenfunction expansion, (4.58), can be applied as in Section 9.2 to give an amplitude for $\underset{\sim}{B}$ of

$$(9.11) \qquad |\underset{\sim}{B}| = A_{o_1} + A_{TOM} \frac{\lambda - \lambda_{o_1}}{\lambda_{TOM} - \lambda} + A_{CW} \frac{\lambda - \lambda_{o_1}}{\lambda_{CW} - \lambda} + A_{NDFW} \frac{\lambda - \lambda_{o_1}}{\lambda_{NDFW} - \lambda}$$

(The CW and TOM were not necessary in (9.10) because of their small (or non-existent) accompanying deformation.) A dimensionless plot of B versus frequency is presented in Figure 11, where the dominant TOM contribution is shown separately. The NDFW excitation is approximately proportional only to the relative torque between the core and mantle and consequently its resonance is quite narrow.

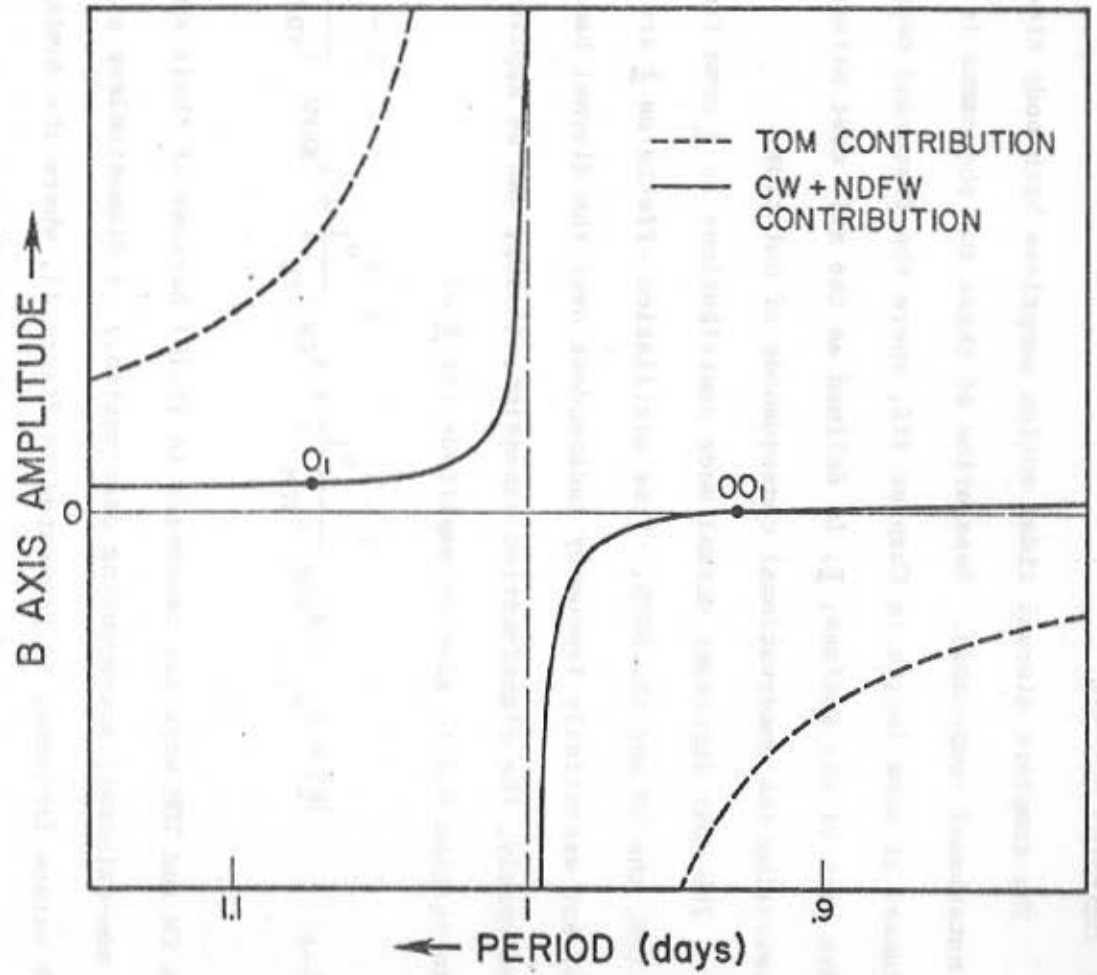

Figure 11. Frequency dependence of the amplitude of the nutating axis, $\underset{\sim}{\beta}$, computed for an assumed frequency independent tidal potential. The large TOM contribution is shown separately.

It is, however, broader than the NDFW resonance in the Love numbers - a consequence of the fact that in the mantle the NDFW is mostly a rigid rotation. Its contribution to $|B|$ is shown in Figure 11 as superimposed on a small non-zero offset - the CW contribution to (9.11).

As discussed in Chapter VII, it proves most expedient to remove the resonant TOM contribution by considering, instead, B_{ratio} - the ratio of the elastic contributions in (9.11) to the amplitude of the rigid Earth figure axis (see equation 7.46). Using the rigid Earth development presented in Section 7.2 gives

$$(9.12) \qquad B_{ratio} = \left[B_{o_1} + B_{CW} \frac{\lambda-\lambda_{o_1}}{\lambda_{CW}-\lambda} - B_{CW_{rigid}} \frac{\lambda-\lambda_{o_1}}{\lambda_{CW_{rigid}}-\lambda} + B_{NDFW} \frac{\lambda-\lambda_{o_1}}{\lambda_{NDFW}-\lambda} \right] \quad [1-\lambda]\left[\lambda-\lambda_{CW_{rigid}}\right]$$

where λ, λ_{NDFW}, λ_{CW} and $\lambda_{CW_{rigid}}$ are the tidal frequency, NDFW frequency, CW frequency and the frequency of the CW on a rigid Earth, all in cycles per sidereal day; and B_{o_1}, B_{CW}, $B_{CW_{rigid}}$ and B_{NDFW} are suitably defined constants. Numerical results for the $\{\lambda\}$ and $\{B\}$ (using $\frac{C-A}{C}$ = .003273952 (Kinoshita, 1977)) are given in Tables 19-23 for all five Earth models. (The notable difference

between B_{CW} for C2 and for the other models seems to be associated with differences in the fluid core CW deformation; the corresponding nutational effects are not large.)

A plot of B_{ratio} versus frequency is given in Figure 12 for model 1066A. The most notable feature is the pronounced NDFW resonance. The constant background slope and the zero crossing at exactly one sidereal day merely reflect division by the results for a rigid Earth.

A complete set of numerical values for B_{ratio} for 1066A is presented in Table 27. Kinoshita's (1977) frequency set is chosen here and his ordering procedure is adopted. Both Brown's (1919) fundamental arguments (ℓ , ℓ', F, D, Ω) and the corresponding Doodson numbers are shown here and his ordering procedure is adopted. The ratios in Table 27 are then convolved with Kinoshita's theory for the figure axis of a rigid Earth, using orbital elements computed at epoch 2000 (results privately communicated by T. Sasao). The resulting perturbations in longitude and obliquity of the axis, B, are shown in Table 28, in units of .0001 seconds of arc.

Longitude and obliquity perturbations are also given for model C2 in Table 29. Although these results for C2 do differ from the results for the other structural models, it is evident from Tables 28 and 29 that agreement is actually quite good. In particular, differences in longitude and obliquity between C2 and

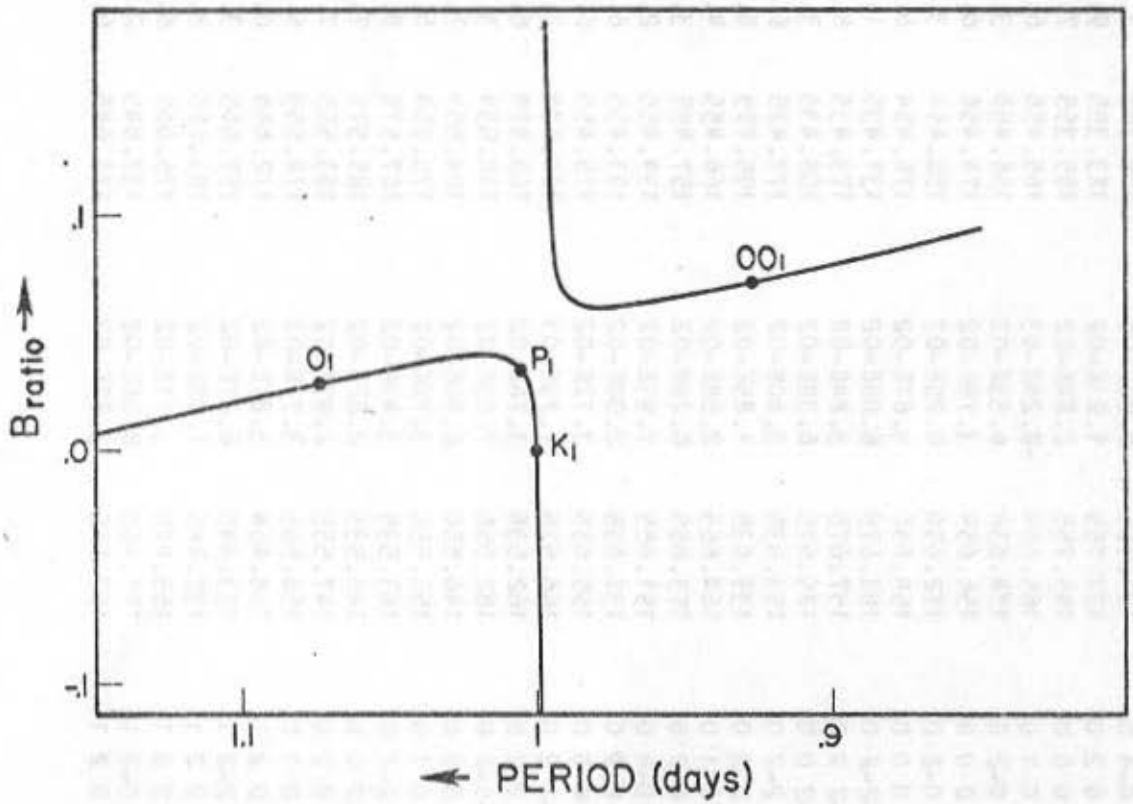

Figure 12. Frequency depencence of B_{ratio} - the elastic contribution to the nutating axis, $\underset{\sim}{B}$.

TABLE 27

RELATIVE NUTATIONS OF B_{ratio} FOR 1066A

	Argument	Negative		Positive	
	l l' F D Ω	Doodson no	ratio	Doodson no	ratio
1	3 0 0 0 0	135.855	1.87E-02	195.255	8.19E-02
2	2 1 0-2 0	162.756	3.69E-02	168.354	7.26E-02
3	2 0-2 0 0	165.775	-3.61E-02	165.335	1.46E-02
4	2 0 0-2 0	163.755	3.33E-02	167.355	9.25E-02
5	2 0 0-4 0	181.755	6.97E-02	149.355	3.09E-02
6	2 0 0 2 0	127.755	1.01E-02	1X3.355	9.05E-02
7	2 0 0 0 0	145.755	2.84E-02	185.355	7.22E-02
8	1-1 0-1 0	165.654	-8.24E-03	165.456	6.17E-03
9	1-1 0-2 0	174.654	6.33E-02	156.456	3.77E-02
10	1-1 0 0 0	156.654	3.78E-02	174.456	6.32E-02
11	1 1 0-2 0	172.656	6.25E-02	158.454	3.87E-02
12	1 1 0 0 0	154.656	3.67E-02	176.454	6.42E-02
13	1 0-2-2 0	193.675	8.08E-02	137.435	1.98E-02
14	1 0-2 2 0	157.675	3.84E-02	173.435	6.27E-02
15	1 0-2 0 0	175.675	6.38E-02	155.435	3.70E-02
16	1 0 2-2 0	153.635	3.60E-02	177.475	6.48E-02
17	1 0 2 0 0	135.635	1.85E-02	195.475	8.21E-02
18	1 0 0-1 0	164.655	2.58E-02	166.455	4.87E-01
19	1 0 0-2 0	173.655	6.28E-02	157.455	3.82E-02
20	1 0 0-4 0	191.655	7.93E-02	139.455	2.14E-02
21	1 0 0 2 0	137.655	2.00E-02	193.455	8.06E-02
22	1 0 0 0 0	155.655	3.72E-02	175.455	6.37E-02
23	0 1-2 2 0	166.576	1.79E-01	164.534	2.84E-02
24	0 1 2-2 0	162.536	3.76E-02	168.574	6.99E-02
25	0 1 0-2 0	182.556	7.03E-02	148.554	3.04E-02
26	0 1 0 2 0	146.556	2.90E-02	184.554	7.17E-02
27	0 1 0 1 0	155.556	3.72E-02	175.554	6.37E-02
28	0 0 2-2 0	163.535	3.49E-02	167.575	8.24E-02
29	0 0 2 0 0	145.535	2.82E-02	185.575	7.25E-02
30	0 0 0 2 0	147.555	2.97E-02	183.555	7.10E-02
31	0 0 0 1 0	156.555	3.77E-02	174.555	6.32E-02
32	-1-1 0 2 1	158.464	3.87E-02	172.646	6.24E-02
33	-1 0 2-2 1	173.445	6.27E-02	157.665	3.83E-02
34	-1 0 2 2 1	137.445	1.98E-02	193.665	8.08E-02
35	-1 0 2 0 1	155.445	3.71E-02	175.665	6.38E-02
36	-1 0 0-2 1	193.465	8.06E-02	137.645	2.00E-02
37	-1 0 0 2 1	157.465	3.82E-02	173.645	6.28E-02

TABLE 27 (contd)

RELATIVE NUTATIONS OF B_{ratio} FOR 1066A

	Argument					Negative		Positive	
	l	l'	F	D	Ω	Doodson no	ratio	Doodson no	ratio
38	-1	0	0	1	1	166.465	3.26E-01	164.645	2.65E-02
39	-1	0	0	0	1	175.465	6.37E-02	155.645	3.72E-02
40	-2	0	2	0	1	165.345	1.29E-02	165.765	-2.71E-02
41	-2	0	0	2	1	167.365	9.04E-02	163.745	3.36E-02
42	-2	0	0	0	1	185.365	7.23E-02	145.745	2.84E-02
43	2	0	-2	0	1	165.785	-4.74E-02	165.325	1.62E-02
44	2	0	2	-2	1	143.745	2.70E-02	187.365	7.37E-02
45	2	0	2	0	1	125.745	8.58E-03	1X5.365	9.21E-02
46	2	0	0	-2	1	163.765	3.31E-02	167.345	9.48E-02
47	2	0	0	0	1	145.765	2.85E-02	185.345	7.22E-02
48	1	1	0	-2	1	172.666	6.25E-02	158.444	3.86E-02
49	1	0	2	-2	1	153.645	3.60E-02	177.465	6.48E-02
50	1	0	2	2	1	117.645	-1.03E-04	1E3.465	1.01E-01
51	1	0	2	0	1	135.645	1.85E-02	195.465	8.21E-02
52	1	0	0	-2	1	173.665	6.29E-02	157.445	3.82E-02
53	1	0	0	2	1	137.665	2.01E-02	193.445	8.05E-02
54	1	0	0	0	1	155.665	3.73E-02	175.445	6.36E-02
55	0	-1	2	-2	1	164.544	2.78E-02	166.566	2.06E-01
56	0	-1	2	0	1	146.544	2.89E-02	184.566	7.17E-02
57	0	-1	0	0	1	166.564	2.06E-01	164.546	2.78E-02
58	0	1	2	-2	1	162.546	3.75E-02	168.564	7.03E-02
59	0	1	2	0	1	144.546	2.75E-02	186.564	7.31E-02
60	0	1	0	0	1	164.566	2.66E-02	166.544	3.16E-01
61	0	0	-2	2	1	167.585	8.12E-02	163.525	3.51E-02
62	0	0	-2	0	1	185.585	7.25E-02	145.525	2.82E-02
63	0	0	2	-2	1	163.545	3.47E-02	167.565	8.36E-02
64	0	0	2	2	1	127.545	9.92E-03	1X3.565	9.07E-02
65	0	0	2	0	1	145.545	2.82E-02	185.565	7.24E-02
66	0	0	0	-2	1	183.565	7.10E-02	147.545	2.97E-02
67	0	0	0	2	1	147.565	2.97E-02	183.545	7.09E-02
68	0	0	0	0	1	165.565	-3.60E-03	165.545	3.14E-03
69	-1	-1	2	2	2	138.454	2.06E-02	192.656	8.00E-02
70	-1	0	4	0	2	135.435	1.83E-02	195.675	8.23E-02
71	-1	0	2	4	2	119.455	1.28E-03	1E1.655	9.94E-02
72	-1	0	2	2	2	137.455	1.99E-02	193.655	8.07E-02
73	-1	0	2	0	2	155.455	3.71E-02	175.655	6.38E-02
74	-1	0	0	0	2	175.475	6.37E-02	155.635	3.72E-02

TABLE 27 (contd)

RELATIVE NUTATIONS OF B_{ratio} FOR 1066A

	Argument					Negative		Positive	
	l	l'	F	D	Ω	Doodson no	ratio	Doodson no	ratio
75	-2	0	2	4	2	129.355	1.13E-02	1X1.755	8.93E-02
76	-2	0	2	2	2	147.355	2.95E-02	183.755	7.11E-02
77	-2	0	2	0	2	165.355	1.10E-02	165.755	-1.98E-02
78	3	0	2	-2	2	133.855	1.72E-02	197.255	8.34E-02
79	3	0	2	0	2	115.855	-1.41E-03	1E5.255	1.02E-01
80	2	0	2	-2	2	143.755	2.70E-02	187.355	7.36E-02
81	2	0	2	2	2	107.755	-1.01E-02	1G3.355	1.11E-01
82	2	0	2	0	2	125.755	8.62E-03	1X5.355	9.20E-02
83	1	-1	2	0	2	136.654	1.93E-02	194.456	8.13E-02
84	1	1	2	-2	2	152.656	3.54E-02	178.454	6.54E-02
85	1	1	2	0	2	134.656	1.78E-02	196.454	8.28E-02
86	1	0	2	-2	2	153.655	3.60E-02	177.455	6.48E-02
87	1	0	2	2	2	117.655	-6.18E-05	1E3.455	1.01E-01
88	1	0	2	0	2	135.655	1.86E-02	195.455	8.21E-02
89	1	0	0	0	2	155.675	3.73E-02	175.435	6.36E-02
90	0	-1	2	2	2	128.554	1.07E-02	1X2.556	8.99E-02
91	0	-1	2	0	2	146.554	2.90E-02	184.556	7.17E-02
92	0	1	2	0	2	144.556	2.75E-02	186.554	7.31E-02
93	0	1	0	0	2	164.576	2.59E-02	166.534	4.62E-01
94	0	0	4	-2	2	143.535	2.67E-02	187.575	7.39E-02
95	0	0	2	-1	2	154.555	3.66E-02	176.555	6.43E-02
96	0	0	2	4	2	109.555	-8.78E-03	1G1.555	1.09E-01
97	0	0	2	2	2	127.555	9.96E-03	1X3.555	9.07E-02
98	0	0	2	1	2	136.555	1.92E-02	194.555	8.14E-02
99	0	0	2	0	2	145.555	2.83E-02	185.555	7.24E-02
100	0	0	0	0	2	165.575	-7.77E-03	165.535	5.90E-03
101	0	2	0	0	0	163.557	3.44E-02	167.553	8.50E-02
102	0	1	0	0	0	164.556	2.72E-02	166.554	2.46E-01
103	0	-1	2	-2	2	164.554	2.72E-02	166.556	2.46E-01
104	0	2	2	-2	2	161.557	3.89E-02	169.553	6.58E-02
105	0	1	2	-2	2	162.556	3.74E-02	168.554	7.07E-02
106	0	0	2	-2	2	163.555	3.44E-02	167.555	8.50E-02

TABLE 28

NUTATIONS IN LONGITUDE AND OBLIQUITY OF THE

AXIS B FOR 1066A

	Argument l l' F D Ω	Period (days)	Longitude (.0001")	Obliquity (.0001")
1	3 0 0 0 0	9.2	2	0
2	2 1 0-2 0	131.7	1	0
3	2 0-2 0 0	1095.2	11	0
4	2 0 0-2 0	205.9	48	1
5	2 0 0-4 0	15.9	-1	0
6	2 0 0 2 0	7.1	1	0
7	2 0 0 0 0	13.8	29	-1
8	1-1 0-1 0	3232.9	-3	0
9	1-1 0-2 0	29.3	1	0
10	1-1 0 0 0	29.8	5	0
11	1 1 0-2 0	34.8	-7	0
12	1 1 0 0 0	25.6	-3	0
13	1 0-2-2 0	9.5	-1	0
14	1 0-2 2 0	32.8	-1	0
15	1 0-2 0 0	26.9	4	0
16	1 0 2-2 0	23.8	-1	0
17	1 0 2 0 0	9.1	3	0
18	1 0 0-1 0	411.8	-4	0
19	1 0 0-2 0	31.8	-158	-1
20	1 0 0-4 0	10.1	-1	0
21	1 0 0 2 0	9.6	6	0
22	1 0 0 0 0	27.6	712	-7
23	0 1-2 2 0	329.8	-1	0
24	0 1 2-2 0	117.5	-1	0
25	0 1 0-2 0	15.4	-4	0
26	0 1 0 2 0	14.2	-1	0
27	0 1 0 1 0	27.3	1	0
28	0 0 2-2 0	173.3	-22	0
29	0 0 2 0 0	13.6	26	-1
30	0 0 0 2 0	14.8	63	-2
31	0 0 0 1 0	29.5	-4	0
32	-1-1 0 2 1	35.0	1	0
33	-1 0 2-2 1	32.6	-2	1
34	-1 0 2 2 1	9.5	-10	5
35	-1 0 2 0 1	27.0	21	-10
36	-1 0 0-2 1	9.6	-2	1
37	-1 0 0 2 1	32.0	16	-8

TABLE 28 (contd)

NUTATIONS IN LONGITUDE AND OBLIQUITY OF THE

AXIS B FOR 1066A

	Argument l l' F D Ω	Period (days)	Longitude (.0001")	Obliquity (.0001")
38	-1 0 0 1 1	388.3	1	0
39	-1 0 0 0 1	27.4	-58	32
40	-2 0 2 0 1	1305.5	46	-24
41	-2 0 0 2 1	199.8	-6	3
42	-2 0 0 0 1	13.7	-2	1
43	2 0-2 0 1	943.2	1	0
44	2 0 2-2 1	12.8	1	-1
45	2 0 2 0 1	6.9	-5	3
46	2 0 0-2 1	212.3	4	-2
47	2 0 0 0 1	13.8	2	-1
48	1 1 0-2 1	34.7	-1	0
49	1 0 2-2 1	23.9	6	-3
50	1 0 2 2 1	5.6	-1	1
51	1 0 2 0 1	9.1	-51	27
52	1 0 0-2 1	31.7	-13	7
53	1 0 0 2 1	9.6	-1	0
54	1 0 0 0 1	27.7	63	-33
55	0-1 2-2 1	346.6	-5	3
56	0-1 2 0 1	14.2	-1	0
57	0-1 0 0 1	346.6	-12	6
58	0 1 2-2 1	119.6	4	-2
59	0 1 2 0 1	13.1	1	0
60	0 1 0 0 1	386.0	-15	9
61	0 0-2 2 1	169.0	1	0
62	0 0-2 0 1	13.6	-1	0
63	0 0 2-2 1	177.8	129	-70
64	0 0 2 2 1	7.1	-7	3
65	0 0 2 0 1	13.6	-386	200
66	0 0 0-2 1	14.7	-5	3
67	0 0 0 2 1	14.8	-6	3
68	0 0 0 0 1	6798.4	-171996	92025
69	-1-1 2 2 2	9.8	-3	1
70	-1 0 4 0 2	9.1	1	0
71	-1 0 2 4 2	5.8	-2	1
72	-1 0 2 2 2	9.6	-59	26
73	-1 0 2 0 2	27.1	123	-53
74	-1 0 0 0 2	27.3	1	-1

TABLE 28 (contd)

NUTATIONS IN LONGITUDE AND OBLIQUITY OF THE

AXIS B FOR 1066A

	Argument l l′ F D Ω	Period (days)	Longitude (.0001")	Obliquity (.0001")
75	-2 0 2 4 2	7.3	-1	1
76	-2 0 2 2 2	14.6	1	-1
77	-2 0 2 0 2	1615.7	-3	1
78	3 0 2-2 2	8.7	1	0
79	3 0 2 0 2	5.5	-3	1
80	2 0 2-2 2	12.8	6	-3
81	2 0 2 2 2	4.7	-1	0
82	2 0 2 0 2	6.9	-31	13
83	1-1 2 0 2	9.4	-3	1
84	1 1 2-2 2	22.5	1	-1
85	1 1 2 0 2	8.9	2	-1
86	1 0 2-2 2	23.9	29	-12
87	1 0 2 2 2	5.6	-8	3
88	1 0 2 0 2	9.1	-301	129
89	1 0 0 0 2	27.8	-2	1
90	0-1 2 2 2	7.2	-3	1
91	0-1 2 0 2	14.2	-7	3
92	0 1 2 0 2	13.2	7	-3
93	0 1 0 0 2	409.2	1	0
94	0 0 4-2 2	12.7	1	0
95	0 0 2-1 2	25.4	-1	0
96	0 0 2 4 2	4.8	-1	0
97	0 0 2 2 2	7.1	-38	16
98	0 0 2 1 2	9.3	2	-1
99	0 0 2 0 2	13.7	-2274	977
100	0 0 0 0 2	3399.2	2062	-895
101	0 2 0 0 0	182.6	17	0
102	0 1 0 0 0	365.3	1426	54
103	0-1 2-2 2	365.2	217	-95
104	0 2 2-2 2	91.3	-16	7
105	0 1 2-2 2	121.7	-517	224
106	0 0 2-2 2	182.6	-13187	5736

TABLE 29

NUTATIONS IN LONGITUDE AND OBLIQUITY OF THE

AXIS B FOR C2

	Argument l l' F D Ω	Period (days)	Longitude (.0001")	Obliquity (.0001"
1	3 0 0 0 0	9.2	2	0
2	2 1 0-2 0	131.7	1	0
3	2 0-2 0 0	1095.2	11	0
4	2 0 0-2 0	205.9	48	1
5	2 0 0-4 0	15.9	-1	0
6	2 0 0 2 0	7.1	1	0
7	2 0 0 0 0	13.8	29	-1
8	1-1 0-1 0	3232.9	-3	0
9	1-1 0-2 0	29.3	1	0
10	1-1 0 0 0	29.8	5	0
11	1 1 0-2 0	34.8	-7	0
12	1 1 0 0 0	25.6	-3	0
13	1 0-2-2 0	9.5	-1	0
14	1 0-2 2 0	32.8	-1	0
15	1 0-2 0 0	26.9	4	0
16	1 0 2-2 0	23.8	-1	0
17	1 0 2 0 0	9.1	3	0
18	1 0 0-1 0	411.8	-4	0
19	1 0 0-2 0	31.8	-157	-1
20	1 0 0-4 0	10.1	-1	0
21	1 0 0 2 0	9.6	6	0
22	1 0 0 0 0	27.6	712	-7
23	0 1-2 2 0	329.8	-1	0
24	0 1 2-2 0	117.5	-1	0
25	0 1 0-2 0	15.4	-4	0
26	0 1 0 2 0	14.2	-1	0
27	0 1 0 1 0	27.3	1	0
28	0 0 2-2 0	173.3	-22	0
29	0 0 2 0 0	13.6	26	-1
30	0 0 0 2 0	14.8	63	-2
31	0 0 0 1 0	29.5	-4	0
32	-1-1 0 2 1	35.0	1	0
33	-1 0 2-2 1	32.6	-2	1
34	-1 0 2 2 1	9.5	-10	5
35	-1 0 2 0 1	27.0	21	-10
36	-1 0 0-2 1	9.6	-2	1
37	-1 0 0 2 1	32.0	16	-8

TABLE 29 (contd)

NUTATIONS IN LONGITUDE AND OBLIQUITY OF THE

AXIS B FOR C2

	Argument l l' F D Ω	Period (days)	Longitude (.0001")	Obliquity (.0001")
38	-1 0 0 1 1	388.3	1	0
39	-1 0 0 0 1	27.4	-58	32
40	-2 0 2 0 1	1305.5	46	-24
41	-2 0 0 2 1	199.8	-6	3
42	-2 0 0 0 1	13.7	-2	1
43	2 0-2 0 1	943.2	1	0
44	2 0 2-2 1	12.8	1	-1
45	2 0 2 0 1	6.9	-5	3
46	2 0 0-2 1	212.3	4	-2
47	2 0 0 0 1	13.8	2	-1
48	1 1 0-2 1	34.7	-1	0
49	1 0 2-2 1	23.9	6	-3
50	1 0 2 2 1	5.6	-1	1
51	1 0 2 0 1	9.1	-51	27
52	1 0 0-2 1	31.7	-13	7
53	1 0 0 2 1	9.6	-1	0
54	1 0 0 0 1	27.7	63	-33
55	0-1 2-2 1	346.6	-5	3
56	0-1 2 0 1	14.2	-1	0
57	0-1 0 0 1	346.6	-12	6
58	0 1 2-2 1	119.6	4	-2
59	0 1 2 0 1	13.1	1	0
60	0 1 0 0 1	386.0	-15	9
61	0 0-2 2 1	169.0	1	0
62	0 0-2 0 1	13.6	-1	0
63	0 0 2-2 1	177.8	129	-70
64	0 0 2 2 1	7.1	-7	3
65	0 0 2 0 1	13.6	-386	200
66	0 0 0-2 1	14.7	-5	3
67	0 0 0 2 1	14.8	-6	3
68	0 0 0 0 1	6798.4	-172006	92028
69	-1-1 2 2 2	9.8	-3	1
70	-1 0 4 0 2	9.1	1	0
71	-1 0 2 4 2	5.8	-2	1
72	-1 0 2 2 2	9.6	-59	25
73	-1 0 2 0 2	27.1	123	-53
74	-1 0 0 0 2	27.3	1	-1

TABLE 29 (contd)

NUTATIONS IN LONGITUDE AND OBLIQUITY OF THE

AXIS B FOR C2

	Argument l l' F D Ω	Period (days)	Longitude (.0001")	Obliquity (.0001")
75	-2 0 2 4 2	7.3	-1	1
76	-2 0 2 2 2	14.6	1	-1
77	-2 0 2 0 2	1615.7	-3	1
78	3 0 2-2 2	8.7	1	0
79	3 0 2 0 2	5.5	-3	1
80	2 0 2-2 2	12.8	6	-3
81	2 0 2 2 2	4.7	-1	0
82	2 0 2 0 2	6.9	-31	13
83	1-1 2 0 2	9.4	-3	1
84	1 1 2-2 2	22.5	1	-1
85	1 1 2 0 2	8.9	2	-1
86	1 0 2-2 2	23.9	29	-12
87	1 0 2 2 2	5.6	-8	3
88	1 0 2 0 2	9.1	-300	128
89	1 0 0 0 2	27.8	-2	1
90	0-1 2 2 2	7.2	-3	1
91	0-1 2 0 2	14.2	-7	3
92	0 1 2 0 2	13.2	7	-3
93	0 1 0 0 2	409.2	1	0
94	0 0 4-2 2	12.7	1	0
95	0 0 2-1 2	25.4	-1	0
96	0 0 2 4 2	4.8	-1	0
97	0 0 2 2 2	7.1	-38	16
98	0 0 2 1 2	9.3	2	-1
99	0 0 2 0 2	13.7	-2271	976
100	0 0 0 0 2	3399.2	2062	-895
101	0 2 0 0 0	182.6	17	0
102	0 1 0 0 0	365.3	1429	55
103	0-1 2-2 2	365.2	217	-95
104	0 2 2-2 2	91.3	-16	7
105	0 1 2-2 2	121.7	-517	224
106	0 0 2-2 2	182.6	-13184	5735

1066A amount to about .4 msec of arc for the 18.6 year term and are never more than .1 msec of arc at other frequencies.

Table 30 shows eight important frequency results for B_{ratio} as computed for models PEM-C, C2, neutral 1066A and stable 1066A. Most notable differences seem to occur near the NDFW resonance. However, results for 1066A and its two fluid core variants do not differ significantly.

The other physical axes defined in Chapter VII are presented in Table 31 for model 1066A for eight important frequencies. Molodensky's (1961) results for $\underset{\sim}{I}_M$ have also been included. Several features deserve discussion.

The angular momentum for the Earth, $\underset{\sim}{H}_E$, is exactly determined by the luni-solar torque and is independent of the elastic response of the Earth. As a result, the $\underset{\sim}{H}_E$ ratio shown in Table 31 should vanish identically. Consequently, the non-zero values presented there serve as an independent check on the numerical procedures used and may be regarded as estimates of the absolute errors in the other axes. In most cases this error amounts to approximately one or two percent of the total axis ratio. (The absolute errors in the figure axes, $\underset{\sim}{F}_M$ and $\underset{\sim}{F}_s$, are, in general, somewhat larger due to independent error sources. However, their values in Table 31 should also be accurate to 1 percent.) Since computation of $\underset{\sim}{H}_E$ involves integration of the tidal solution over the Earth's volume, its deviation from zero is probably mostly a measure of

TABLE 30

VALUES OF THE OBSERVATIONAL AXIS, B, FOR 4 OF THE 5 EARTH MODELS.
H_E REPRESENTS AN ABSOLUTE ERROR ESTIMATION

Doodson tidal Variables	PEM-C		1066A neutral		1066A stable		C_2	
	B	H_E	B	H_E	B	H_E	B	H_E
145.555	.0283	.00022	.0284	.00031	.0284	.00032	.0270	-.0014
163.555	.0344	.00019	.0345	.00027	.0345	.00027	.0342	.0001
164.556	.0272	.00015	.0273	.00021	.0273	.00021	.0270	.0001
165.545	.00314	.000017	.00315	.000024	.00315	.000024	.00310	-.000012
165.565	-.00359	-.000019	-.00361	-.000027	-.00361	-.000027	-.00356	-.000014
166.554	.249	.00133	.247	.0019	.247	.0019	.251	.0011
167.555	.0852	.00045	.0852	.00063	.0852	.00064	.0848	.0004
185.555	.0725	.00037	.0725	.00046	.0725	.00045	.0711	.0001

TABLE 31

COMPLETE AXIS SET FOR MODEL 1066A. NUMBERS REPRESENT RATIOS OF THE NON-RIGID CONTRIBUTIONS TO THE CORRESPONDING RIGID BODY RESULTS. H_E GIVES AN ABSOLUTE ERROR ESTIMATION (SEE TEXT)

Doodson tidal Variables	corresponding nutational term	B	I_M	I_E	H_E	H_M	F_M	F_s	I_N Molodensky Model I	I_N Molodensky Model II
145.555	fortnightly	.0283	.0283	-.0230	.00021	.0488	5.74	4.62	.026	.022
163.555	semi-annual	.0344	.0344	-.0015	.00025	.0359	.478	.394	.0359	.0316
164.556	annual	.0273	.0273	-.0007	.00020	.0280	.245	.205	.0286	.0251
165.545	18.6 year	.00314	.00314	-.00003	.000023	.00318	.0141	.0123	.00333	.00291
165.565	18.6 year	-.00360	-.00360	.00002	-.000026	-.00364	-.0144	-.0126	-.00383	-.00334
166.554	annual	.246	.246	.002	.0018	.245	-.0977	-.00483	.247	.225
167.555	semi-annual	.0850	.0850	.0023	.00063	.0833	-.418	-.311	.0884	.0786
185.555	fortnightly	.0724	.0724	.0237	.00055	.0517	-6.58	-5.27	.080	.071

the accuracy of that integration. Consequently, it provides a fairly conservative error estimate for the non-integrated axis, $\underset{\sim}{B}$.

It is convenient to think of the values in Table 31 as resulting from two distinct phenomena: 1) elastic deformation in the mantle, and 2) near resonance excitation of the Nearly Diurnal Free Wobble. The NDFW differential rotation between core and mantle is clearly evident in Table 31 by comparing $\underset{\sim}{H}_M$ with $\underset{\sim}{H}_E$ or $\underset{\sim}{I}_M$ with $\underset{\sim}{I}_E$ at any of the tidal lines. The differences are the largest at 166.554 which lies very near the Nearly Diurnal Free Wobble eigenfrequency.

The elastic mantle deformation, on the other hand, is particularly evident at those frequencies, such as 145.555 and 185.555, which are farthest from the Nearly Diurnal Free Wobble. Here, differences between the mantle angular momentum, $\underset{\sim}{H}_M$, and the mean mantle rotation, $\underset{\sim}{I}_M$, are quite pronounced, suggesting the inadequacy of $\underset{\sim}{H}_M$ as an observational reference axis. In addition, as predicted, the figure axes $\underset{\sim}{F}_M$ and $\underset{\sim}{F}_S$ are strongly perturbed by the mantle deformation. They are included in Table 31 strictly for illustrative purposes.

In Table 32 we compare our nutation results for 1066A with those of earlier theories for a small set of important frequencies. Kinoshita's (1977) results for the figure axis of a rigid Earth are shown as are the non-rigid results of Molodensky (1961), Shen and Mansinha (1976), and Sasao et al. (1979) for the Tisserand mean figure axis of

TABLE 32

A comparison of the nutations of the axis, B,

with the results of other theories

	18.6 years		1 year		6 months		13.7 days	
	Obliquity	Longitude	Obliquity	Longitude	Obliquity	Longitude	Obliquity	Longitude
Present Theory	9.2025"	-6.8416"	.0054"	.0567"	.5736"	-.5245"	.0977"	-.0905"
Kinoshita (rigid Earth)	9.2278	-6.8743	-.0001	.0499	.5534	-.5082	.0949	-.0881
Molodensky (Model II)	9.2044	-6.8441	.0049	.0561	.5719	-.5232	.0972	-.0899
Shen and Mansinha	9.1966	-6.8328			.5768	-.5274	.0973	-.0899
Sasao, et al (Wang model)	9.2018	-6.8407	.0051	.0565	.5739	-.5249	.0977	-.0904

the mantle (although our results describe motion of the Tisserand mean figure axis of the surface, differences between the two axes have been shown above to be insignificant). Molodensky's (1961) results in Table 32 are found by convolving his elastic nutation corrections, $\frac{\varepsilon-\varepsilon_o}{\varepsilon_o}$, for his Model II with Kinoshita's (1977) rigid Earth figure axis (convolution results privately communicated by T.Sasao), and are the results currently favored for adoption by the IAU Working Group on Nutation (P. K. Seidelmann, personal communication).

The most pronounced absolute differences between the rigid and non-rigid results occur at 18.6 years and at six months, with offsets of around .02" to .03" (seconds of arc). Differences between the non-rigid results are smaller, but still potentially important. For example, results for both the 18.6 year and six month nutations differ between our model and Molodensky's by around .002": about 10% of the total non-rigid correction. This can be compared with the difference between our results for 1066A and for C2 of .0004" for the 18.6 year nutation and .0001" for the six month term.

9.4 Changes in Angular Position of the Earth (UT1-UTC)

As discussed in Chapter VIII, the long period tidal solution consists of body tide components and an incremental rotation about the $\hat{\underset{\sim}{z}}$-axis. Relationships between the rotation amplitude, $\eta_s(\omega)$, and observations are given in equations (8.6). Results for $\omega\eta_s(\omega)$ for an assumed unit potential are nearly constant across the long period band and do not vary significantly between models. In particular, we find

(9.13) $$-i\omega\eta_g(\omega) = -.726 \text{ msec/sidereal day.}$$

By convolving with a long period potential theory we find frequency dependent amplitudes of UT1-UTC in msec as

(9.4) $$[\text{UT1-UTC}](\omega) = -H_s(\omega)\frac{\Omega}{\omega}(.726)\sin(\omega t+\alpha)$$

where the $\{H_s(\omega)\}$ represents equatorial coefficients in meters of the $\ell=2$ long period tidal potential, $\frac{\Omega}{\omega}$ is the period in sidereal days and α is the tidal phase. Taking the $\{H_s\}$ from Cartwright and Edden (1973) gives the UT1-UTC amplitudes for 1066A listed in the third column of Table 33. Only those terms with amplitude larger than .05 msec are kept. (The large annual (S_a) and semi-annual (S_{sa}) amplitudes must be added to even larger atmospheric contributions at the same frequencies to compare with observation. The total observed annual term, for example, is over ten times as large as predicted tidal contribution.)

Also in Table 33 are corresponding results for $\frac{2\pi\omega}{\Omega}$ [UT1-UTC](ω), with [UT1-UTC](ω) given by (9.14), which roughly corresponds to changes in the length of day ($\Delta\ell$od). The usual method of computing $\Delta\ell$od (see e.g. Munk and McDonald, 1960) uses conservation of angular momentum on an assumed solid Earth to equate

TABLE 33

TIDAL VARIATIONS IN ROTATION RATE

Doodson no	Period (days)	UT1-UTC (msec)	LOD Change (msec)	Solid Earth LOD (msec)
055.565	6798.4	-138.	-.127	-.142
055.575	3399.2	.693	.0013	.0014
056.554 (S_a)	365.3	1.31	.0224	.0251
056.556	365.2	-.069	-.0012	-.0013
057.555 (S_{sa})	182.6	4.12	.141	.158
057.565	177.8	-.100	-.0035	-.0039
058.554	121.7	.160	.0083	.0092
063.655	31.8	.156	.0307	.0343
065.455 (M_m)	27.6	.706	.160	.179
073.555	14.8	.063	.0266	.0297
075.555 (M_f)	13.7	.663	.304	.340
075.565	13.6	.274	.126	.141
085.455	9.1	.085	.0582	.0651

$$(9.15) \qquad \frac{\Delta \ell od}{\ell od} = \delta C_{33}/C$$

where δC_{33} is the tidally induced change in the Earth's greatest moment of inertia and C is the unperturbed greatest moment. Expressing δC_{33} in terms of the spherical Love number, k, as

$$(9.16) \qquad \delta C_{33} = k \frac{gR_E^3}{3G} \times \text{tidal potential}$$

gives

$$(9.17) \qquad \frac{\Delta \ell od}{\ell od} = \frac{k}{R_E} \times \text{tidal potential}$$

We have used (9.17) together with k = .299 to derive the fifth column in Table 33. Differences between these results and the correct values (fourth column) amount to around 10%. These discrepancies are caused by the fluid core. In particular, for our axisymmetric and non-dissipative model of the Earth, mantle rotation will not be affected by mass redistribution within the core. Consequently, (9.15) should be replaced by

$$(9.18) \qquad \frac{\Delta \ell od}{\ell od} = \delta C_{33}^M / C^M$$

where δC_{33}^{M} and C^{M} are computed for the mantle only. The use of (9.18) should give results identical to $\frac{2\pi\omega}{\Omega}$ [UT1-UTC](ω), which is used to compute the fourth column in Table 33.

CHAPTER X

SUMMARY

The tidal motions of the Earth are conveniently separated conceptually into the body tide (i.e. the Earth's deformation), the Earth's precession and nutation, and changes in the Earth's rotation rate. A separation is effected, above, which maintains the intuitive observational significance of each of these three phenomena.

The traditional use of Love numbers as dimensionless parameters representing the surface tidal deformation is complicated by rotation and ellipticity. The latitude dependence of the response becomes more involved, and new Love numbers must be defined to maintain 1% or better accuracy. The relationships between the various observational quantities (e.g. gravity, tilt, strain) and the Love numbers are also affected by ellipticity and rotation at the 1% level. Consequently, to successfully exploit the high accuracy of the body tide solution (one part in 300), we have found it useful to model each observable separately. In each case, small (< 1%) latitude dependent modifications must be added to the familiar, spherical results. Comparable differences are also found between the different tidal bands. These smaller effects are overshadowed in the diurnal band by the much studied fluid core resonance. This resonance results from excitation of the nearly

diurnal free wobble (NDFW) which, in turn, depends roughly on the differential tidal torque between the core and mantle. Since this differential torque is small the resonance is quite narrow.

The most pronounced body tide differences between the five Earth models considered here (PEM-C, C2, 1066A, and two variants of 1066A obtained by modifying the stability of the fluid core) occur near the NDFW resonance in the diurnal band. These differences are due to the slight variations between models of the NDFW eigenfrequency. Unfortunately, no computationally significant differences are found between the results for 1066A and its two variants.

The Earth's forced nutational motion is simply one component of its diurnal tidal response. Separate identification of nutation is desirable, however, to avoid contamination with errors in available tidal potential theories. Observational considerations have prompted the use of the axis, $\underset{\sim}{B}$, (the Tisserand mean figure axis of the surface) to describe the forced nutational motion. The most notable non-rigid characteristic in the results for $\underset{\sim}{B}$ is the narrow NDFW resonance. As for the body tide, most model-dependent differences in $\underset{\sim}{B}$ occur near this resonance. Again, no significant differences are found between results for the three models of the fluid core stability (1066A and its two variants).

Tidally induced changes in the Earth's rotation rate are part of the long period tidal motion. These changes are found to

be about 10% less than previously supposed due to relative axial rotation between the fluid core and mantle. No significant variations in the results are found for any of the five models.

The numerical results described in Chapter IX may be applied either to remove the tidal signal from geodetic or astrometric data as an undesirable source of noise, or to use observed tidal motion to investigate the geophysical behavior of the Earth. Our success in achieving these ends depends on the answers to three questions:

1) Is our model of the Earth's dynamical behavior adequate?
2) Have we chosen models for the material structure which are sufficiently close to the real Earth?
3) Is our computational process reliable (i.e. do we accurately solve the posed problem)?

The computational accuracy here is quite good; we have argued that the results are uniformly accurate to at least one part in 300. In view of the current large modelling uncertainties associated with the effects of ocean loading and local geological and topographical inhomogeneities, it appears that these computational limits should pose no problems.

For the structure of the Earth we have chosen what seems to be a fairly representative sample of contemporary dissipationless models, each of which has been designed to accommodate great quantities of free oscillation and seismic wave data. Differences

between results for the various structural models are usually near the level of computational accuracy. Once again, deficiencies in our current ability to correct for the oceans and for other local effects are probably much larger than these differences. We must conclude that measurements of the different tidal motions are not likely to greatly improve our knowledge of the global structure of the Earth within the near future (at least not within the limits imposed by the dynamical model used here). On the other hand, the close agreement between these results does allow for relatively unambiguous removal of the tidal signal from observations, if desired.

The dynamical model used here is incomplete. By far the most serious known defects are the absence of both oceans and local near surface inhomogeneities in geology and topography, which must be corrected for independently. Uncertainties in these corrections currently present the most formidable obstacles to a successful interpretation of tidal observations.

Other unmodelled dynamical behavior could conceivably be important, however. Probably most likely to be observed, either geodetically or astrometrically, is any phenomenon which affects the NDFW resonance in the diurnal tides and nutations. The anomalous frequency behavior associated with this resonance is not likely to be masked by the effects of oceans or local inhomogeneities (as one qualification: the oceanic tide may exhibit

some structure near the resonance since it must in part respond to any resonant tidal motion of the solid ocean floor).

Of particular geophysical interest are proposed mechanisms of dissipative coupling between the fluid core and the mantle. Since the NDFW resonance depends on relative rotation between the core and mantle, any mechanism (i.e. viscosity, electro-magnetic coupling, an irregular core-mantle boundary) which could impede this slippage might be observed. Such coupling could also show up in astrometric observations of the changes in rotation rate, since these also involve a large relative core-mantle rotation.

The elliptictiy of the core-mantle boundary determines the inertial pressure coupling between core and mantle and is very important in controlling the frequency of the NDFW resonance. Although the core-mantle ellipticity has not been directly observed seismically, it is thought to be well determined by the core density structure and the assumption of hydrostatic equilibrium. It seems unlikely that tidal observations can offer improvement over these estimates. However, should there be large unknown processes in the core (such as large scale convective flows) which alter the state of hydrostatic equilibrium, the ellipticity of the boundary could be affected. It should be understood that if such processes exist or if hydrostatic equilibrium is violated in the core (a most unlikely situation) all existing theories of the tidal resonance must be suspect.

REFERENCES

Alsop, L. E., 1963. Free spheroidal vibrations of the earth at very long periods, Part II, Effect of rigidity of the inner core, Bull. Seism. Soc. Am., 53, 503-515.

Anderson, D.L., and Hart, R.S., 1976. An Earth model based on free oscillations and body waves, J. Geophys. Res., 81, 1461-1475.

Atkinson, R. d'E, 1973. On the "dynamical variation" of latitude and time, Astron. J., 78, 147-151.

Atkinson, R. d'E, 1975. On the Earth's axes of rotation and figure, Mon. Not. R. astr. Soc., 71, 381-386.

Baker, T. F., 1979, What can earth tides tell us about ocean tides or earth structure? To be published in the Proceedings of the 9th GEOP Conference on the Application of Geodesy to Geodynamics, Columbus, Ohio, October 2-5, 1978.

Bartels, J., 1957. Geszeitenkräfte, in Encyclopedia of Physics Volume 48 (Geophysics II), p. 734-774, Springer-Verlag, Berlin.

Beaumont, C., and Berger, J., 1974. Earthquake Prediction: modification of the earth tide tilts and strains by dilatancy, Geophys. J. R. astr. Soc., 39, 111-121.

Beaumont, C. and Berger, J., 1975. An analysis of tidal strain observations from the United States of America I. the homogeneous tide, Bull. Seism. Soc. Am., 65, 1613-1629.

Beaumont, C., and Lambert, A., 1972. Crustal structure from surface load tilts using a finite element model, Geophys. J. R. astr. Soc., 29, 203-226.

Berger, J., and Beaumont, C., 1976. An analysis of tidal strain observations from the United States of America, II. the inhomogeneous tide, Bull. Seism. Soc. Am., 66, 1821-1846.

Brown, E. W., 1919. Tables of the motion of the Moon, Yale University Press, New Haven.

Busse, F. H., 1970. The dynamical coupling between inner core and mantle of the Earth and the 24-year libration of the pole in Earthquake Displacement Fields on the Rotation of the Earth, ed. by L. Mansinha, p. 88, D. Reidel, Dordrecht, Netherlands.

Busse, F. H., 1974. On the free oscillations of the earth's inner core, J. Geophys. Res., 79, 753-757.

Busse, F. H., 1975. A model of the Geodynamo, Geophys. J. R. astr. Soc., 42, 437-459.

Cartwright, D.E. and Edden, A. C., 1973. Corrected tables of tidal harmonics, Geophys. J. R. astr. Soc., 33, 253-264.

Cartwright, D.E. and Tayler, R. J., 1971. New computations of the tide-generating potential, Geophys. J. Roy. Astr. Soc., 23, 45-74.

Counselman III, C.C., 1976. Radio Astrometry, Annual review of astronomy and astrophysics, 14, 197-214.

Crossley, D. J., 1975. Core undertones with rotation, Geophys. J. R. astr. Soc., 42, 477-488.

Dahlen, F. A., 1968. The normal modes of a rotating elliptical Earth, Geophys. J. R. astr. Soc., 16, 329-367.

Dahlen, F. A., 1969. The normal modes of a rotating elliptical Earth - II: Near-resonance multiplet coupling, Geophys. J. R. astr. Soc., 18, 397-436.

Dahlen, F. A., 1972. Elastic dislocation theory for a self-gravitating elastic configuration with an initial static stress field, Geophys. J. R. astr. Soc., 28, 357-383.

Dahlen, F. A. and Smith, M. L., 1975. The influence of rotation on the free oscillations of the Earth, Phil. Trans. Roy. Soc. Lond. A., 279, 583-624.

Darwin, G. H., 1883. Report of a committee for the harmonic analysis of tidal observations, Brit. Ass. Rep., 48-118.

Doodson, A. T., 1922. The harmonic development of the tide-generating potential, Proc. Roy. Soc. Lond., Ser. A, 100, 305-329.

Dziewonski, A.M., Hales, A.L., and Lapwood, E.R., 1975. Parametrically simple Earth models consistent with geophysical data, Phys. Earth Planet. Interiors, 10, 12-48.

Edmonds, A.R., 1960. Angular Momentum in Quantum Mechanics, Princeton University Press, Princeton, New Jersey.

Farrel, W.E., 1972. Deformation of the earth by surface loads, Rev. Geophys. Space Phys., 10, 761-797.

Gilbert, F., and Dziewonski, A.M., 1973. The structure of the Earth retrieved from eigenspectra, EOS, 54, 374.

Gilbert, F., and Dziewonski, A.M., 1975. An application of normal mode theory to the retrieval of structural parameters and source mechanisms from seismic spectra, Phil. Trans. R. Soc. Lond. A278, 187-269.

Greenspan, H.P., 1968. The Theory of Rotating Fluids, Cambridge University Press.

Harrison, J.C., 1976. Cavity and topographic effects in tilt and strain measurement, J. Geophys. Res., 81, 319-328.

Hough, S.S., 1895. The oscillations of a rotating ellipsoidal shell containing fluid, Phil. Trans. R. Soc. Lond. A186, 469-506.

Jeffreys, H., 1948. The earth core and the lunar nutation, Mon. Not. R. astr. Soc., 108, 206-209.

Jeffreys, H., Dyanmic effects of a liquid core, Mon. Not. R. Astr. Soc., 109, 670-687.

Jeffreys, H., 1950. Dynamic effects of a liquid core (II), Mon. Not. R. astr. Soc., 110, 460-466.

Jeffreys, H., 1970. The Earth, Cambridge University Press, 5th edition.

Jeffreys, H. and Vicente, R.O., 1957a. The theory of nutation and the variation of latitude, Mon. Not. R. astr. Soc., 117, 142-161.

Jeffreys, H. and Vicente, R.O., 1957b. The theory of nutation and the variation of latitude: the Roche model core, Mon. Not. R. astr. Soc., 117, 162-173.

Jordan, T.H. and Anderson, D.L., 1974. Earth structure from free oscillations and travel times, Geophys. J. R. astron. Soc., 36, 411-459.

Kinoshita, H., 1977. Theory of the rotation of the rigid Earth. Celestial Mech., 15, 277-326.

Kudlick, M.D., 1966. On transient motions in a contained rotating fluid, Ph.D. Thesis, Math. Dept., MIT.

Larmor, J., 1909. The relation of the Earth's free precessional nutation to its resistance against tidal deformation, Proc. R. Soc. Lond. A, 82, 89-96.

Longman, I.M., 1962. A Green's function for determining the deformation of the Earth under surface mass loads, 1, Theory, J. Geophys. Res., 67, 845-850.

Longman, I.M., 1963. A Green's function for determining the deformation of the Earth under surface mass loads, 2, Computations and numerical results, J. Geophys. Res., 68, 485-496.

Love, A.E.H., 1909. The yielding of the Earth to disturbing forces, Proc. R. Soc. Lond. A., 82, 73-88.

Masters, G., 1978, Observational constraints on the chemical and thermal structure of the earth's deep interior, Ph.D. thesis, Cambridge.

McClure, P., 1976. Core-resonance effects on the Earth's angular momentum vector and rotation axis - a generalized model, Bull. Geod., 50, 262.

Melchior, P., 1966. The Earth Tides, Pergamon Press, Oxford.

Messiah, A., 1958. Quantum Mechanics, North-Holland Publishing Company-Amsterdam.

Molodensky, M.S., 1961. The theory of nutation and diurnal Earth tides. Comm. Obs. R. Belgique, 288, 25-56.

Munk, W.H. and McDonald, G.J.F., 1960. The Rotation of the Earth, Cambridge University Press, London.

Oppolozer, T.R.V., 1880. Bahnbestimmung der Kometen und Planeten, Engelmann, Leipzig Union, 2nd ed., vol. I, p. 154-155.

Pekeris, C.L., and Accad, Y., 1972. Dynamics of the liquid core of the Earth, Phil. Trans. R. Soc. Lond. A, 273, 237-260.

Phinney, R.A. and Burridge, R., 1973. Representation of the elastic-gravitational excitation of a spherical Earth model by generalized spherical harmonics, Geophys. J. R. astr. Soc., 34, 451-487.

Poincaré, H., 1910. Sur la Précession des Corps Deformables, Bull. Astr., 27, 321-356.

Robertson, D.S., Carter, W. E., Corey, B. E., Cotton, W. D., Counselman, C. C., Shapiro, I. I., Hinteregger, H. F., Knight, C. A., Rogers, A. E. E., Whitney, A. R., Ryan, J. W., Clark, T. A., Coates, R. J., Ma, C., Moran, J. M., 1978. Recent results of radio interferometric determinations of a trans-continental baseline, polar motion, and Earth rotation, presented at I.A.U. Symposium No. 82 "Time and Earth's Rotation", Cadiz,Spain, May 1978.

Rochester, M.G., 1976. The secular decrease of obliquity due to dissipative core-mantle coupling, Geophys. J. R. astr. Soc., 46, 109-126.

Rudin, W., 1973. Functional Analysis, McGraw-Hill, New York.

Sasao, T., Okamoto, J., and Sakai, S., 1977. Dissipative core-mantle coupling and nutational motion of the Earth, Publ. Astron. Soc. Japan, 29, 83-105.

Sasao, T., Okubo, S., Saito, M., 1979. A simple theory on dynamical effects of stratified fluid core upon nutational motion of the earth, to be published in Proceedings of IAU Symposium No. 78 "Nutation and the Earth's Rotation" (Kiev, May 1977), in press.

Shen, P-Y, and Mansinha, L., 1976. Oscillation, nutation, and wobble of an elliptical rotating Earth with liquid outer core, Geophys. J. R. astr. Soc., 46, 467-496.

Silverberg, E. C., 1978. On the effective use of lunar ranging for determination of the Earth's orientation, presented at I.A.U. Symposium No. 82 "Time and the Earth's Rotation", Cadiz, Spain, May 1978.

Slichter, L. B., 1961. The fundamental free mode of the earth's inner core, Proc. Nat. Acad. Sci., U.S.A., 47, 186-190.

Smith, D. E., Kolenkiewicz, R., Dunn, P. J., and Torrence, M., 1978. Determination of polar motion and Earth rotation from laser tracking of satellites, presented at I.A.U. Symposium No. 82 "Time and the Earth's Rotation"; Cadiz, Spain, May 1978.

Smith, M.L., 1974. The scalar equations of infinitesimal elastic-gravitational motion for a rotating, slightly elliptical earth, Geophys. J. R. astr. Soc., 37, 491-526.

Smith, M.L., 1976. Translational inner core oscillations of a rotating, slightly elliptical earth, J. Geophys. Res., 81, 3055-3065.

Smith, M.L., 1977. Wobble and nutation of the Earth, Geophys. J. R. astr. Soc., 50, 103-140.

Toomre, A., 1974. On the 'nearly diurnal wobble' of the Earth, Geophys. J. Roy. Astron. Soc., 38, 335-348.

Warburton, R.J., Beaumont, C., and Goodkind, J.M., 1975. The effect of ocean tide loading on tides of the solid earth observed with the superconducting gravimeter, Geophys. J. R. astr. Soc., 43, 707-720.

Williams, J.G., 1977. Present scientific achievements from lunar laser ranging in Scientific Applications of Lunar Laser Ranging, ed. J.D. Mulholland, Reidel, Dordrecht.

Woolard, E.W., 1953. Theory of the rotation of the earth around its center of mass. Astronomical Papers for the American Ephemeris and Nautical Almanac (Govt. Printing Office, Washington, D.C., 1953), Vol. XV, Pt. 1.

Zschau, J., 1976. Tidal sea load tilt of the crust and its application to the study of crustal and upper mantle structure, Geophys. J. R. astr. Soc., 44, 577-593.

Zscahu, J., 1978. Tidal Friction in the Solid Earth: Loading Tides versus Body Tides in Tidal Friction and Earth's Rotation, Ed. by P. Brosche and J. Sündermann, Springer-Verlag, New York.

APPENDIX A

GENERALIZED SPHERICAL HARMONICS

The most analytically tractable partial differential equations are usually those possessing some degree of global symmetry. Exploitation of symmetry usually leads to separation of variables and a corresponding expansion in terms of some complete set of orthogonal functions. Thus, spherically symmetric scalar equations are most usefully solved in spherical polar coordinates with spherical harmonics, Y_ℓ^m, chosen as a basis set. In particular, any scalar function of position, f, is conveniently expanded over each spherical surface as

$$f(\theta,\phi) = \sum_{\ell=0}^{\infty} \sum_{m=-\ell}^{\ell} a_{\ell m}\, Y_\ell^m(\theta,\phi) \tag{A.1}$$

where the $a_{\ell m}$ are constants and the Y_ℓ^m are defined here with normalization

$$Y_\ell^m(\theta,\phi) = (-1)^m \left[\frac{2\ell+1}{4\pi} \frac{(\ell-m)!}{(\ell+m)!} \right]^{1/2} e^{im\phi}\, P_\ell^m(\cos\theta) \quad \text{for } m \geq 0$$

$$Y_\ell^{-m} = (-1)^m\, (Y_\ell^m)^* \tag{A.2}$$

$$P_\ell^m(x) = \frac{(1-x^2)^{m/2}}{2^\ell \ell!} \frac{d^{\ell+m}}{dx^{\ell+m}} (x^2-1)^\ell$$

Unfortunately, extension to spherical vector and tensor equations is not easily realized. For example, vector completeness of the Y_ℓ^m takes the form

$$\underset{\sim}{v}(\theta,\phi) = \sum_{\ell,m} \left[a^1_{\ell m} \hat{\underset{\sim}{e}}_r Y^m_\ell + a^2_{\ell m} \underset{\sim}{\nabla} Y^m_\ell + a^3_{\ell m} \hat{\underset{\sim}{e}}_r \times \underset{\sim}{\nabla} Y^m_\ell \right] \tag{A.3}$$

where $\hat{\underset{\sim}{e}}_r$ is the unit vector along r. Tensor fields prove even more awkward.

To overcome these difficulties we introduce generalized spherical harmonics, $D^\ell_{mn}(\theta,\phi)$, as (Phinney and Burridge, 1973; Edmonds, 1960)

$$D^\ell_{mn}(\theta,\phi) = (-1)^{m+n} P^{nm}_\ell(\cos\theta)\, e^{im\phi} \tag{A.4}$$

where

$$P^{nm}_\ell(x) = \frac{(-1)^{\ell-n}}{2^\ell(\ell-n)!} \left[\frac{(\ell-n)!\ (\ell+m)!}{(\ell+n)!\ (\ell-m)!} \right]^{1/2} (1-x)^{-1/2(m-n)} \tag{A.5}$$

$$(1+x)^{-1/2(m+n)} \left(\frac{d}{dx}\right)^{\ell-m} \left[(1-x)^{\ell-n}\ (1+x)^{\ell+n} \right]$$

(D^{ℓ}_{mn} in (A.4) differs from the Y^{nm}_{ℓ} of Phinney and Burridge, 1973, by the factor $(-1)^{m+n}$.) Any spherically symmetric tensor of arbitrary order is conveniently represented by the D^{ℓ}_{mn} with components along complex spherical unit vectors, $\hat{\underset{\sim}{e}}_-$, $\hat{\underset{\sim}{e}}_o$ and $\hat{\underset{\sim}{e}}_+$. These are related to the conventional spherical basis vectors, $\hat{\underset{\sim}{e}}_r$, $\hat{\underset{\sim}{e}}_\theta$, $\hat{\underset{\sim}{e}}_\phi$ by

$$
\begin{aligned}
\hat{\underset{\sim}{e}}_- &= \frac{1}{\sqrt{2}} (\hat{\underset{\sim}{e}}_\theta - i\hat{\underset{\sim}{e}}_\phi) \\
\hat{\underset{\sim}{e}}_o &= \hat{\underset{\sim}{e}}_r \\
\hat{\underset{\sim}{e}}_+ &= -\frac{1}{\sqrt{2}} (\hat{\underset{\sim}{e}}_\theta + i\hat{\underset{\sim}{e}}_\phi)
\end{aligned}
\tag{A.6}
$$

In particular, any scalar, ϕ, vector, $\underset{\sim}{v}$, and second order tensor, $\underset{\sim}{T}$, can be expanded over a spherical surface as

$$
\begin{aligned}
\phi(r,\theta,\phi) &= \sum_{\ell=0}^{\infty} \sum_{m=-\ell}^{\ell} \phi^m_\ell(r)\, D^{\ell}_{mo}(\theta,\phi) \\
\underset{\sim}{v}(r,\theta,\phi) &= \sum_{\ell=0}^{\infty} \sum_{m=-\ell}^{\ell} \sum_{n=-1}^{+1} v^{mn}_\ell(r)\, D^{\ell}_{mn}(\theta,\phi)\, \hat{\underset{\sim}{e}}_n \\
\underset{\sim}{T}(r,\theta,\phi) &= \sum_{\ell=0}^{\infty} \sum_{m=-\ell}^{\ell} \sum_{\alpha,\beta=-1}^{+1} T^{m\alpha\beta}_\ell(r)\, D^{\ell}_{m(\alpha+\beta)}(\theta,\phi)\, \hat{\underset{\sim}{e}}_\alpha \hat{\underset{\sim}{e}}_\beta
\end{aligned}
\tag{A.7}
$$

Furthermore, the D^{ℓ}_{mn} are orthogonal in the familiar sense that

$$\text{(A.8)} \qquad \int_0^{2\pi}\int_0^{\pi} D^{\ell}_{mn}(\theta,\phi)\left(D^{\ell'}_{m',n}(\theta,\phi)\right)^{*} \sin\theta d\theta d\phi = \left(\frac{4\pi}{2\ell+1}\right)\delta_{\ell\ell'}\delta_{mm'}$$

Useful recurrence relations for the D^{ℓ}_{mn} are found in Phinney and Burridge (1973).

The D^{ℓ}_{mn} are related to the Y^{m}_{ℓ} defined by (A.2) according to

$$D^{\ell}_{mo} = \sqrt{\frac{4\pi}{2\ell+1}}\; Y^{-m}_{\ell}$$

$$D^{\ell}_{m-} + D^{\ell}_{m+} = \sqrt{\frac{4\pi}{2\ell+1}}\;\frac{2}{\sqrt{\ell(\ell+1)}}\;\frac{m}{\sin\theta}\,Y^{-m}_{\ell}$$

(A.9)

$$D^{\ell}_{m-} - D^{\ell}_{m+} = -\sqrt{\frac{4\pi}{2\ell+1}}\;\frac{2}{\sqrt{\ell(\ell+1)}}\;\partial_{\theta}\,Y^{-m}_{\ell}$$

$$D^{\ell}_{m+2} + D^{\ell}_{m-2} = 4\sqrt{\frac{4\pi}{2\ell+1}}\sqrt{\frac{1}{\ell(\ell+1)(\ell+2)(\ell-1)}}\left[\partial^{2}_{\theta}Y^{-m}_{\ell} + \frac{\ell(\ell+1)}{2}\,Y^{-m}_{\ell}\right]$$

$$D^{\ell}_{m+2} - D^{\ell}_{m-2} = 4\sqrt{\frac{4\pi}{2\ell+1}}\sqrt{\frac{1}{\ell(\ell+1)(\ell+2)(\ell-1)}}\;\frac{m}{\sin\theta}\left[\partial_{\theta}Y^{-m}_{\ell} - \frac{\cos\theta}{\sin\theta}\,Y^{-m}_{\ell}\right]$$

Of equal importance is the product of two generalized spherical harmonics:

$$D^{\ell'}_{m'n'}\, D^{\ell''}_{m''n''} = \sum_{\ell=|\ell''-\ell'|}^{|\ell''+\ell'|} \begin{vmatrix} \ell & \ell' & \ell'' \\ n & n' & n'' \\ m & m' & m'' \end{vmatrix} D^{\ell}_{mn} \tag{A.10}$$

where

$$\begin{vmatrix} \ell & \ell' & \ell'' \\ n & n' & n'' \\ m & m' & m'' \end{vmatrix} = (2\ell+1)(-1)^{m+n} \begin{pmatrix} \ell & \ell' & \ell'' \\ -n & n' & n'' \end{pmatrix} \begin{pmatrix} \ell & \ell' & \ell'' \\ -m & m' & m'' \end{pmatrix} \tag{A.11}$$

and the $\begin{pmatrix} \ell & \ell' & \ell'' \\ -n & n' & n'' \end{pmatrix}$ are Wigner 3-j symbols (see e.g., Edmonds, 1960; Messiah, 1958). A more complete discussion may be found in Smith (1974).